



Assessment of Channel Morphology and Fluvial Geomorphic Processes in the Lower McCloud River (GS-S2)

TECHNICAL MEMORANDUM 68 (TM-68)

DATE: January 30, 2009

TO: Relicensing Participants

FROM: Steve Nevares (PG&E) and Jay Stallman (Stillwater Sciences)

SUBJECT: Assessment of Channel Morphology and Fluvial Geomorphic Processes (GS-S2)

The preliminary assessment of channel morphology and fluvial geomorphic processes in the Lower McCloud River was presented in Licensee's Initial Study Report (ISR) (PG&E 2008). This technical memo presents the final version of this assessment, as well as text presented in Section 2.2 of Licensee's Initial Study Report and additional data not previously presented. This technical memorandum supersedes Section 2.2 of Licensee's ISR.

1 STUDY OBJECTIVES

Study Description GS-S2 has three primary goals: (1) assess the potential geomorphic effects of reducing coarse sediment supply and altering coarse sediment transport in the Lower McCloud River, (2) provide information required to assess potential ecological effects of any geomorphic changes in the Lower McCloud River resulting from Project operations and maintenance, and (3) provide information for developing protection, mitigation, and enhancement (PM&E) measures aimed at mitigating any coarse sediment imbalance.

The specific objectives of the study are to:

1. Characterize coarse sediment supply rates upstream and downstream of McCloud Reservoir;
2. Classify channel reach morphology and response reaches in the Lower McCloud River from McCloud Dam to Squaw Valley Creek;
3. Characterize channel morphology, fluvial processes, and coarse sediment transport rates at intensive study sites in the Lower McCloud River from McCloud Dam to Squaw Valley Creek;
4. Estimate the mass balance between coarse sediment supply and transport at intensive study sites in the Lower McCloud River from McCloud Dam to Squaw Valley Creek;
5. Estimate coarse alluvial sediment storage (*i.e.*, gravel and cobble) in the Lower McCloud River from McCloud Dam to Squaw Valley Creek;
6. Estimate the downstream extent of any geomorphic effects of a coarse sediment deficit based on (1) coarse sediment mass balance, (2) coarse sediment storage characteristics, and (3) surveys of channel morphology and fluvial processes at



intensive study sites in the Lower McCloud River from McCloud Dam to Squaw Valley Creek; and

7. Provide information required for aquatic resource studies aimed at characterizing the ecological significance of any geomorphic effects associated with Project operation and maintenance.

2 STUDY AREA

The GS-S2 Study Area encompasses connected sediment source areas to McCloud Reservoir and the McCloud River between McCloud Reservoir and the confluence of Squaw Valley Creek (Figure 1). The Study Area was divided into 12 subbasin areas based on drainage area, magnitude of flow and sediment inputs, potential to alter channel morphology and bed surface texture, and relationship to hydroelectric Project facilities (Table 1). Specific study locations in the GS-S2 Study Area include:

- McCloud Reservoir,
- The Lower McCloud River channel between McCloud Dam and Squaw Valley Creek (where analyses of sediment supply, transport, and storage are conducted),
- Five intensive study sites on the Lower McCloud River between McCloud Dam and Squaw Valley Creek, and
- Three bed texture study sites on major tributaries to the Lower McCloud River between McCloud Dam and Squaw Valley Creek.

Specifically excluded from field study were areas where access was unsafe or private property for which Licensee did not receive approval from landowners to enter the property to perform the study. The Licensee made a good faith effort to obtain access to private property where necessary to conduct field studies.

2.1 Geology and Geomorphology

Bedrock geology within the McCloud River basin can be divided into three major bedrock terranes with characteristic surficial processes, erodibility, and drainage development: the Eastern Klamath belt, the Western Cascades terrane, and the High Cascades terrane (Figure 2, Table 1, Figure 3) (Irwin 1966, Wagner and Saucedo 1987, Irwin and Wooden 1999, Irwin 2003).



Table 1. Geologic terranes in the Study Area

Subbasin	Total Connected Source Area (km ²)	Connected Source Area (km ²)							
		High Cascades Terrane		Eastern Klamath Terrane					Western Cascades Terrane
		Quaternary Volcanics	Surficial Deposits	Meta-sedimentary	Meta-volcanic	Sedimentary	Igneous Intrusive	Older Volcanics	Tertiary Volcanic and Sedimentary
Upper McCloud River (including reservoir tributaries)	268	36	31	49	15	3.2	0	0.19	134
Mud/Huckleberry Creek	33	12	9.9	7.1	0	0	0.31	0	3.4
McCloud Dam to Hawkins Creek	3.6	0	0	0	3.6	0	0	0	0
Hawkins Creek	46	0	0	33	2.5	0	0	11	0
Hawkins Creek to Squirrel Creek (including Squirrel Creek)	6.6	0	0	5.2	1.4	0	0	0	0
Squirrel Creek to Fitzhugh Creek (including Fitzhugh Creek)	4.9	0	0	0	4.9	0	0	0	0
Fitzhugh Creek to Ladybug Creek (including Ladybug Creek)	19	0	0	10	8.8	0	0	0	0
Ladybug Creek to Bald Mountain Creek (including Bald Mountain Creek)	9.6	0	0	0.20	9.4	0.03	0	0	0
Bald Mountain Creek to Claiborne Creek	18	0	0	4.6	13	0.50	0	0	0
Claiborne Creek	42	0	0	34	6.5	0.08	0	0.54	0
Claiborne Creek to Squaw Valley Creek	7.6	0	0	3.4	4.1	0	0	0	0
Squaw Valley Creek	104	0	0.05	70	25	7.5	0.08	0.19	1.4



The Lower McCloud River occurs entirely within the Redding subterrane of the Eastern Klamath belt, which consists of arcuate belts of predominantly metavolcanic, metasedimentary, and limestone rocks of Paleozoic age. These foliated, fractured, and weathered metamorphic rocks are relatively weak and prone to mass wasting in areas with steep slopes. Soils mantling steep slopes are typically thin and rocky, except in areas with convergent topography, where a thicker mantle of soil and colluvium may be susceptible to landsliding and debris flow during intense storm events. Secondary erosion by rock fall and shallow debris slides commonly occurs in active and dormant landslide scars. Basement rocks of the Eastern Klamath belt are overlain by late Cretaceous and early Tertiary marine and non-marine sedimentary rocks northeast of McCloud Reservoir. In the Upper McCloud River watershed, these sedimentary rocks are buried by late Tertiary volcanic rocks of the Western Cascades terrane and by Quaternary and Holocene volcanic rocks in the Modoc Plateau and High Cascades terrane. The western half of the Upper McCloud River watershed encompasses the southern flanks of Mt. Shasta, a High Cascades compound stratovolcano consisting of at least four overlapping cones that range in age from 250,000 years to a few thousand years (Christiansen *et al.* 1977). The south flank of Mt. Shasta developed by accumulation of andesitic, dacitic, and basaltic lava flows and cones; unconsolidated pyroclastic, debris flow, and alluvial deposits; and glacial erosion and deposition (Christiansen *et al.* 1977). The eastern half of the Upper McCloud River watershed encompasses Neogene and younger volcanic rocks in the Medicine Lake Highlands of the Modoc Plateau. Mt. Shasta and the Medicine Lake Highlands have both erupted in the last 1,000 years.

Glacial advance and retreat during the Late Pleistocene transferred large amounts of coarse sediment to the Lower McCloud River. These deposits remain as fill terraces and coarse channel lag deposits in high-order valley bottoms. Field observations suggest that sediment supplied to the Lower McCloud River during Quaternary glacial episodes was much larger (boulder and large cobble) than typical of current bedload material (cobble and gravel). Much of the sediment produced during late Pleistocene glaciation remains in long-term storage, armors the bed surface, and is mobilized only during extreme flood events.

Principle tributaries to the Upper McCloud River originating from the southern and southeastern slopes of Mt. Shasta include Ash Creek, Mud Creek, Pilgrim Creek, and Brewer Creek. Mud Creek originates from Konwakiton Glacier and Ash Creek originates from Wintun glacier, two of seven active glaciers on Mt. Shasta. The Mud-Ash debris fan covers much of the southeast flank of Mt. Shasta and is formed from andesitic lava flows and pyroclastic, debris-flow, glacial, and fluvial deposits (Osterkamp *et al.* 1986). Although Mud and Ash creeks incise the upper parts of the fan by up to 200 m, much of the surface runoff from the southeast flanks of Mt. Shasta infiltrates the lower parts of the debris fan and emerges at springs on the Upper McCloud River.

At least five large debris flow events in Mud Creek have delivered large quantities of sediment to the McCloud River during the last 1,200 years, giving a recurrence interval of about 250 years for large debris flows (Osterkamp *et al.* 1986). The last large debris flow occurred in 1924. Smaller debris flows occur more frequently (at least one per decade) and result from failure of inner gorge slopes in Mud Creek Canyon and by entrainment of stored sediment in Mud Creek during high discharges caused by rapid meltwater release from the Konwakiton glacier. Osterkamp *et al.* (1986) estimate that debris flow sediment yields from Mud Creek to the Upper McCloud River may be as



much as 11,000 tonnes $\text{km}^{-2} \text{y}^{-1}$. Debris flow activity in Pilgrim Creek and Brewer Creek is infrequent and smaller in magnitude.

2.2 Hydrology

The Study Area experiences warm, dry summers and cool winters with moderate snowfall at elevations above 5,000 ft and heavy rainfall at lower elevations. In the Lower McCloud River watershed mean annual precipitation exceeds 70 in. throughout the basin and exceeds 80 in. in Claiborne Creek and Chatterdown Creek drainages (USFS 1998). Approximately 90 percent of the mean annual precipitation occurs from October to April during winter storms. Mean annual precipitation is less in the upper watershed as a greater percentage occurs as snowfall. At the National Weather Service monitoring station (#045449) located in the town of McCloud, mean annual precipitation is 47.7 in. and mean annual snowfall is 88.4 in. (WRCC 2008).

The hydrology of the Upper McCloud River watershed, which includes the southern and eastern flanks of Mt. Shasta, differs substantially from the hydrologic regime of the Lower McCloud River. Differences can be attributed in large part to large unchannelized areas where surface runoff is disconnected due to low gradient topography, rapid infiltration, and subsurface flow through relatively unweathered and rapidly permeable volcanic rocks and unconsolidated surficial deposits (Freeman 2001). As a result of these hillslope characteristics, springs that discharge groundwater from the aquifer to the east of Mt. Shasta contribute a large component to baseflow (estimated at 700 cfs [Davidson and Rose, 1997]) in the upper watershed. The Upper McCloud River watershed also includes the highest altitudes within the Study Area and has a much greater snowmelt influence than the Lower McCloud River watershed. As snowpack melts onto highly permeable volcanic sediments, a significant percent of the snowmelt infiltrates as recharge to the volcanic aquifer and later discharges as spring flow to the Upper McCloud River and its tributaries. Freeman (2001) estimated an approximate 3-year lag between rainfall/runoff in a given year and baseflow 3 years later. Hydrographs from historical gage data in the upper watershed generally show a slower response to precipitation events due to snowpack accumulation, porous surficial geology and flatter topography (TM-46, *Unimpaired Hydrology Development* [PG&E 2009a]).

In contrast to the upper watershed, the Lower McCloud River drains steeper and more dissected hillslopes that are primarily composed of much older (Paleozoic age) metasedimentary and metavolcanic rocks (Table 1). As a result, the Lower McCloud River basin generally exhibits a “flashier” hydrologic response to precipitation events, and is driven more by rainfall-runoff than by the snowmelt and spring-fed baseflow that characterize Upper McCloud River hydrology.

2.3 Disturbance History

The Lower McCloud River watershed is an unpopulated area with low road density (1.7 mi per mi^2). Although roads were constructed to the McCloud River Club in 1916 and to Ah-Di-Na in the 1950s, it is unlikely that roads significantly influenced erosion processes and sediment delivery to the Lower McCloud River until the mid-1960s, when a more extensive road system was developed to support timber harvest activities on both public and private lands (USFS 1998). Timber harvest activities on public lands began in 1966, but development of unroaded areas for timber production



on National Forest ceased in 1975. Road building in other areas continued, with the latest road built in 1996 to access private land in North Fork Chatterdown Creek (USFS 1998). Although surface erosion and failure of drainage structures on roads have undoubtedly increased fine sediment production during the past 40 years, little is known about changes in landslide frequency and coarse sediment production as a result of timber harvest and road construction in the basin.

This sediment budget does not explicitly account for variability in sediment production and yield resulting from wildfire, but long-term patterns in fire frequency and distribution in the Study Area provide a context for qualitatively interpreting how wildfires may affect sediment dynamics. Aerial photography from 1944 and reporting from the early 1900s indicate that much of the Lower McCloud River watershed was covered in early seral vegetation as a result of large wildfires, some of which burned through the entire southern portion of the watershed in the late 1800s (USFS 1998). During the past 100 years, fire suppression activities have decreased the size and frequency of fires in the watershed, presumably reducing sediment production by mass wasting and surface erosion associated with fire-related ground disturbance. The Lower McCloud River watershed currently has a high potential for catastrophic wildfire due to abundant standing fuels, dense fire ladders, and a moderate to high probability of ignition start from lighting (USFS 1998). Although fire is generally understood to increase erosion rates, the duration and long-term effects of fire on sediment production, storage, and yield are not clearly understood (Swanson 1981, Wondzell and King 2003, Roering and Gerber 2005). Geomorphic effects of fire can include increased surface erosion by increased overland flow, increased dry ravel of cohesive soil aggregates, and increased shallow landsliding and debris flow due to loss of root strength. Increased runoff and higher peak flows can alter channel sediment storage following fire (Swanson 1981). While large stand-replacing fires in the watershed could dramatically increase the short-term sediment supply and cause temporary fining of bed surface texture in the Lower McCloud River, it is unlikely that large fires would have a long-term influence on channel morphology due to the coarse, relatively immobile framework and high existing transport capacity.

3 SEDIMENT SUPPLY

3.1 Methods

The overall approach to estimating sediment supply to the Lower McCloud River involved (1) measuring sediment accumulation in McCloud Reservoir and estimating average annual sediment yield from the reservoir source area based on sedimentation rate, (2) applying a sediment delivery model to the connected source area to McCloud Reservoir and testing model results against average annual sediment yield from sedimentation rate, and (3) extrapolating and/or modeling sediment delivery rates to The Lower McCloud River under regulated and unimpaired conditions.

3.1.1 Measuring Reservoir Sedimentation

Sediment accumulation in a reservoir reflects sediment yield from the source area and can be used to estimate average annual sediment yield. Calculating sediment yield to a reservoir requires measuring or estimating (1) the volume of accumulated sediment, (2) bulk sediment properties (*e.g.*, density, grain size, and percent organic matter), (3) reservoir trap efficiency (TE), and (4) connected



source area to the impoundment. This study estimated the average annual sedimentation rate in McCloud Reservoir and used this rate to extrapolate average annual sediment yield to locations along the McCloud River.

The volume of sediment accumulated since reservoir construction was determined by differencing two digital grid surfaces of reservoir floor elevations—one based on topography prior to sediment filling and the other based on modern bathymetry. The grid surface prior to sediment filling was derived from topography of McCloud Reservoir that was photogramatically prepared prior to construction of McCloud Dam by Hammon, Jenson, and Wallen Mapping and Forestry Services using 1:12,000 scale aerial photography dated May 5, 1953. Topography of the reservoir basin was typically represented by 10-ft contour intervals. The drawings were scanned, rectified to the NAD83 UTM zone 10 north coordinate system, and used to screen-digitize elevation contours that were converted to a 5-ft grid using the TopoGrid function in ArcInfo. Modern bathymetry was surveyed when the reservoir was near maximum pool (elevation 2,677.3 ft) during June 2007, using survey-grade hydroacoustic and GPS equipment. Data were collected using an onboard laptop computer running software that merged position data with depth measurements. Raw data points were converted to x, y, and z coordinates and filtered to remove anomalous points resulting from turbulence, turbidity, aquatic vegetation, and poor GPS resolution. Bathymetric data were used to construct a 5-ft grid surface by kriging, a weighted-moving-average interpolation method. To improve georeferencing between the historical and current grids, the historical grid was rubber-sheeted to tie points (*e.g.*, points that have remained unchanged over time) selected along 11 reservoir cross sections. The coincident grids of post-construction and modern reservoir floor elevations were then subtracted to determine sediment thickness and calculate accumulated sediment volume (Morris and Fan 1998, Childs *et al.* 2003, Snyder *et al.* 2004, 2006). Isopach contours were used to evaluate the distribution of sediment accumulated in the reservoir and the relative sediment contributions from different source areas.

Average annual yield to McCloud Reservoir was estimated using the following procedure:

1. Accumulated sediment volume was converted to accumulated mass using published values for reservoir sediment density;
2. Total mass yield was calculated from accumulated mass using TE estimates derived from commonly used empirical equations (*e.g.*, Brown 1943, Churchill 1948, Brune 1953); and
3. Average annual, unit-area sediment yield was calculated by dividing the total mass sediment yield by the duration of accumulation and the connected source area to the reservoir.

The High Cascades terrane in the source area to the Upper McCloud River encompasses large unchannelized areas where surface runoff is disconnected due to low gradient topography, rapid infiltration, and subsurface flow through relatively unweathered and rapidly permeable volcanic rocks and unconsolidated surficial deposits. Areas with low relief and without connected surface runoff do not produce or transfer sediment, and therefore do not contribute to the sediment budget. For the purposes of this study, these areas were not considered part of the connected source area to McCloud Reservoir. Disconnected areas in the High Cascades terrane were mapped by a



combination of field observations, terrane analysis, existing map information, and professional judgment (personal communication, S. Bachmann, Hydrologist, USFS, McCloud, CA, and J. Stallman, Geomorphologist, Stillwater Sciences, Arcata, CA, September 28, 2007). In addition, the low gradient and relatively unconfined morphology of the Upper McCloud River channel upstream of Lakin Dam (located approximately 13.8 km [8.6 mi] upstream of McCloud Reservoir), combined with the lack of coarse sediment deposits in the impoundment, suggest that coarse sediment sourced from Western Cascades terrane upstream of Lakin Dam is sequestered in upstream reaches (personal communication, S. Bachmann, Hydrologist, USFS, McCloud, CA, and J. Stallman, Geomorphologist, Stillwater Sciences, Arcata, CA, September 28, 2007). For the purposes of this study, these areas were not considered part of the *bedload* connected source area (*i.e.*, source area for coarse sediment) to McCloud Reservoir.

Estimating sediment yield from the source area to McCloud Reservoir requires estimating the bulk properties of reservoir sediment (*e.g.*, density, grain size, and percent organic matter). Little existing information was available to describe bulk sediment properties in McCloud Reservoir, and a coring effort to characterize the spatial variability (longitudinal, lateral, and vertical) in grain size of sediment deposits was beyond the scope of this study. Bulk sediment properties were therefore assigned β -PERT distributions based on published values for other reservoirs with similar geology and from a larger sample of reservoirs located throughout the United States. β -PERT distributions allow flexibly shaped distributions to be defined in terms of minimum, modal, and maximum values (referred to here as low, most likely, and high). A disproportionately large amount of fine sediment is delivered to McCloud Reservoir by Mud Creek during debris flow events, and estimated values for bulk sediment properties in McCloud Reservoir could be reevaluated if more information about the grain size and proportional volume of fine sediment contributions from debris flows becomes available.

Reservoir TE is influenced by sediment transport processes in a reservoir, particle-size distribution of the incoming sediment, the mean flow velocity through the impoundment, and the average length of time water is impounded. These variables were not measured in McCloud Reservoir. Trap efficiencies were estimated using empirical equations relating TE to a capacity:annual inflow ratio (Brune 1953), a capacity:watershed area ratio (Brown 1943), and a sedimentation index (Churchill 1948). The Brune relation resulted in a lower TE estimate (78 percent) than estimates based on Brown (90 percent) and Churchill (92 percent). An unknown portion of fine sediment delivered to the proximal end of McCloud Reservoir by Mud Creek is transported to more distal parts of the reservoir by bottom turbidity currents. Bottom turbidity currents can efficiently transport a large fraction of fine sediment through the reservoir to a depositional pile located upstream of the dam face, and in some situations, through outlets in the dam to the Lower McCloud River. These processes may result in fine sediment trap efficiencies that differ from those predicted by empirical equations. Reservoir trap efficiencies could be reevaluated if more information about transport of fine sediment by turbidity currents in McCloud Reservoir becomes available.

3.1.2 Modeling Sediment Delivery Rates

The GEO model (USFS 2005), an empirically calibrated approach to modeling sediment delivery from mass wasting, was used to independently estimate coarse sediment delivery to the McCloud



River in the Study Area. The GEO model was developed by the U.S. Forest Service to estimate sediment delivery to streams by mass wasting as part of watershed analysis. The model accounts for the influence of geomorphic terranes, roads, timber harvest activity, and recent wildfires on sediment delivery by assigning a matrix of empirically defined sediment delivery coefficients in a GIS environment using Arc/Info. The approach was developed and calibrated in the Salmon sub-basin (de la Fuente and Haessig 1993), where topography and metamorphic bedrock geology are similar to the Redding subterrane of the Eastern Klamath belt in the Lower McCloud River source area (Figure 2 and Figure 3). Sediment delivery coefficients developed in the Salmon Sub-basin Sediment Analysis were modified for the Klamath Cumulative Watershed Effects Analysis (2004) and Shasta-Trinity Cumulative Watershed Effects Analysis (2005). A study of six streams in the Klamath National Forest found that estimates of sediment supply from the GEO and Universal Soil Loss Equation (USLE) models were correlated to fine sediment storage, median grain size, and subsurface flow rates (Cover *et al.* 2006).

The GEO model was applied to the connected source areas in the McCloud River Study Area using the geo13 geomorphic terrane coverage and associated sediment delivery rates developed by the U.S. Forest Service for the Shasta Trinity National Forest (USFS 2005). The geo13 coverage divides the landscape into 18 geomorphic terrane types with similar surface processes and sediment delivery rates (Figure 4, Table 2, Figure 5). Timber harvest history on private lands (1996–2006) was obtained from the California Department of Forestry and Fire Protection (CDF 2000). Timber management on public lands (1978–2008) was obtained from the USFS Stand Record System. Roads in the Study Area were clipped from a roads line coverage updated by the USFS ACT2 Enterprise Team in 2004. Mapping of recent wild fires and burn intensity (1988–2003) was obtained from the Shasta Trinity National Forest.

Sediment delivery from mass wasting is the primary source of coarse sediment to the McCloud River. Sediment delivered by mass wasting, however, is comprised of both coarse and fine sediment, the proportion of which varies by process (*e.g.*, shallow landslide, deep-seated landslide, debris flow). Because the ratio of coarse and fine sediment delivered by landslides in the Study Area is unknown, we assume that GEO model estimates of sediment delivery represent a maximum estimate of coarse sediment delivery to the McCloud River.

Table 2. Geomorphic terranes in the Study Area

Subbasin	Total Connected Source Area (km ²)	Connected Source Area (km ²)															
		Active Landslides	Dormant Landslides	Toe Zone Dormant Slides	Debris Basins	Inner Gorge on Granitic Bedrock	Inner Gorge on Unconsolidated Deposits	Other Inner Gorge	Cenozoic Volcanic Bedrock, Gentle Slopes	Cenozoic Volcanic Bedrock, Moderate Slopes	Cenozoic Volcanic Bedrock, Steep Slopes	Granitic Bedrock, Low to Moderate Slopes	Granitic Bedrock, Steep Slopes	Non-Granitic Bedrock, Low to Moderate Slopes	Non-Granitic Bedrock, Steep Slopes	Glacial Moraine, Terrace and Fan Deposits	Waterbodies, Lakes and Polygon Streams
Upper McCloud River	268	0.09	0.97	0.13	3.1	0	0	9.4	107	76	1.3	0	0	54	0.30	14	2.1
Mud/Huckleberry Creek	33	0	0.23	0	0	0.29	3.8	1.8	18	0.81	0.09	0	0	3.3	0	4.7	0.22
McCloud Dam to Hawkins Creek	3.6	0.01	1.4	0	0.76	0	0	0.12	0	0	0	0	0	1.3	0	0.01	0.04
Hawkins Creek	46	0.02	0.80	0.15	15	0	0	1.1	0	0	0	0	0	29	0.05	0.27	0
Hawkins Creek to Squirrel Creek (including Squirrel Creek)	6.6	0	0.01	0	4.2	0	0	0.68	0	0	0	0	0	1.7	0.01	0.06	0.02
Squirrel Creek to Fitzhugh Creek (including Fitzhugh Creek)	4.9	0	0.01	0	1.0	0	0	0.20	0	0	0	0	0	3.2	0.34	0.05	0.06
Fitzhugh Creek to Ladybug Creek (including Ladybug Creek)	19	0.17	3.4	0.13	5.5	0	0	0.91	0	0	0	0	0	7.8	0.02	0.77	0.08
Ladybug Creek to Bald Mt. Creek (including Bald Mt. Creek)	9.6	0	0.30	0	3.2	0	0	0.43	0	0	0	0	0	5.4	0.06	0.09	0.05
Bald Mountain Creek to Claiborne Creek	18	0	0.24	0.02	8.1	0	0	0.70	0	0	0	0	0	8.3	0.13	0.44	0.14
Claiborne Creek	42	0.14	2.1	0.02	1.8	0	0	2.0	0	0	0	0	0	34	0.70	0.83	0
Claiborne Creek to Squaw Valley Creek	7.6	0	0.16	0.01	0.49	0	0	0.46	0	0	0	0	0	5.7	0.52	0.22	0
Squaw Valley Creek	104	0.18	0.30	0.04	11	0.01	0	7.3	0.32	0.89	0.02	0.04	0.01	83	1.0	0.18	0



3.2 Results

3.2.1 Sedimentation in McCloud Reservoir

McCloud Reservoir (original capacity 35,234 acre-ft) has a connected source area of 301 km² (116 mi²). The connected source area is composed of 29.5 percent High Cascades terrane, 24.6 percent eastern Klamath terrane, and 45.8 percent Western Cascades terrane. The bedload source area to McCloud Reservoir (excluding the area upstream of Lakin Dam) is 154 km² (59 mi²). McCloud Reservoir accumulated 4,134,539 m³ (3,352 acre-ft) of sediment over the 43-year period between 1964 and 2007, reducing the original capacity by approximately 10 percent and resulting in an average annual sedimentation rate of 96,152 cubic meters per year (m³y⁻¹) (Figure 6, Table 3). The longitudinal geometry of the reservoir deposit in the mainstem valley forms a massive delta containing the coarsest fraction of the sediment load (Figure 7). The topset beds, composed of rapidly settling sediment at the proximal end of the delta, form a relatively continuous surface with an elevation of about 803 m (2,635 ft). This surface reflects the approximate water surface elevation during the normal minimum water surface elevation for McCloud Reservoir. The foreset beds at the face of advancing delta form a distinctive slope break approximately 5.2 km from the dam and steeply descend to the reservoir bottom. A thickening wedge of sediment is also apparent in the 1.8 km closest to the dam, likely related to transport of fine sediment through the reservoir by turbidity currents.

Average annual sediment yield to McCloud Reservoir was approximately 470 t km⁻² y⁻¹. Considering uncertainties in historical and current bathymetric surfaces, bulk sediment properties, and TE, this estimate of sediment yield is accurate to within about 20 percent. Sediment yield calculated from sedimentation rates in McCloud Reservoir is comparable to but on the higher end of the range in yields reported for other reservoirs in the Siskiyou region (200–650 t km⁻² y⁻¹), western Cascades (250–300 t km⁻² y⁻¹), and western slope of the northern Sierra Nevada (350–600 t km⁻² y⁻¹). The relatively high estimate of sediment yield is most likely due to the large volume of sediment delivered to McCloud Reservoir by debris flows from Mud Creek. The average annual coarse (>2 mm) sediment yield to the reservoir is estimated at approximately 140±30 t km⁻² y⁻¹, assuming 100 percent coarse sediment TE in Lakin and McCloud reservoirs and an estimated coarse:total ratio (coarse sediment > 2mm) of 0.15–0.20 for sediment in McCloud Reservoir (Vanoni 1977, U.S. Bureau of Reclamation 1987, Morris and Fan 1998, Snyder *et al.* 2004). Long-term average annual rates calculated from the volume of sediment accumulated since reservoir construction do not account for variability in sediment yield between dry years when little sediment production or bedload transport occurs, and wet years when large storm events trigger landslides and mobilize coarse sediment stored in channels. Sediment deposited in McCloud Reservoir during large floods in 1974, 1986, and 1997 may skew results toward higher estimates of long-term average annual sediment yield.



Table 3. Sedimentation in McCloud Reservoir and estimated sediment yield

Characteristics of McCloud Reservoir				
Placed in service	1964			
Bathymetric survey	June, 2007			
Duration of accumulation	43 years (y)			
Connected source area (including connected area upstream of Lakin Dam)	301 km ²			
Bedload connected source area (excluding area upstream of Lakin Dam)	154 km ²			
Accumulated sediment volume ^a	4,134,539 m ³			
Estimated Parameters	Units	Low	Most Likely	High
Bulk density ^b	t m ⁻³	1.18	1.31	1.44
Organic mass ^c	%	2%	4%	6%
Coarse-to-total ratio ^d	%	15%	18%	20%
Trap efficiency ^e	%	78%	86%	91%
Reservoir Sedimentation	Units	Low	Most Likely	High
Accumulated sediment mass	tonnes (t)	4,690,924	5,207,721	5,724,518
Mass accumulation rate	t y ⁻¹	109,091	121,110	133,128
Average annual unit sediment yield ^f	t km ⁻² y ⁻¹	388	468	583
Average annual coarse sediment yield ^g	t km ⁻² y ⁻¹	107	142	173
Denudation rate	mm y ⁻¹	0.18	0.18	0.18

^a Accumulated sediment volume determined by differencing two grids of reservoir floor elevations; one based on historical topography in 1964 prior to sediment filling and the other based on 2007 bathymetry.

^b Bulk density inferred from published sources (Ambers 2001, McBain and Trush 2002, Stillwater Sciences 2003, Snyder *et al.* 2004, Lara and Pemberton 1963 cited in Morris and Fan 1998).

^c Percent organic matter based on loss on ignition measured in sediment cores from Dorena Lake (Ambers 2001) and Englebright Reservoir (Snyder *et al.* 2004).

^d Coarse sediment yield based on a coarse-to-total ratio (proportion of sediment >2mm).

^e Trap efficiency averaged from empirical relations by Brune (1953), Churchill (1948) and Brown (1943).

^f Unit-area estimate for total sediment yield (fine and coarse) includes connected source areas upstream of Lakin Dam.

^g Unit-area estimate for coarse sediment yield excludes areas upstream of Lakin Dam.



3.2.2 Model Estimates of Sediment Delivery

Estimates of sediment delivery to McCloud Reservoir using the GEO model were 34 percent of the average annual sedimentation rate (Table 4). Low model results for sediment delivery largely result from using low sediment delivery coefficients assigned to geomorphic terranes in the Upper McCloud River source area. While GEO sediment delivery coefficients have been calibrated for metavolcanic and metasedimentary bedrock terranes similar to those encompassing the Lower McCloud River source area, sediment delivery coefficients are uncalibrated for Cenozoic volcanic bedrock terranes, unconsolidated glacial moraine and fan deposits, and associated inner gorges (Figure 4). In particular, GEO does not account for the large quantities of predominantly fine sediment delivered to McCloud Reservoir by debris flows originating from the inner gorge of Mud Creek Canyon, and likely underestimates sediment delivery from Tertiary volcanic and sedimentary rocks on steep slopes in the Western Cascades terrane located northeast of McCloud Reservoir (Figure 2). Calibration of sediment delivery coefficients in these terranes requires extensive air photo interpretation and field survey of sediment sources beyond the scope of this relicensing study. Estimates of sediment delivery using the GEO model do not account for fine sediment delivery related to surface erosion.

While reservoir sedimentation rate provides a reliable estimate of sediment delivery from the dominantly Cenozoic volcanic terranes in the Upper McCloud River source area, extrapolation of this high rate to source areas in the Eastern Klamath terrane downstream of McCloud Dam overestimates sediment delivery to the Lower McCloud River by a factor of 3 to 4. In addition, annual yield derived from reservoir sedimentation averages variability in erosion rates across different geomorphic terranes (stable and potentially unstable) and does not account for the geomorphic effects of land use changes on sediment production, variables that are incorporated into the GEO model.

Because reservoir sedimentation rate provides a reliable estimate of sediment delivery from the dominantly Cenozoic volcanic terranes in the Upper McCloud River source area, and GEO model estimates are a reasonably good predictor of sediment delivery from metamorphic bedrock and associated geomorphic terranes in the Lower McCloud River source area, a combined approach was used to estimate sediment supply in the McCloud River watershed under regulated and unimpaired conditions (Table 4, Figure 8). The cumulative coarse sediment supply using this combined approach provides the basis for subsequent analyses of the balance between annual coarse sediment supply and bedload transport under regulated and unimpaired conditions. The largest tributaries contributing coarse sediment to Lower McCloud River between McCloud Dam and Squaw Valley Creek are Hawkins Creek (46 km² adding 1,250 t y⁻¹), Claiborne Creek (42 km² adding 1,060 t y⁻¹), and Squaw Valley Creek (104 km² adding 2,200 t y⁻¹). Reduction in cumulative sediment supply to Lower McCloud River due to sediment trapping in McCloud Reservoir decreases with distance downstream of McCloud Dam, ranging from a 94 percent reduction at the Hawkins Creek confluence (1,500 t y⁻¹ regulated, 26,500 t y⁻¹ unimpaired) to a 78 percent reduction at the Squaw Valley Creek confluence (7,000 t y⁻¹ regulated, 32,000 t y⁻¹ unimpaired).



Table 4. Summary of sediment supply estimates

Subbasin	Source Area (km ²)	Sediment Delivery Estimated from Reservoir Sediment Rate (t y ⁻¹)	Sediment Delivery Estimated from GEO Model (t y ⁻¹)	Sediment Delivery Estimated Using Combined Approach ^b		
				Coarse Sediment Supply (t y ⁻¹)	Cumulative Coarse Sediment Supply (t y ⁻¹)	
					Unimpaired	Regulated
Upper McCloud River (including reservoir tributaries)	268.0	21,518	5,304	21,518	21,518	n/a
Mud/Huckleberry Creek	32.8	3,511	3,286	3,511	25,028	n/a
McCloud Dam to Hawkins Creek	3.6	381	197	197	25,225	197
Hawkins Creek	46.2	4,949	1,253	1,253	26,478	1,450
Hawkins Creek to Squirrel Creek (including Squirrel Creek)	6.6	708	227	227	26,705	1,677
Squirrel Creek to Fitzhugh Creek (including Fitzhugh Creek)	4.9	526	88	88	26,792	1,764
Fitzhugh Creek to Ladybug Creek	10.1	1,084	443	443	27,236	2,208
Ladybug Creek	8.6	924	845	845	28,081	3,053
Ladybug Creek to Bald Mountain Creek (including Bald Mountain Creek)	9.6	1,026	197	197	28,278	3,250
Bald Mountain Creek to Claiborne Creek	18.1	1,933	394	394	28,672	3,644
Claiborne Creek	41.4	4,428	1,061	1,061	29,733	4,705
Claiborne Creek to Squaw Valley Creek	7.6	809	142	142	29,875	4,847
Squaw Valley Creek	104.4	11,168	2,202	2,202	32,077	7,049

^a Sediment production excluded from Quaternary volcanics, unconsolidated surficial deposits, and ice/water in the Upper McCloud River subbasin.

^b Sedimentation rate is used to estimate sediment supply in the upper watershed and GEO model estimates are used to estimate sediment supply in the lower watershed.



4 CHANNEL MORPHOLOGY AND TEXTURE IN LOWER MCCLOUD RIVER

4.1 Methods

4.1.1 Classification of Channel Reach Morphology and Response Potential

Channel reach morphology in the Lower McCloud River was classified from McCloud Dam to Squaw Valley Creek to (1) group functional similar valley and channel morphology into reaches with similar sediment transport characteristics and sediment storage potential, and (2) stratify the relative responsiveness of channels to alterations in flow, sediment supply, and sediment transport. Channel reaches were classified using a process-based classification system emphasizing sediment supply, sediment transport, links to hillslope processes, and external forcing by valley confinement (Montgomery and Buffington 1998, 1997). The Montgomery and Buffington system was adapted to the Lower McCloud River by recognizing four dominant reach types (pool riffle, plane bed, step pool, and cascade) and two transitional reach types (riffle bar and riffle step) (Figure 9). Reach morphology was classified based on video footage from a low-altitude helicopter flight in July 2006, high resolution color aerial photography from 2007, channel gradient derived from USGS 10-m digital elevation model (DEM) data, and direct field observations. Reach morphology was delineated on a channel network coverage (the centerline for the Lower McCloud River).

Responsive reaches are those channel reaches where morphology and sediment storage (*e.g.*, gravel patches or alluvial channel bed, bars, and floodplains) are most likely to show Project effects from altered sediment supply and transport. A responsive reach is defined as having the following attributes: (1) slope less than 1.5 percent; (2) relatively unconfined; (3) plane bed, riffle bar, or pool riffle morphology; (4) predominantly alluvial sediment storage (cobble facies or finer); and (5) relatively abundant riparian vegetation.

4.1.2 Study Site Selection

4.1.2.1 Intensive Study Sites in Lower McCloud River

Subsequent to classifying channel morphology in the Lower McCloud River, potentially suitable and accessible response reaches were identified for intensive field study. Channel morphology, confinement, bedrock controls, and alluvial sediment storage were initially assessed, to the extent possible, using aerial photographs and video footage from a low-altitude helicopter flight. Final site selection occurred following field reconnaissance to all potentially suitable and accessible sites identified in the steps above. Intensive study sites were selected that were most likely to show a response to Project alterations in hydrology and sediment supply, were suitable for bed mobility analysis, and allowed for interpretations about the mass balance between coarse sediment supply and transport. Other criteria used to evaluate the suitability of responsive study sites for intensive study included minimal direct sediment input from streamside mass wasting (*i.e.*, from bank collapse or shallow landsliding) that may have caused localized changes in channel morphology or bed surface texture; minimal localized land use effects (*e.g.*, timber



harvest, channel constrictions due to road construction or crossings, bank protection), and safe access with landowner approval.

The Lower McCloud River from McCloud Dam to Squaw Valley Creek was divided into four reaches based on major tributary junctions that potentially alter channel morphology and bed texture due to flow and sediment inputs:

- McCloud Dam to Hawkins Creek (Reach 1),
- Hawkins Creek to Ladybug Creek (Reach 2),
- Ladybug Creek to Claiborne Creek (Reach 3), and
- Claiborne Creek to Squaw Valley Creek (Reach 4).

Five responsive study sites were selected for intensive field study within these reaches (Figure 1). The five intensive study sites are consistently spaced about 4 to 6 km apart, and where possible, were located to capture the influence of the larger tributaries on sediment supply, transport, and storage. The final intensive study sites were selected during field reconnaissance based on the above criteria, as well as observations of minimum stream power and maximum potential for sediment storage, where any effects resulting from Project-related alterations in hydrology and sediment supply were most likely to be observed. Other important considerations in selecting intensive study sites included maximizing site length and co-locating Study Description GS-S2 sites with sites selected for other related studies (*e.g.*, riparian and instream flow studies), although all sites selected for Study Description GS-S2 met the physical criteria for response reaches discussed above. These study sites represent the range of geomorphic characteristics found in response reaches in the Lower McCloud River, and are the sites most suited for study using the methods outlined in the GS-S2 study description. Other, less-suited potential study sites in the Lower McCloud River are unlikely to provide additional information critical to understanding potential ongoing Project effects on fluvial geomorphology.

4.1.2.2 Bed Texture Study Sites in Lower McCloud River Tributaries

Study sites were also selected in three major tributaries to the Lower McCloud River to map the spatial distribution of bed surface texture and quantitatively describe the grain-size distribution of the mobile bed material supplied to the mainstem of the Lower McCloud River (Figure 1). Major tributaries were delineated by drainage area and geology in an effort to characterize the primary sediment sources to the Lower McCloud River. Three bed texture study sites were located in the Lower McCloud River basin: one in Hawkins Creek, one in Claiborne Creek, and one in Squaw Valley Creek. Results were used to characterize (1) the grain-size distribution of the coarse sediment supply and (2) the bed surface texture where sediment supply and transport are unimpeded by Project operations. Where possible, bed texture study sites were located in tributary response reaches similar in morphology to the intensive study sites located in the Lower McCloud River, and were located in lower reaches of the tributary channels close to the Lower McCloud River confluence.



4.1.3 Study Site Characterization

4.1.3.1 Intensive Study Sites on the Lower McCloud River

The objectives of the intensive study site characterization were to quantitatively describe channel morphology, texture, and grain size. Intensive study sites typically encompassed lengths about 8 to 11 times the bankfull channel width. Although attempts were made to maximize the length of study sites during site selection and field survey, reach endpoints were confined by major changes in slope and channel morphology that changed the potential response to Project operation and violated the assumptions of uniform, steady-state flow necessary for sediment transport modeling. Reach lengths, although shorter than initially targeted, were considered long enough to adequately characterize reach morphology, grain-size distribution, sediment storage, and responsiveness to Project operations.

Three representative cross sections and a long profile of the channel bed and water surface were surveyed at each site. Surveys included identifying location coordinates, standard field indicators, and other appropriate geomorphic characteristics (Harrelson *et al.* 1994). Alluvial coarse sediment storage reservoirs and sediment facies (delineation of the surface bed texture into distinct units by dominant and sub-dominant grain-size classes) were mapped onto aerial photographs at a scale of 1:225 using methods modified from Buffington and Montgomery (1999). Pebble counts (Wolman 1954) were conducted to verify facies mapping and provide roughness parameters at cross sections used in bed mobility analyses. A total of three bulk samples were collected from predominantly gravel-cobble sized alluvial sediment deposits at each site. Submerged bulk samples were collected from sediment patches in flow depths of 2.5 ft or less with an 18-in. diameter McNeil sampler. Bulk samples were collected from subaerial deposits by shoveling gravel from within a square meter sample area marked at the corners. Bulk samples were sieved in the field to 1/2 Φ classes (*i.e.*, 16, 22, 32, 45, 64, 90, 128 mm), Φ classes 11 mm and greater were weighed in the field, and the fraction less than 11 mm underwent laboratory particle-size analysis (Bunte and Abt 2001). Characteristics of the channel bed and banks relevant to channel stability (*e.g.*, bank erosion, aggradation, or degradation) were also noted.

Discharge measurement records collected at the Gage MC-1 cableway near Ah-Di-Na (same as cross-section 2B surveyed at Site 2 during the GS-S2 study) were used to assess long-term changes in bed elevation and channel geometry. The discharge summary notes record the distance from initial position (*i.e.*, stationing) and water depth for each vertical used in the discharge measurement, which can be used to create a historical cross section. Positions created from stationing and water depth measurements taken during high discharge measurements (*i.e.*, when the maximum channel width was inundated) were converted to elevation and distance coordinates using the discharge stage height on the staff plate as a datum and adjusted to tie points (*i.e.*, points that have remained unchanged over time) on the cross section. A total of seven cross section profiles calculated from historical discharge measurements were developed from the following years and flows: 1974 (1,167 cfs), 1978 (6,150 cfs), 1982 (2,050 cfs), 1983 (1,993 cfs), 1986 (6,800 cfs), 2004 (3,400 cfs), and 2006 (2,160 cfs). These data were compared to the cross section survey in 2007 at approximately 200 cfs. Two metrics were used to assess



changes in the channel cross section: (1) change in minimum bed elevation (thalweg), and (2) change in the highest elevation within the low-flow wetted channel (between stations 24–83 ft).

4.1.3.2 Bed Texture Study Sites on the Lower McCloud River Tributaries

The objectives of the bed texture study site characterization were to (1) map bed surface texture and (2) quantitatively describe the grain-size distribution of mobile, alluvial sediment deposits in order to better understand the characteristics of the dominant bedload supply to the Lower McCloud River. Study site lengths were approximately 10–20 bankfull channel widths, depending on the length necessary to adequately characterize reach morphology and grain-size distribution. Data collection at each site was similar to those at intensive study sites and included: (1) measurements of active and bankfull channel widths and water surface slope, (3) mapping of alluvial coarse sediment storage reservoirs and sediment facies, and (4) three bulk samples collected from alluvial sediment deposits. Vegetation in aerial photographs obscured the channel at tributary sites, so the dimensions of storage reservoirs and facies patches were measured with a range finder or tape and tabulated. Bulk samples from bed texture study sites were collected and processed as described above for intensive study sites.

4.2 Results

4.2.1 Classification of Channel Reach Morphology and Response Potential

The Lower McCloud River from McCloud Dam to Squaw Valley Creek is a steep (average gradient 1.25 percent [Figure 10]), confined, and coarse-grained (predominantly boulder and cobble) channel. Local channel gradient varies by channel reach and by channel reach type (Figure 11). Bankfull channel widths are typically 30 to 40 m, and floodplain surfaces are uncommon. Large boulders comprising the channel bed framework are thought to be relict of wetter climate during periods of late Pleistocene glaciation, but may also reflect supply from mass wasting (*e.g.*, shallow streamside landslides and tributary debris flows) and high transport capacity. The boulder and large cobble framework is typically immobile except during large, infrequent floods. The river channel typically maintains low volumes of active sediment storage, although reaches with relatively low stream power and sediment transport capacity store more mobile sediment in association with large roughness elements (*e.g.*, boulders and bedrock outcrops), local backwater effects from channel or valley width contraction, local flow expansion from channel or valley widening, and high local sediment supply relative to local bedload transport capacity. Large wood does not influence channel morphology or sediment storage in the Lower McCloud River, but it does provide habitat complexity along channel margins.

Channel reach morphology in the Lower McCloud River broadly transitions from predominantly step pool upstream of Ah-Di-Na to alternating plane bed and pool riffle downstream of Ah-Di-Na (Figure 12), reflecting an overall decrease in slope and confinement and an increase in mobile sediment supply. Between McCloud Dam and approximately Fitzhugh Creek, average channel gradient is steep (1.72 percent) and the active channel is tightly confined by valley walls, bedrock, and boulders. Channel morphology is predominantly step pool (75 percent of length) separated by plane bed segments (22 percent of length) with boulder substrate. Riffle step



morphology makes up the remainder of the reach (4 percent). A short, steep, and highly bedrock-confined gorge occurs in this reach from approximately 3.1 km to 4.5 km downstream of McCloud Dam. Between Fitzhugh Creek and Ladybug Creek, average channel gradient drops to 1.24 percent, and morphology becomes dominantly plane bed (48 percent of length) and pool riffle (26 percent of reach), with lesser amounts of step pool and riffle step morphology (17 percent and 9 percent, respectively). The channel is confined by valley walls, bedrock, large boulders, and Quaternary river terraces. Large pool tails begin to store the majority of mobile sediment. Average gradient between Ladybug Creek and Bald Mountain Creek increases slightly to 1.31 percent. The dominant channel morphology is distributed equally between pool riffle (44 percent) and plane bed (42 percent of reach), with step pool and riffle step morphologies making up 3 percent and 11 percent of the remaining reach length, respectively. Mobile sediment storage in large pool tails continues to increase. Average gradient between Bald Mountain Creek and Claiborne Creek decreases to 1.04 percent, and channel morphology remains predominantly pool riffle (45 percent of reach) and plane bed (33 percent of reach), with lesser amounts of riffle step (13 percent), riffle bar (6 percent), and step pool (1 percent). Average gradient between Claiborne Creek and Squaw Valley Creek decreases again to 0.83 percent, and channel morphology is predominantly pool riffle (57 percent of reach); with lesser amounts of plane bed (20 percent of reach), riffle step (13 percent) and step pool (10 percent). Downstream of Squaw Valley Creek, channel morphology becomes dominated by very large pools separated by steep, bedrock and boulder controlled steps.

Potentially responsive reaches where morphology and sediment storage are most likely to show Project effects from altered sediment supply and transport are summarized in Table 5. Responsive channel lengths in Table 5 include plane bed, riffle bar, or pool riffle morphology with slopes less than 1.5 percent. Note that 10-m DEM is the best available information for determining channel gradient along the complete length of the Lower McCloud River channel. Channel gradient derived from 10-m DEM data, however, averages actual channel gradient over short channel lengths (<300 m) and may differ from channel gradient measured in the field.



Table 5. Potential response reaches in the Lower McCloud River

Reach	Reach Length (m)	Potential Response Reach Types ^a							
		Pool-Riffle		Riffle-Bar		Plane- Bed		Total	
		Length (m)	Percent of Reach Length	Length (m)	Percent of Reach Length	Length (m)	Percent of Reach Length	Length (m)	Percent of Reach Length
McCloud Dam to Hawkins Creek	1,804	0	0%	0	0%	0	0%	0	0%
Hawkins Creek to Fitzhugh Creek	3,224	0	0%	0	0%	0	0%	0	0%
Fitzhugh Creek to Ladybug Creek	3,392	869	26%	0	0%	43	1%	912	27%
Ladybug Creek to Bald Mt. Creek	2,419	0	0%	0	0%	1,028	43%	1,028	43%
Bald Mt. Creek to Claiborne Creek	8,754	2,929	33%	572	7%	2,609	30%	6,110	70%
Claiborne Creek to Squaw Valley Creek	3,295	1,865	57%	0	0%	674	20%	2,539	77%

^a Potential response reaches include pool riffle, riffle bar, and plane bed channel reach morphology with gradients less than 1.5 percent. Channel gradient is based on 10-m DEM data, and is superseded by more detailed channel surveys at intensive study sites.

4.2.2 Main Stem Intensive Study Sites

The five intensive study sites on the Lower McCloud River are discussed below in consecutive downstream order. Note that the sites 3, 4, and 5 have been renumbered from how they were reported in the Initial Study Report.

4.2.2.1 Site 1

Intensive Study Site 1 is located in Reach 1 (McCloud Dam to Hawkins Creek) about 1.7 km downstream of McCloud Dam (Figures 1 and 10). Few other suitable sites exist in Reach 1. The valley within the reach is developed into Paleozoic metavolcanic bedrock of the Eastern Klamath terrane. Floodplain and terrace surfaces occur only along the left bank at the downstream end of the reach, where incision of the alluvial fan at the mouth of Hawkins Creek has created terraces on which Ash Camp is developed. A footbridge for the Pacific Crest Trail (PCT) crosses the channel within the site (Figure 13); the footbridge is supported by concrete pillars that may alter channel hydraulics during large flood flows. The downstream extent of

field surveys at Site 1 terminate at the Hawkins Creek confluence with the Lower McCloud River. Refer to Attachment 1 for a detailed summary of survey results at Site 1.



The average water surface slope at Site 1 was 0.0135 (Attachment 1, Figure A1-1). The site exhibited step pool morphology upstream of the PCT Bridge and plane bed morphology between the bridge and the Hawkins Creek confluence (Table 6). The channel within the reach had an average bankfull width of 31.2 m (Attachment 1, Figure A1-2) and was confined by stable boulder and bedrock banks and steep valley walls that grade directly into the channel. The average bankfull depth at the cross-sections was 1.5 m and the width-to-depth ratio was 21.5. Hillslopes and channel banks along Site 1 appeared stable. Instability associated with road failure and sidecast from Hawkins Creek Road (Forest Road 38N11) and the access road to Ash Camp was observed directly upstream of the site, however, and is likely the dominant source of angular to subangular gravel and cobble in the reach.

The channel bed surface at Site 1 was dominated by boulder (75 percent of facies area) and cobble (21 percent of facies area) (Table 7, Figure 13). Gravel within the reach was primarily found as a sub-dominant facies; only 2 percent of the reach was gravel dominant. Gravel dominant facies average 17 m² in size and were found in the lee and stoss of large boulders and along the margin of a lateral cobble bar at the upstream end of the reach. Three bulk samples were excavated from the bed within these gravel dominant facies. The D₅₀ of these bulk samples ranged from 10–20 mm and the D₈₄ ranged from 26–55 mm (Attachment 1, Figure A1-3 and Table A1-1). Pebble counts of the surface grain size at the three cross-sections were similar and exemplified a wide range of clasts on the bed surface: D₈₄ was boulder (range 380–500 mm), D₅₀ was large cobble (range 130–150 mm), and D₁₆ was medium sized gravel (range 14–20 mm) (Attachment 1, Figure A1-3 and Table A1-1).

4.2.2.2 Site 2

Intensive Study Site 2 is located in Reach 2 (Hawkins Creek to Ladybug Creek) about 5.5 km downstream of McCloud Dam (Figure 1 and Figure 7). The flow gage at Ah-Di-Na (Gage MC-1, USGS Gage No. 11367800) is located within Site 2, and a cross-section (2B) was established under the cableway at the gaging station (Figure 14). The site was co-located with the gage in order to potentially use historical gage records to assess any long-term changes in bed elevation and channel geometry. The valley within the reach is developed into Paleozoic metavolcanic bedrock within the Eastern Klamath terrane. Valley walls were steep and graded directly into the channel on the left bank, except at Ah-Di-Na Campground, which is developed on a terrace along the right bank in the downstream half of the reach. Refer to Attachment 1 for a detailed summary of survey results at Site 2.

The average water surface slope at the site was 0.0119 (Attachment 1, Figure A1-5), and the reach exhibited plane bed morphology transitioning to step pool morphology downstream of cross-section 2C (Table 6, Figure 14). The channel within the reach had an average bankfull width of 29.7 m (Attachment 1, Figure A1-6) and was confined by stable boulder and bedrock banks. The average bankfull depth for the cross-sections was 1.9 m and the width-to-depth ratio was 16. Field observations indicated that the channel, hillslope, and banks at Site 2 were stable. No evidence of channel aggradation or degradation was observed.



The channel bed surface at Site 2 was dominated by boulder (69 percent of facies area) and cobble (24 percent of facies area) (Table 7, Figure 14). Gravel within the reach was primarily found as a sub-dominant facies; only 6 percent of the reach was mapped as gravel dominant. Gravel was absent, even as a sub-dominant facies, in the majority of the higher energy step pool portions of the site. Nine gravel dominant facies were mapped in the reach, averaging 42 m² in size. Gravel deposits were most prevalent along channel margins, but were also found in velocity shadows downstream of large boulders. Two bulk samples were excavated from the bed within the gravel dominant facies, and contained similar grain-size distributions with D₅₀ ranging from 20–27 mm and D₈₄ ranging from 71–79 mm (Attachment 1, Figure A1-7, and Table A1-2). A third bulk sample (BS2C) was taken from a large gravel-sand bar deposited on the inside channel bend downstream of the long profile extent (Figure 14). This bulk sample had the finest distribution of all bulk samples collected in this study (Figure 15), in large part due to the high content (44 percent) of sand and finer material. This distribution is indicative of an eddy deposit formed during high flow, and may be similar to other large deposits in the Lower McCloud River formed during floods at points with pronounced planform curvature (*e.g.*, the deposit at intensive Study Site 3 where bulk sample BS3c was collected). Pebble counts of the surface grain size at the three cross-sections were similar and exemplified a wide range of clasts on the bed surface; D₈₄ was boulder (range 480–513 mm), D₅₀ was small cobble (range 87–105 mm), and D₁₆ was medium sized gravel (range 15–18 mm) (Attachment 1, Figure A1-7 and Table A1-2).

Comparison of historical cross sections indicates negligible net change in channel geometry or mean bed elevation at the cableway (Site 2, cross section 2B) (Figure 16). Over the historical period analyzed (1974–2006), the total variation in thalweg elevation was 0.8 ft, and the total variation in the highest elevation within the low-flow wetted channel was 1.1 ft (Figure 17). Gravel dominant facies occur on the left channel margin at station distances of 20–40 ft, where the 2006 and 2007 channel bed elevations are approximately 0.5 ft lower than the 1974 and 1986 elevations. The 1986 channel bed is approximately 1.0 ft lower between stations 37–52 and near station 81. Although the historical cross section comparison suggests minor localized bed aggradation and degradation within the low flow wetted channel, these elevation differences are within expected error ranges given the sampling method (discharge equipment measuring water depth from a cableway) applied to a coarse grained (dominantly cobble and boulder) channel that influences where the depth-sounder encounters the bed.



Table 6. Summary of GS-S2 intensive study sites and bed texture study sites

Study Site	Distance from McCloud Dam ^a (km)	Distance from McCloud River Confluence (km)	Reach ^b	Channel Type ^c	Drainage Area ^d (km ²)		Length (m)	Gradient (m/m)	Bankfull Width (m)	Bankfull Depth (m)	Width-to-Depth (W/D)
					Regulated	Unimpaired					
Intensive Site 1	1.7	NA	1	PB, SP	1.7	987	248	0.0135	31.2	1.5	21.5
Intensive Site 2	5.5	NA	2	PB, SP	16.5	1,047	303	0.0119	29.7	1.9	16.0
Intensive Site 3	11.3	NA	3	PB	26.3	1,073	305	0.0074	29.3	2.0	21.0
Intensive Site 4	16.8	NA	3	PB	40.8	1,088	242	0.0094	42.8	1.6	18.1
Intensive Site 5	20.8	NA	4	PB	50.2	1,138	286	0.0043	28.7	1.5	19.7
Hawkins Creek Bed Texture Site	1.9	2.6	1	SP	NA	41.6	207	0.0344	15.1	NA	NA
Claiborne Creek Bed Texture Site	19.3	0.6	3	PB	NA	41.1	91	0.0060	9.3	NA	NA
Squaw Valley Creek Bed Texture Site	22.5	1.5	4	PB, PR	NA	268	198	0.0119	18.7	NA	NA

^a For tributary sites, distance from McCloud Dam denotes the distance along the Lower McCloud River to the tributary confluence.

^b Reach 1 from McCloud Dam to Hawkins Creek, Reach 2 from Hawkins Creek to Ladybug Creek, Reach 3 from Ladybug Creek to Claiborne Creek, Reach 4 from Claiborne Creek to Squaw Valley Creek.

^c Channel reach classification based on Montgomery and Buffington (1997): step pool (SP), plane bed (PB), pool riffle (PR).

^d Drainage area is calculated at the upstream end of study site.



Table 7. Summary of dominant textural facies on the channel bed at intensive study sites

Dominant Facies	Site 1			Site 2			Site 3			Site 4			Site 5		
	Area (m ²)	% of Area	D ₅₀ ^a (mm)	Area (m ²)	% of Area	D ₅₀ ^a (mm)	Area (m ²)	% of Area	D ₅₀ ^a (mm)	Area (m ²)	% of Area	D ₅₀ ^a (mm)	Area (m ²)	% of Area	D ₅₀ ^a (mm)
Bedrock	109	2	NA	71	1	NA	0	0	NA	0	0	NA	280	4	NA
Boulder	4,532	75	296	4,261	69	264	4,895	77	244	2,295	34	260	4,098	65	225
Cobble	1,276	21	146	1,468	24	91	584	9	180	4,409	65	111	1,487	24	116
Gravel	133	2	15	376	6	26	797	12	25	85	1	21	415	7	27
Sand	0	0	NA	0	0	NA	109	2	NA	0	0	NA	0	0	NA
Total	6,050	100	NA	6,176	100	NA	6,385	100	NA	6,789	100	NA	6,280	100	NA

^a D₅₀ is the median grain size estimated for the specified dominant facies at the site.



4.2.2.3 Site 3

Intensive Study Site 3 is located about 11.3 km downstream of McCloud Dam immediately downstream of Bald Mountain Creek in Reach 3 (Ladybug Creek to Claiborne Creek)(Figure 1 and Figure 7). Site 3 is located in a straight reach and is predominantly plane bed morphology with a large pool at the upstream end of the reach (Figure 18). The valley within the reach is developed into Paleozoic metavolcanic bedrock within the Eastern Klamath terrane. The left channel bank was bordered by a terrace 7.2 m above the thalweg at cross-section 3C. Floodplain indicators of recent alluvial activity were not observed on the terrace surface. Refer to Attachment 1 for a detailed summary of survey results at Site 3.

Average water surface slope was 0.0074 (Attachment 1, Figure A1-8). The three cross-sections were located in the plane bed portions of the reach (Attachment 1, Figure A1-9). The reach had an average bankfull width of 29.3 m and depth of 1.5 m, which results in a width-to-depth ratio of 20 (Table 6). The reach was confined by coarse substrate and bedrock banks. Much of the right channel bank was formed in bedrock with minimal vegetation, and similar bedrock controlled channel banks are prevalent upstream and downstream of Site 3. Small areas of bedrock also outcropped in the thalweg of this reach and likely function as gradient control. Site 3 appeared stable, and no evidence of channel aggradation or degradation was observed.

The channel bed surface at Site 3 was dominated by boulder (77 percent of facies area) (Table 7, Figure 15). Gravel and cobble dominated facies were found in similar proportions at Site 3 (12 percent and 9 percent by area, respectively). Gravel dominated facies were primarily associated with the large pool at the upstream end of the reach and as part of a lateral gravel and sand bar deposited in a high flow eddy environment adjacent to the pool thalweg. This lateral bar extended downstream into the pool tail-out as a lobe of mobile gravel from which one bulk sample (BS3B) was excavated. Two additional bulk samples were excavated just beyond the extent of the long profile survey: one upstream in a pool tail-out that stored a significant volume of mobile sediment (BS3A), and another downstream in a large cobble and gravel bar deposited on the inside of a sharp channel bend (BS3C) (Figure 18). Bulk sample BS3C was finer than the other samples at Site 3. The three bulk samples were almost entirely gravel; the D_{10} through D_{90} was in the gravel range and diverged from the bulk sample distributions found at the two adjacent intensive study sites (sites 2 and 4), where the D_{84} was typically small cobble or larger (Figure 15; Attachment 1, Figure A1-10 and Table A1-3). Pebble counts of the surface grain size at the three cross-sections showed a coarsening downstream with distance away from mobile sediment stored in the pool. These surface pebble counts depicted a wide range of clasts on the bed surface; D_{84} was very large cobble to boulder (range 235–310 mm), D_{50} was very coarse gravel to medium cobble (range 50–125 mm), and D_{16} was medium sized gravel (range 14–20 mm) (Attachment 1, Figure A1-10 and Table A1-3).

4.2.2.4 Site 4

Intensive Study Site 4 is located in Reach 3 (Ladybug Creek to Claiborne Creek) about 16.8 km downstream of McCloud Dam and 2.5 km upstream of Claiborne Creek (Figure 1 and Figure 7). The valley within the reach is developed into Paleozoic metavolcanic bedrock within the Eastern



Klamath terrane. The reach was confined on both banks by steep valley walls extending to the bankfull channel margins. Refer to Attachment 1 for a detailed summary of survey results at Site 4.

Site 4 is located in a straight reach with plane bed morphology and an average water surface slope of 0.0094 (Figure 19; Attachment 1, Figure A1-11). The three cross-sections had an average bankfull width of 42.8 m and depth of 2.0 m, which results in a width-to-depth ratio of 21 (Table 6, Attachment 1 Figure A1-12). Although bankfull width and depth values at Site 4 were the highest measured at any intensive study site, the width-to-depth ratios at Site 4 were similar to other study sites. The channel at Site 4 appeared stable, with no evidence of channel aggradation or degradation. Shallow landslides and slumps were observed, however, at several locations along the left valley toeslope.

The channel bed surface at Site 4 was dominated by cobble (65 percent of facies area) and boulder (34 percent of facies area) (Table 7, Figure 19). Site 4 was the only intensive study site where boulder dominant facies did not occupy the greatest area. Gravel dominant facies, however, were small in Site 4, averaging about 11 m² in area and occupying only about 1 percent of the total facies area. Gravel dominant facies were found in the lee of large boulders and along the channel margin. Two bulk samples were collected from lee deposits downstream of large boulders within the reach, and an additional bulk sample (BS4A) was excavated from a pool tail upstream of the extent of the long profile survey (Figure 19). The pool tail sample was the coarsest of the three samples and the coarsest bulk sample collected from any study site (Figure 15). Pebble counts of the surface grain size at the three cross-sections depicted a wide range of clasts on the bed surface; D₈₄ was boulder (range 332–513 mm), D₅₀ was large cobble (range 137-180 mm), and D₁₆ was medium to coarse gravel (range 12–27 mm) (Attachment 1, Figure A1-13 and Table A1-4). On average, surface pebble counts at Site 4 had the coarsest distributions of any study site, which coupled with the sediment facies results, indicates a higher percentage of immobile material (large cobble) and less gravel than at other study sites.

4.2.2.5 Site 5

Intensive Study Site 5 is located in Reach 4 (Claiborne Creek to Squaw Valley Creek) about 20.8 km downstream of McCloud Dam and 1.5 km downstream of Claiborne Creek (Figure 1, Figure 7). The valley within the reach is developed into Paleozoic metavolcanic bedrock within the Eastern Klamath terrane. Refer to Attachment 1 for a detailed summary of survey results at Site 5.

Site 5 was characterized as plane bed morphology with an average water surface slope of 0.0043 (Table 6, Figure 20, Attachment 1 Figure A1-14). The three cross-sections had an average bankfull width of 29.3 m and depth of 1.5 m, which results in a width-to-depth ratio of 20 (Table 6, Attachment 1 Figure A1-15). Bedrock outcrops in the channel bed and on the left bank, as well as Quaternary terraces confined both sides of the channel. The right bank terrace exhibited at least 3 distinct elevation benches, the lower of which measured 4.3 m above the thalweg at cross-section 5B. Debris trapped against trees at this elevation indicated periodic flood inundation. A left bank terrace parallels the downstream half of the site and occurred at a higher



elevation above the channel than the right bank terrace, measuring 7.6 m above the thalweg at cross-section 5C. No evidence of channel aggradation or degradation was observed. A small, shallow landslide was observed on the left bank, although sediment delivery from the slide to the channel was impeded by bedrock outcrops.

The channel bed surface at Site 5 was dominated by boulder (65 percent of facies area) and cobble (24 percent of facies area) (Table 7, Figure 20). Gravel dominant facies occupied only 7 percent of the reach, but gravel deposits occurred along the channel margin and in the lee and stoss of large boulders. Two bulk samples were excavated from the bed within the larger gravel dominant facies patches along the channel margin. Both bulk samples had similar gravel-sized distributions, with D_{50} of 18 and 20 mm (Figure 15; Attachment 1 Figure A1-16 and Table A1-5). Pebble counts of the surface grain size at the three cross-sections were nearly identical at cross-sections 5A and 5B, while cross-section 5C was slightly finer (Attachment 1 Figure A1-16). The grain-size distributions at the cross sections exhibited a wide range of clasts on the bed surface; D_{84} was boulder (range 260–430 mm), D_{50} was large cobble (range 113–135 mm), and D_{16} was medium to coarse gravel (range 15–27 mm) (Attachment 1, Figure A1-16 and Table A1-5).

4.2.3 Tributary Bed Texture Study Sites

Bed texture study sites were selected in the three largest tributaries to the Lower McCloud River: (1) Hawkins Creek, (2) Claiborne Creek, and (3) Squaw Valley Creek.

4.2.3.1 Hawkins Creek

Hawkins Creek enters the Lower McCloud River 1.9 km downstream of McCloud Dam (Figure 1 and Figure 7). Hawkins Creek has a drainage area of 41.6 km² and is sourced primarily in metasedimentary and metavolcanic rocks within the Eastern Klamath terrane, as well as some older volcanic rocks in the Western Cascades terrane (Figure 2). The bed texture site in Hawkins Creek was located 2.6 km upstream of the Lower McCloud River confluence to avoid the steep channel gradient (> 0.04) in the immediate vicinity of the Lower McCloud River and to avoid disturbance related to tunnel construction and spoil. The channel within the Hawkins Creek site exhibited typical step pool morphology with very coarse boulder framework. Channel gradient was approximately 0.0344 and average bankfull width was 15.1 m (Table 6). The only mobile deposits in the reach were forced by large roughness (*i.e.*, large boulders). The three bulk samples excavated from Hawkins Creek had the finest grain-size distributions of any tributary study site (Figure 21; Attachment 1, Figure A1-17 and Table A1-6). Bulk samples from Hawkins Creek were almost entirely gravel, with 10–23 percent of the material less than 2 mm (*i.e.*, sand or finer); D_{50} of the bulk samples ranged from 8 to 13 mm.

4.2.3.2 Claiborne Creek

Claiborne Creek enters the Lower McCloud River 19.3 km downstream of McCloud Dam (Figure 1 and Figure 7). Claiborne Creek has a drainage area of 41.1 km² and is sourced primarily in metasedimentary rock within the Eastern Klamath terrane (Figure 2). The bed texture site in Claiborne Creek was located 0.6 km upstream of the Lower McCloud River



confluence in a relatively low gradient (0.006) reach with plane bed morphology. The average bankfull width was 9.3 m (Table 6). The channel was narrowly entrenched approximately 2.5–3.0 m within Holocene and Quaternary river terrace deposits. Mobile sediment deposits in the reach were associated with planform curvature and a large woody debris jam. Two bulk samples were excavated from Claiborne Creek, both with relatively uniform grain-size distributions trending towards the coarser range of the tributary bulk samples (Figure 21). Sample CB2 ranged from 2 to 180 mm with a D_{50} of 23 mm, and sample CB3 ranged from 2 to 90 mm with a D_{50} of 19 mm (Attachment 1, Figure A1-18 and Table A1-7).

4.2.3.3 Squaw Valley Creek

Squaw Valley Creek enters the Lower McCloud River 22.5 km downstream of McCloud Dam and is the largest tributary to the Lower McCloud River (drainage area 268 km²). Sediment production from the High Cascades terrane in the upper Squaw Valley Creek watershed, however, is disconnected from the lower basin (Figure 1). The majority of the connected portion of the Squaw Valley Creek basin drains metasedimentary and metavolcanic rock within the Eastern Klamath terrane (Figure 2). The bed texture site in Squaw Valley Creek was located 1.5 km upstream of the Lower McCloud River confluence and directly downstream of Tom Dow Creek, the most downstream large tributary in the Squaw Valley Creek basin. The channel within the Squaw Valley Creek site was classified as plane bed and pool riffle morphology with a channel gradient of 0.0119 and average bankfull width of 18.7 m (Table 6). Two of the three bulk samples collected at the site (SV1 and SV2) were strongly unimodal and had a high percentage of grains in the 11–22 mm range (Figure 21; Attachment 1, Figure A1-19 and Table A1-8). The third bulk sample (SV3) was more uniformly distributed between 2 and 180 mm. D_{50} of the two strongly unimodal deposits was 15–16 mm, while the D_{50} of SV3 bulk sample was 34 mm. All Squaw Valley Creek bulk samples contained less than 8 percent sand or finer material, which was a smaller fraction of fine material than found at the other tributary bed texture sites.

5 BED MOBILITY AND BEDLOAD TRANSPORT

The amount of bed material transport and the residence time of bed material in a channel reach strongly influence the potential effects of reducing sediment supply on channel form and aquatic habitat. The objectives of this component of the study were to (1) evaluate critical discharges that mobilize the channel bed, (2) estimate coarse (>2 mm) bedload transport capacity, (3) determine bedload grain-size distributions in Project-affected reaches, and (4) assess potential effects of Project operation on the frequency and magnitude of sediment transport.

5.1 Methods

5.1.1 Tracer Rock Studies

To evaluate flows at which the bed is initially mobilized and to calibrate reference Shields stress used for sediment transport modeling (Attachment 2), approximately 20–30 tracer rocks with grain size ranging from small cobble (64 mm) to coarse cobble (180 mm) were placed within the



bankfull channel at two of the three cross sections at each intensive study site. Three size classes were each painted a different color to facilitate recognition of selective mobility: rocks 64–90 mm were painted purple, rocks 90–128 mm were painted yellow, and rocks 128–180 mm were painted blue. This range encompassed the surface D_{50} at all cross sections. Cross sections were selected for tracer deployment based on their suitability for monitoring and numerically modeling sediment transport. Generally, one cross section per intensive study site was unsuitable for sediment transport monitoring and modeling due to large roughness, bedrock exposure, or other factors that substantially complicate assumptions regarding normal flow used in sediment transport modeling. Tracer rocks were placed in a line along the cross section by removing a particle from the bed, placing a tracer rock of similar size in the same location, and pushing the rock slightly into the bed to emulate natural particle packing and embeddedness. Locations of tracer rocks along the cross section and the distance upstream or downstream of the cross-section line were documented to determine the direction and extent of movement during high flow events. Tracer rocks were considered mobilized if they moved at least 1 m (Haschenburger and Wilcock 2003). A total of 253 tracer rocks were placed at 10 cross-sections (*i.e.*, 2 cross sections at 5 sites) in November 2007. Tracer rocks at cross sections were resurveyed to determine the amount and direction of movement following relatively high flow events during Water Year 2008 (456 cfs on January 4, 2008 and 1,382 cfs on May 19, 2008).¹ In addition to the 64-180 mm tracer rocks deployed along cross sections, 32-90 mm tracer rocks were deployed on mobile sediment patches at intensive study sites. Tracer rocks were deployed on mobile sediment patches following the peak spill of 1,382 cfs that occurred on May 19, 2008 and prior to the release of 617 cfs on June 17, 2008 for Study Description FA-S8, *Instream Flow Evaluation on the Lower McCloud River*. The smaller tracer rocks deployed on patches were used to evaluate initial mobility of mobile coarse sediment deposits characteristic of those documented in the sediment storage analysis (Section 6 of this technical memo) and bulk sampled at study sites.

5.1.2 Flow Frequency and Duration Analyses

As part of Study Description WR-S1, *Unimpaired Hydrology Development*, long-term synthetic hydrologic flow records were developed for regulated and unimpaired conditions at intensive study sites and bed texture study sites in the Lower McCloud River. Summation uses mass balance equations (*e.g.*, change in reservoir storage equals inflow minus outflow) for all points where gaging station records and/or observer's reports were available. The summation method also assimilates stream flow gage data from contributing drainage areas and accounts for losses from diversion flows. The proration method estimates daily, unimpaired flows for a given watershed of interest based on unimpaired flow data in a similar (reference) watershed. Unimpaired flow data in the reference watershed are then prorated to the watershed of interest by applying a drainage area ratio factor. The long-term gaging records at MC-1 (USGS Gage No. 113367800 McCloud River at Ah-Di-Na) and MC-5 (USGS Gage No. 11368000 McCloud River above Shasta Lake) were also used to calculate the synthetic discharge records by prorating the differences in flow based on a drainage area ratio factor. Accretion to the channel is assumed to

¹ Discharges are peak flows recorded by Gage MC-1 at Ah-Di-Na.



be positive and is estimated based on contributing area. Refer to TM-46, *Unimpaired Hydrology Development* (PG&E 2009a) for a more detailed discussion of hydrology methods.

Synthetic discharge records for the Lower McCloud River were calculated for the upstream end of all intensive study sites and bed texture study sites using the methods described above. From these synthetic flow records, annual flow duration curves under regulated and unimpaired hydrologic conditions were generated for all intensive study sites. Recurrence intervals of peak flows assuming Log-Pearson Type III distributions were calculated for annual maximum daily discharges from synthetic hydrologic records. Note that recurrence intervals for peak flows are typically calculated for annual instantaneous peak discharges recorded at long-term gaging stations, but due to the synthetic nature of the hydrology data, only annual maximum daily discharges were available for recurrence interval calculations.

5.1.3 Modeling Bed Mobility Thresholds and Bedload Transport Capacity

The Enhanced Acronym Series with Interface (EASI) model, which implements Parker's surface-based sediment transport equation (Parker 1990a,b), was applied to each intensive site to estimate surface-based dimensionless Shields stress (τ_{sg}^*), critical discharges (Q_{cr}) to mobilize the channel bed, coarse (> 2 mm) bedload transport capacity, and bedload grain-size distributions. The model input parameters include channel cross-section data, water surface slope, grain-size (channel roughness) data for either the channel surface substrate or bedload supply, and current or reference annual flow duration curves (refer to Attachment 2 for model documentation). The model output parameters include Shields stress versus discharge rating curves, average annual bedload transport capacity, and grain-size distributions of either the bedload supply or channel surface (depending on whether the input parameter was surface or bedload supply grain size). All sediment transport modeling used in this study assumes normal (uniform and steady-state) flow. Sediment density was assumed to be $2,650 \text{ kg m}^{-3}$ (refer to Attachment 2 for additional model assumptions). Coarse sediment bedload transport capacities are estimated for regulated and unimpaired scenarios, where the flow duration curve is the only variable changed between the scenarios. Thus, the unimpaired scenario assumes that channel geometry, channel gradient, and grain size data measured in 2007 is applicable to pre-dam conditions.

The sediment transport equations used in this study require a reference Shields stress (τ_r^*) that corresponds to where the dimensionless bedload transport rates (W^*) of different sized fractions collapse to a single, constant low value, referred to as the reference transport rate (e.g., Parker 1990a,b; Wilcock and Crowe 2003). Parker (1990a,b) and this study use a $W^* = 0.00218$ as the reference transport rate. A reference Shields stress can be viewed as a parameter similar to a critical Shields stress because the bedload transport equation used in the EASI model (Parker 1990a,b) is constructed such that bedload transport rates quickly approach zero when local Shields stress drops below the reference Shields stress. This is similar to the concept of a critical Shield stress where zero transport occurs at local Shield stresses below the critical value. Reference Shield stresses in this study were determined from tracer rock studies and from published values. In particular, the τ_r^* and channel gradient relationship developed by Mueller *et al.* (2005), which was based on field measurements of discharge and bedload transport in 45



gravel-bed streams, was used in this study. Model coefficients (*i.e.*, references Shield stress and roughness values) were also calibrated to results from the tracer rock studies (see section 5.2.1).

A friction factor correction was used in the sediment transport modeling for this study due to the abundance of large roughness elements on the channel bed in the Lower McCloud River. Large, relatively immobile grains in mountain stream channels consume a significant portion of the total shear stress, thereby reducing the stress available for transporting finer, mobile sediment. This process can lead to over prediction of sediment flux (Yager *et al.* 2007). The friction factor correction was calculated by partitioning the grain size distribution (determined from pebble counts of the surface material at each cross-section) into a mobile fraction (< 256 mm) and immobile fraction. For the mobile fraction, a grain roughness was calculated based on the geometric mean and standard deviation of the mobile size distribution (see Attachment 2 for equations and details). A separate roughness for the entire channel was determined based on published relations for friction factors in steep, coarse-grained streams (see Attachment 2 for details) and from roughness values calculated from stage-discharge observations at the sediment transport modeling cross-sections which were surveyed as part of Study Description BR-S4 (see TM-65, *Assess Ongoing Project Effects on Riparian Vegetation Community Types in the Project Area* [PG&E 2009b]). The range of main channel roughness values calculated from these two methods were used to bracket a high and low bedload mobility threshold and bedload transport capacity (see Attachment 2 for details). Using a ratio of the mobile roughness value to the entire channel roughness, the effective grain stress flow depth for the mobile sediment fraction was calculated and then used to determine a mobile grain shear stress. Because the mobile grain size roughness is less than the main channel roughness value at the intensive study sites, the shear stress available for transporting mobile grains is less than the total boundary shear stress at each cross-section.

5.2 Results

5.2.1 Tracer Rock Studies

On February 13, 2008, a helicopter was used to survey movement of tracer rocks deployed along cross sections at intensive study sites. Three relatively low magnitude flood events occurred between the time tracer rocks were deployed and the field effort on February 13. Peak discharge for the three events occurred on January 4, 2008, and was approximately 456 cfs at Gage MC-1 near Ah-Di-Na and 4,467 cfs at Gage MC-5 above Shasta Lake. The helicopter was unable to land during the field effort at study sites due to vegetation, wind, and snow cover. Tracers were observed while hovering approximately 50–100 ft above the water surface. Nearly all of the tracer rocks were observed in their original locations. The few tracer rocks not accounted for during the field effort were of the smallest size class (64–90 mm) and were unrecognized in only the deepest thalweg sections where turbulence and boulders obscured a clear view of the channel bed from the air. Results indicated that the bed at the five intensive study sites was immobile during the January 4, 2008 flow event. No additional natural flow events of equal or greater magnitude occurred on the Lower McCloud River during the 2008 winter storm season.



Flows of 800 cfs and 1,000 cfs released for Study Description FA-S8, *Instream Flow Evaluation on the Lower McCloud River*, and Study Description RL-S3, *Lower McCloud River Recreational Flow Study*, during early May 2008 provided additional opportunity for mobilization of tracer rocks. Attempts were made to observe tracer rocks during flows of approximately 800 cfs and 1000 cfs at Sites 1, 2, 3, and 5; but water depth and velocity, turbulence, and turbidity prohibited an accurate account of rock mobility during these flow events. Shortly after these managed flow releases, uncontrolled spills to the Lower McCloud River resulted in a peak discharge of 1,382 cfs at Gage MC-1 near Ah-Di-Na on May 19, 2008. Tracer rocks were resurveyed by ground at all sites on May 27, 2008. Movement based on surveys following the 1,382 cfs peak flow on May 19, 2008 is summarized in Table 8. Results indicate that the 64–128 mm grain sizes began mobilizing at flows less than or equal to the 1,382 cfs peak at Site 1, and to a lesser degree at Site 2. The small percentage of mobilized tracer rocks suggests that the 1,382 cfs peak flow was near the threshold of bed mobility at these sites. Few tracer rocks were mobilized at intensive study sites 3, 4, and 5 during this flow event, and the small percentage that did move (8.3 percent) were all in the 64–90 mm size class. These results suggest that the flow event did not exceed the threshold of bed mobility at these sites.

The 32-90 mm rocks deployed on mobile patches at Sites 1, 2, 3, and 5 during late May, 2008 were resurveyed by ground during the first week in July, 2008 after a peak discharge of 617 cfs at Ah-Di-Na on June 17, 2008. No movement was observed, although small amounts of fine and medium gravel (4–16 mm) were deposited on and around tracer rocks at Site 2 and Site 3. These results suggest that the 617 cfs flow did not exceed the threshold of mobility for any mobile sediment patches at intensive study sites.



Table 8. Summary of tracer rock mobility at intensive study sites during the period November 2007–July 2008

	Size of Rocks Deployed at Cross Sections ^a			Size of Rocks Deployed on Mobile Patches ^b		
	64–90 mm	90-128 mm	128–180 mm	32–64 mm	64–90 mm	64–90 mm
Site 1						
Rocks Deployed	21	20	12	33	0	0
Discharge (cfs)	1,382	1,382	1,382	617	617	617
Rocks Mobilized	12	5	0	0	0	0
Site 2						
Rocks Deployed	26	30	18	54	18	0
Discharge (cfs)	1,382	1,382	1,382	617	617	617
Rocks Mobilized	5	8	0	0	0	0
Site 3						
Rocks Deployed	20	20	8	63	10	2
Discharge (cfs)	1,382	1,382	1,382	617	617	617
Rocks Mobilized	1	0	0	0	0	0
Site 4						
Rocks Deployed	20	20	8	65	19	3
Discharge (cfs)	1,382	1,382	1,382	617	617	617
Rocks Mobilized	1	1	0	0	0	0
Site 5						
Rocks Deployed	20	20	12	65	19	0
Discharge (cfs)	1,382	1,382	1,382	617	617	617
Rocks Mobilized	3	0	0	0	0	0

^a All 64–180 mm rocks were deployed at cross sections during November, 2007. All sites were resurveyed by helicopter on February 13, 2008 after a peak discharge of 456 cfs at Ah-Di-Na on January 4, 2008, at which time, no movement was observed. All sites were resurveyed by ground on May 27–29, 2008 after a peak discharge of 1,382 cfs at Ah-Di-Na on May 19, 2008. Movement resulting from this flow is summarized in the table.

^b All 32–90 mm rocks were deployed on mobile patches during late May, 2008. Sites 1, 2, 3, and 5 were resurveyed by ground during the first week in July 2008 after a peak discharge of 617 cfs at Ah-Di-Na on June 17, 2008, at which time, no movement was observed.

5.2.2 Flow Frequency and Duration Analyses

Differences between the regulated and unimpaired hydrologic regimes at the five intensive study sites on the Lower McCloud River are greater at sites closer to McCloud Dam and are more pronounced at lesser discharges (*i.e.*, higher exceedance probabilities of the daily flow series)



(Figures 22). Flow increases monotonically in the downstream direction from Site 1 to Site 5, and the primary flow accretions between study sites are from tributary input, which is most pronounced during high flow events. The median flow (50 percent exceedance probability) for the regulated period of record ranged from 174 cfs at Site 1 to 243 cfs at Site 5. For comparison, median flow for the unimpaired record ranged from 930 cfs at Site 1 to 1,007 cfs at Site 5, an 81 percent reduction at Site 1 and 76 percent reduction at Site 5, respectively (Figure 22). The percent reduction in flow remains consistently high (>75 percent reduction) for all exceedance probabilities >15 percent (Figure 23). At less frequent, higher magnitude flows (*i.e.*, exceedance probabilities <15 percent), the percent reduction begins to decrease and at the highest flows (0.1 percent exceedance probability), the percent reduction ranges from 24 percent at Site 1 to 21 percent at Site 5.

The shape and slope of an annual flow exceedance curve is an indicator of hydrologic variability within a system. A relatively flat exceedance curve, for example, illustrates limited average annual flow variance. Flow exceedance curves for intensive study sites illustrate a relatively stable flow regime under unimpaired conditions with little variability between 20 percent and 90 percent exceedance probabilities, and even less variability in this range for the regulated flow regime (Figure 22). Limited flow variability in the Lower McCloud River for *unimpaired* conditions in large part can be attributed to the relatively high year-round baseflow from spring-fed groundwater contributions originating in the upper watershed, and in the *regulated* conditions from relatively constant minimum flow releases from McCloud Dam. Primary tributaries to the study reach show significantly more flow variability, with distinct differences between median, high, and base flow periods (Figure 24). Discharges from major tributaries are the primary driver for differences in high flows (exceedance probabilities < 10 percent) between study sites (Figure 22). Differences in high flows between Site 1 and 2, for example, can be attributed to Hawkins Creek. However, significant tributary contribution to mainstem flow is limited to periods associated with precipitation events, and tributary high flows are generally not sustained for extended periods in the Lower McCloud River (Figure 23). For regulated flow exceedance probabilities <20 percent, Squaw Valley Creek contributes similar flow magnitudes as the mainstem of the Lower McCloud River at Site 5 (*i.e.*, regulated flow approximately doubles downstream of the Squaw Valley Creek confluence during higher flows).

Recurrence intervals of peak flows illustrate a similar pattern as the flow exceedance analysis: reductions in recurrence intervals under regulated conditions are highest at sites near the dam and are more pronounced for the more frequent, small return period peak flows (Table 9, Attachment 3). A 2-year return interval flow under regulated conditions is less than or equal to a 1.2-year return interval flow under unimpaired conditions. A 2-year flow under regulated conditions ranges from 1,040 cfs at Site 1 to 2,800 cfs at Site 5 compared to 3,380 cfs and 5,210 cfs under unimpaired conditions, respectively. The reduction in return interval flows from regulated to unimpaired conditions at Site 1 ranges from 77 percent for a 1.5-year flow to 20 percent for a 10-year flow. At Site 5, the reduction ranges from 54 percent for a 1.5-year flow to 14 percent for a 10-year flow (Table 9). For the 33 years of record used in the analysis, the unimpaired peak flow was higher for all years except water years (WY) 1974 and 1997 (Figure 25). The highest flow over the period of synthetic record occurred during WY 1997, which is the primary reason the regulated 50-year return interval flow is listed as greater than the unimpaired 50-year return



interval flow in Table 9. Because this is primarily based on one peak flood, it is insufficient to conclude that very large return interval flows have increased under the regulated flow regime.

Table 9. Summary of peak flow recurrence interval based on the annual maximum daily flow for regulated and unimpaired conditions

	Peak Flow (cfs) for Specified Return Period (years [y])					
	1.2 y	1.5 y	2 y	5 y	10 y	50 y
Site 1						
Regulated	260	560	1,040	3,610	7,040	21,900
Unimpaired	1,690	2,480	3,380	6,300	8,780	15,900
% Difference ^a	85	77	69	43	20	-38
Site 2						
Regulated	500	960	1,660	4,920	8,760	23,800
Unimpaired	2,030	2,990	4,090	7,600	10,530	18,700
% Difference ^a	75	68	59	35	17	-27
Site 3						
Regulated	640	1,190	1,980	5,500	9,470	24,400
Unimpaired	2,180	3,220	4,410	8,190	11,320	20,000
% Difference ^a	71	63	55	33	16	-22
Site 4						
Regulated	720	1,320	2,170	5,840	9,890	24,700
Unimpaired	2,220	3,330	4,590	8,720	12,230	21,900
% Difference ^a	68	60	53	33	19	-13
Site 5						
Regulated	990	1,760	2,800	7,000	11,340	26,300
Unimpaired	2,550	3,790	5,210	9,620	13,230	23,000
% Difference ^a	61	54	46	27	14	-14

^a % difference is calculated as the change from unimpaired to regulated conditions.

5.2.3 Bed Mobility Thresholds and Bedload Transport Capacity

Bed mobility thresholds and bedload transport capacities are a function of channel slope, channel geometry, grain size distributions of the channel surface, bed material, and sediment supply. Discharge frequency is also a factor controlling average annual transport capacities. The primary variable controlling differences in bed mobility and transport capacity estimates at intensive study sites is channel slope, which follows a downstream decreasing continuum that ranges from



0.0135 at Site 1 to 0.0043 at Site 5 (Table 6). Changes in channel geometry between sites are modest, as illustrated by (1) the relatively consistent bankfull widths and depths between sites (Table 6), (2) the dominantly coarse (boulders and cobbles with ≤ 12 percent gravel by facies area) surface grain size distributions at all sites (Table 7), and (3) the consistent range in grain size of subsurface bulk samples collected from mobile sediment patches (Figure 15 and Attachment 1). Although discharge increases in the downstream direction, the increases are modest at all sites upstream of Squaw Valley Creek, the primary tributary flow input to the Lower McCloud River (Figure 22). Thus, bedload mobility thresholds and annual average coarse sediment (>2 mm) transport capacities at the intensive study sites reflect the decreasing downstream slope continuum and have the following trends: (1) bedload transport capacities generally decrease with distance downstream and (2) threshold discharges for bed mobility increase with downstream distance (Figures 24a and 25a).

Annual average coarse sediment bedload transport capacities under both regulated and unimpaired flow regimes peak at Site 2 (17,800 t yr⁻¹ and 54,700 t yr⁻¹ for regulated and unimpaired flow, respectively) and then decline downstream until they reach a minimum at Site 5, where the rates are about half the capacity estimated at Site 2 (Table 10 and Figure 26a). Sediment transport capacities under the regulated flow regime are reduced at all sites relative to the unimpaired flow regime. Reductions in transport capacities are higher at sites near the dam (70 percent at Site 1) and decrease with distance downstream (51 percent at Site 5) primarily due to increased tributary flow input with downstream distance. Bedload transport capacities at specific discharges also follow a general decreasing trend in the downstream direction, although Site 1 and Site 2 show similar capacities per discharge, as do Site 3 and Site 4 (Figure 26b). Significant bedload transport capacity (estimated at rates $>1,000$ t day⁻¹ based on the order of magnitudes of the annual average transport capacity and coarse sediment supply) begins at around 2,500 cfs for Site 1 and Site 2, at 3,500 cfs for Site 3 and Site 4, and at 4,400 cfs for Site 5.

Estimated bed mobility thresholds are based on where normalized Shield stresses equal 1 (see Attachment B for details). As described in section 5.2.1, tracer rock observations indicated that bed mobilization initiated at a discharge of 1,382 cfs or less at Site 1 and Site 2, but did not initiate at this discharge at sites further downstream. Initial model results predicted similar boundaries for bed mobilization as observed with the tracer rocks at all sites except Site 2, where slight calibrations to the model were made based on tracer observations. Bed mobility thresholds indicate an increase in the discharge required for mobility with increasing distance downstream, with bed mobilization occurring at 1,030 cfs at Site 2 and at 2,060 cfs at Site 5 (Table 10 and Figure 27). Due to the high frequency of large roughness elements on the channel bed in the Lower McCloud River that creates significant divergence in the stress fields (*i.e.*, localized areas of high and low velocities and shear stress), bed mobility thresholds likely vary considerably within a reach as indicated by the region of bed mobility in Figure 27b. Initial mobilization of more mobile sediment patches in most locations occurs at flows > 620 cfs based on tracer observations, and may occur at the lower range of the region of bed mobility in Figure 27b. The EASI model that utilizes Parker's (1990a, b) surface based bedload transport equations is able to predict the bedload grain size at a site. This predicted bedload grain size distribution is dependent on the input surface grain size distribution, which in this study was truncated at 256



mm to reflect the population of mobile grains (see section 5.1.2). Comparing the predicted bedload grain size distributions with bulk samples of mobile material shows similar ranges of grain size distributions at all of the sites, except for Site 5, where the predicted bedload distribution is coarser by about a factor of 2 (Attachment 4). This implies the model is reasonably simulating the transport of the more mobile sediment sampled in the field, which was the objective of partitioning the bed into mobile and immobile grain sizes and calculating stresses specifically available for transporting the mobile fraction (see section 5.1.2 and Attachment 2).

Table 10. Estimated average annual coarse sediment transport capacity and bed mobility thresholds at intensive study sites

Site	Distance Downstream of McCloud Dam (km)	Slope (%)	Regulated Flow			Unimpaired Flow			Bed Mobility Threshold Q (cfs)		
			Average Annual Coarse Sediment Transport Capacity (t y-1)								
			Low	Middle	High	Low	Middle	High	Low	Middle	High
Site 1	1.71	1.35	8,889	12,072	17,423	24,825	40,906	72,651	750	1,130	1,490
Site 2	5.49	1.19	12,045	17,813	27,627	32,072	54,719	96,868	862	1,175	1,515
Site 3	11.33	0.74	10,603	14,149	20,380	22,312	32,906	55,545	1,050	1,460	1,825
Site 4	16.77	0.94	7,510	10,857	15,764	15,854	25,514	42,357	1,350	1,734	2,175
Site 5	20.78	0.43	6,893	8,970	10,993	13,242	18,122	23,192	1,813	2,060	2,415

6 SEDIMENT STORAGE

The quantity and time that coarse alluvial sediment (*e.g.*, gravel and cobble) is stored in a channel reflects the mass balance between coarse sediment supply and bedload transport. A reduction in coarse sediment supply with little change in the frequency and duration of effective discharges that transport bedload can force a coarse sediment deficit in responsive reaches, potentially resulting in degradation (*e.g.*, reduced sediment storage, coarsening of the bed surface, and incision).

In the Lower McCloud River, where the channel bed is comprised of a coarse framework (*i.e.*, boulders and large cobbles) and active sediment storage is relatively low due to high sediment transport capacity, a Project-induced coarse sediment deficit is unlikely to influence channel morphology, gradient, or large alluvial features (*e.g.*, point bars and island bars). These large alluvial bedforms occur infrequently, are relatively immobile due to their coarse-grained composition, and the Project does not affect the frequency or magnitude of large floods capable of mobilizing them (*i.e.*, greater than 10–20 yr recurrence interval). Instead, the extent and magnitude of a coarse sediment deficit downstream of McCloud Dam would be expressed as coarsening of the bed surface (*e.g.*, loss of gravel from the interstices of larger framework grains) and in the frequency and size of smaller mobile sediment deposits created by large roughness



elements, local backwater effects, and local flow expansion. Closer to the dam, where the deficit is greatest, channel sediment storage is expected to be small relative to the storage potential. Downstream contributions of coarse sediment will increase the amount of sediment stored in responsive reaches until the storage potential becomes saturated. Once this condition is achieved, the amount of sediment in storage will fluctuate around an approximate equilibrium in response to local changes in channel morphology (slope, width, and confinement) that influence unit stream power and sediment transport.

6.1 Methods

Mobile coarse sediment stored in the Lower McCloud River downstream of McCloud Dam was mapped in an effort to identify the reach where sediment storage approaches an equilibrium value, signifying an approximate balance between coarse sediment supply, storage, and transport.

Available aerial photographs of the Lower McCloud River from 1944, 1952, 1971, and 1985 were compiled, scanned, and examined on screen to determine if alluvial features could be identified in the Lower McCloud River channel. Coverage of the Lower McCloud River was incomplete for 1952, 1971, and 1985. Historical aerial photographs were unsuitable for mapping and quantitatively analyzing change in alluvial storage because the coarse resolution (typically 1:24,000 or larger), glare and reflection from the water surface, and vegetation obscuring the channel prohibited recognition of alluvial features. Similar efforts were made to use the same historical aerial photographs of the Lower McCloud River during preparation of the Lower McCloud River Watershed Analysis (USFS 1998), but the resolution and scale did not allow an evaluation of changes in channel morphology or alluvial features (personal communication, S. Bachmann, Hydrologist, USFS, McCloud, CA, J. Stallman, Stillwater Sciences, Arcata, CA, January 11, 2008). To the extent possible, historical aerial photographs were used to qualitatively evaluate sediment supply and large scale controls on channel morphology, but mapping of alluvial features and quantitative analysis of change in alluvial features was not possible using the available aerial photography.

6.1.1 Sample Site Selection

Sample reaches with comparable sediment storage potential were selected for study between McCloud Dam and Squaw Valley Creek based on coarse-level stratification of channel reach morphology. Video footage from a low-altitude helicopter flight in July 2006 and high-resolution aerial photography from 2007 were reviewed to evaluate the distribution of mobile coarse sediment deposits in the Lower McCloud River. Sample reaches had slopes less than three percent, a length typically greater than twice the bankfull width, and were longitudinally distributed in order to characterize downstream trends in sediment storage. Study sites were grouped according to their classification as flatwater, pool, or riffle units. The *area* of mobile sediment in flatwater (*e.g.*, pocketwater, run, step-run, and glide) is most responsive to Project operation and most feasible to detect because (1) these deposits are patchy and primarily associated with large roughness, (2) the thickness of these deposits is typically less than the depth of scour during a large bed mobilizing flood event, and (3) a shift in mass balance toward



supply limitation in these reaches would reduce the size and frequency of mobile sediment patches. Pool tail deposits, important in providing spawning habitat in the Lower McCloud River, may coarsen or change thickness and therefore volume in response to Project operation, but the Project is unlikely to influence the planform area of mobile coarse sediment stored in pools.

6.1.2 Sample Site Characterization

Channel sediment storage was characterized in sample reaches starting at McCloud Dam and working downstream to Squaw Valley Creek. Field mapping was conducted using methods modified from Kelsey *et al.* (1987) and Curtis *et al.* (2005). Stored sediment was defined as the fraction of the bed material that is mobile during frequent flood events (*e.g.*, 1.5–5 year recurrence interval) most affected by the Project (refer to Section 5.2.2 for discussion of regulated and unimpaired flood frequency). For the purposes of mapping channel sediment storage, mobile sediment deposits were defined as having a D_{90} grain size of approximately 150 mm or less. This grain-size criterion was based on the upper limit of the D_{90} from bulk sampling of mobile sediment deposits at intensive study sites on the Lower McCloud River and at bed texture study sites in major tributaries (Figures 12 and 16, Attachment 1). This definition of mobile sediment storage is generally consistent with the bed material mapped during the spawning gravel assessment conducted as part of Study Description FA-S3, *Characterize Fish Populations in Project Reservoirs and Project-Affected Streams Reaches*. Specific habitat parameters of mobile sediment deposits (*e.g.*, water depth, flow velocity, and grain-size preferences of spawning fish) were evaluated as part of Study Description FA-S3.

Boundaries of each sediment storage patch were mapped in the field on color aerial photo tiles (2006, scale 1:500). The minimum mapable area was approximately 4 m². Each sediment storage patch was described in geomorphic terms, assigned an activity class (*e.g.*, active or semiaactive) based on relative position and indicators of residence time, and characterized with a textural facies and an estimated D_{50} and D_{84} grain size (refer to sample data sheet in Attachment 5). Depth of each patch was measured with a Silvy rod or estimated relative to the depth to bedrock controls or the thalweg elevation. Because mobile coarse sediment in the Lower McCloud River is often distributed in thin, discontinuous, and transitory sheets within a bed of immobile framework grains (mobile sediment that cannot be mapped in discrete patches), field data collection also included a visual estimate of the percentage of transitory mobile bed (TMB) in each sample reach. TMB estimates were binned in 10 classes (0–2 percent, 2–5 percent, 5–10 percent, and 10 percent classes thereafter). Bankfull width, wetted channel width, water surface slope, and length were measured in each sample reach.

6.1.3 Analytical methods

Sediment storage areas mapped in the field on air photo tiles were digitized, and the area of each patch was determined in GIS using ArcInfo. GIS was also used to determine the distance along the mainstem channel from McCloud Dam to the midpoint of each sample reach, as well as the unimpaired drainage area to the reach midpoint. Unit storage area (*i.e.*, area of sediment storage per unit area of bankfull channel in m²/m²) and unit storage volume (*i.e.*, volume of sediment



storage per unit area of bankfull channel in m^3/m^2) were calculated for each sample reach from field measurements of channel width, reach length, and depth of storage. Normalizing sediment storage values by channel area was necessary to account for differences in the length and width of sample reaches.

Unit stream power is the time rate of potential energy expenditure per unit channel area. Unit stream power is generally proportional to bedload transport rate and inversely related to storage potential (*e.g.*, higher unit stream power is commonly associated with higher sediment transport rate and lower sediment storage). Unit stream power was calculated for each sample reach to evaluate the extent to which trends in sediment storage may be controlled by reach-scale factors related to sediment transport rate (*i.e.*, channel gradient, width, and bankfull discharge) rather than by project effects on sediment supply and transport.

6.2 Results

Sediment storage and associated attributes were mapped in 50 sample reaches from McCloud Dam to Ladybug Creek (Figure 28, Attachment 6). A total of 5,803 m of channel was surveyed, or 25.8 percent of the total channel length from McCloud Dam to Squaw Valley Creek (Table 11). The survey included 3,743 m of flatwater (64.5 percent of the survey length) at 24 sites, 1,748 m (29.6 percent of the survey length) of pool at 23 sites, and 312 m of riffle (4 percent of reach length) at three sites. Sampling of riffle units in the first 8.5 km downstream of the dam was limited to the few sites with slopes less than 3 percent. Riffles were eliminated from further study after preliminary results indicated that the small sample of suitable riffles had little potential for sediment storage and were a poor indicator of project effects on channel sediment storage compared to flatwater and pool units.

Table 11. Summary of channel length sampled during sediment storage mapping

Channel Type	Count	Survey Length (m)	Percent of Total Survey Length	Percent of Total Length (McCloud Dam to Squaw Valley Creek)
Flatwater	24	3,743	64.5	16.6
Pools	23	1,748	29.6	7.8
Riffles	3	312	5.3	1.4
Total	50	5,803	100	25.8

Storage area is the most relevant metric in flatwater because a shift in mass balance toward supply limitation may reduce the size and frequency of the ubiquitously small and thin mobile sediment patches (typically less than the depth of scour during a large bed mobilizing flood event) associated with large roughness. Storage volume is a more relevant metric in pools because pools typically contain a large and thick sediment deposit in the tail, and a shift in mass balance toward supply limitation may reduce the volume of the pool tail deposit without changing the areas or frequency of mobile sediment patches.



Unit storage area in flatwater is low ($\leq 3 \text{ m}^2 100\text{m}^{-2}$) in the first 5.2 km downstream of McCloud Dam, where coarse sediment supplied by the larger tributaries (*i.e.*, Hawkins Creek, Squirrel Creek, Fitzhugh Creek) is efficiently routed through the steep and confined the McCloud River channel with little storage potential (Figure 28 and Figure 29). Sediment storage increases by a small amount in the wider, lower gradient, and less confined channel reach near Ah-Di-Na. Approximately 8 km downstream of McCloud Dam (a short distance upstream of Ladybug Creek), sediment storage *area* in flatwater reaches a global maximum of $15 \text{ m}^2 100\text{m}^{-2}$ and sediment storage *volume* in pools reaches a significant local peak of $58 \text{ m}^3 100\text{m}^{-2}$ (Figure 28, Figure 29, and Figure 30). The peak in storage is related to both lower stream power and higher rates of sediment delivery from potentially unstable terrane (*e.g.*, debris basins and domant landslides) in this vicinity, including a large active landslide entering the channel from the left bank (Figure 28a). The size and variability in size of individual stored sediment patches in flatwater also increases in the reach from Fitzhugh Creek to Ladybug Creek, with patches generally reaching their largest size in the reach from Ladybug Creek to Bald Mountain Creek (Figure 31). Trends in sediment *storage area* in flatwater reaches, sediment *storage volume* in pools, and individual *patch size* in flatwater reaches are also supported by a peak in transitory mobile bed (TMB) in both flatwater and pools at approximately 8 km downstream of McCloud Dam (Figure 32). Downstream of 8 km, overall trends in sediment storage are less clear and are punctuated by variability related to local changes in channel morphology, stream power, and sediment transport rate that influence storage potential, as well as local variability in coarse sediment supply. Storage area and patch size in flatwater units tend to decline, while storage volume and patch size in pools tend to remain high or increase.

Longitudinal patterns in sediment storage and sediment storage potential (*i.e.*, stream power) suggest that the Project forces or at least exacerbates supply limitation (deficit of coarse sediment supply relative to bedload transport capacity) in responsive reaches in the first 7 or 8 km downstream of McCloud Dam. From McCloud Dam to approximately Fitzhugh Creek (5 km) there is little responsive reach length, and therefore the reach of the Lower McCloud River potentially most affected by the Project is from 5 to 8 km downstream of McCloud Dam. Downstream of 8 km, sediment supply appears to be in approximate equilibrium with unit stream power and the amount of sediment in storage fluctuates in response to local changes in channel morphology (slope, width, and confinement) that influence storage potential.

7 SYNTHESIS

This synthesis combines analyses of geologic and geomorphic controls, sediment supply, hydrologic regimes, channel morphology and composition, bed mobility and transport, and sediment storage to describe the unimpaired (pre-dam) and regulated (post-dam) sediment mass balance in the Lower McCloud River and the effects of the regulated mass balance on fluvial processes.

7.1 Geologic and Geomorphic Controls on Sediment Supply

McCloud Dam is located near the boundary between distinctly different geologic terranes that strongly influence the supply, transport, and storage of fluvial sediment in the McCloud River.



The majority of the upper basin (connected source area 301 km²) occurs in the High Cascades and Western Cascades terranes comprised of predominantly young (late Tertiary to Holocene age) volcanic rocks and related surficial deposits, while the lower basin (connected source area 261 km²) occurs almost entirely in the Eastern Klamath belt comprised of older (Paleozoic age) metamorphic rocks (Figure 2 and Figure 3).

Young volcanic rocks and unconsolidated surficial deposits of the High Cascades terrane in the Upper McCloud River basin forms large areas of low-gradient topography with little surface runoff and little or no sediment delivery to the Upper McCloud River. Debris flows originating from the unconsolidated inner gorge slopes of the Mud Creek canyon high on the southeast flank of Mount Shasta, however, historically delivered large quantities of fine sediment (sand and finer) to the McCloud River during the summer months (Osterkamp *et al.* 1986), and sediment delivery from debris flows in Mud Creek constitutes a large fraction of the 4,134,500 m³ of sediment currently stored in McCloud Reservoir (Figure 6, Table 3). Sediment delivered by tributaries draining the steep Western Cascades terrane upstream of Upper Fowler Falls (near the present location of Lakin Dam) and south of the McCloud River (*e.g.*, Tate, Racoon, and Bull creeks) is sequestered in the low gradient, relatively unconfined upstream river valley (Figure 1) and historically contributed little coarse sediment to downstream reaches of the McCloud River. Tributaries draining the steep topography of the Eastern Klamath Terrane and Western Cascades Terrane surrounding McCloud Reservoir (*e.g.*, Angel, Lick, and Star City creeks) historically delivered the majority of the coarse sediment to the McCloud River upstream of McCloud Dam, and sediment delivery from these tributaries constitutes the majority of the coarse sediment stored in McCloud Reservoir. An estimated 937,400 tonnes of coarse sediment (>2 mm) is stored in McCloud Reservoir, representing an average annual coarse sediment yield of approximately 140±30 t km² y⁻¹ (Table 3)

In contrast to the Upper McCloud River basin, the Lower McCloud River basin is comprised almost entirely of the Eastern Klamath terrane, a landscape typified by steep slopes and a dense, deeply incised channel network that promote a more peaked response to storm events and higher rates of coarse sediment delivery by mass wasting from unstable areas (Figure 4 and Figure 5). The largest tributaries that contribute coarse sediment to the 22.5 km of the Lower McCloud River study reach are Hawkins Creek (46 km² adding 1,250 t y⁻¹), Claiborne Creek (42 km² adding 1,060 t y⁻¹), and Squaw Valley Creek (104 km² adding 2,200 t y⁻¹) (Table 4). Other named tributaries that contribute lesser quantities of water and sediment to the Lower McCloud River in the Study Area include Squirrel Creek, Fitzhugh Creek, Ladybug Creek, Bald Mountain Creek, and Hat Mountain Creek. Cumulative sediment supply to the Lower McCloud River under regulated conditions ranges from 1,450 t y⁻¹ at the Hawkins Creek confluence (5.5 percent of the cumulative unimpaired supply) to 7,050 t y⁻¹ at the Squaw Valley Creek confluence (22 percent of the cumulative unimpaired supply) (Table 4, Figure 8).

7.2 Hydrologic Regimes

The Upper and Lower McCloud River watersheds exhibit different hydrologic regimes in response to differences in geology and topography, elevation, precipitation, and spring-fed groundwater discharge. The predominance of young, porous volcanic and volcanoclastic



materials forming smooth, undissected topography in the upper watershed leads to year-round, spring-fed groundwater discharge that contributes at least 700 cfs to baseflow in the Upper McCloud River (Davidson and Rose, 1997). The Upper McCloud River watershed also includes the highest altitudes within the Study Area and is strongly influenced by snowmelt that recharges volcanic aquifers and groundwater springs. Hydrographs from historical gage data in the upper watershed generally show a slower response to precipitation events due to snowpack accumulation, porous surficial geology, and gentle topography (WR-S1 *Unimpaired Hydrology Development*). In contrast to the upper watershed, the Lower McCloud River watershed drains steeper and more dissected hillslopes that are primarily composed of much older metasedimentary and metavolcanic rocks (Table 1). As a result, the Lower McCloud River basin generally exhibits a “flashier” hydrologic response to precipitation events, and is driven more by rainfall-runoff than by the snowmelt and spring-fed baseflow that characterize Upper McCloud River hydrology.

Hydrograph analyses at intensive study sites in the Lower McCloud River indicate a relatively stable baseflow regime with relatively minimal annual variance outside of high flow events driven by prolonged moderately intense rainfall (Figure 22). Limited baseflow variability in the Lower McCloud River under *unimpaired* conditions can be attributed in large part to relatively high year-round flow from spring-fed groundwater contributions originating in the upper watershed, and under *regulated* conditions to relatively consistent minimum flow releases from McCloud Dam. Discharge from major tributaries are primarily responsible for differences in high flows (exceedance probabilities < 10 percent) between mainstem study sites (Figure 23). Squaw Valley Creek contributes the most significant tributary flow input to the Lower McCloud River during high flow events, doubling the mainstem discharge during higher flows under regulated conditions (Figure 24).

Differences between regulated and unimpaired hydrologic regimes at the five intensive study sites on the Lower McCloud River are greater at sites closer to McCloud Dam and are more pronounced at lesser daily and peak flow discharges (*i.e.*, higher exceedance probabilities of the daily flow series and lower return period of the peak flow series) (Figures 20 and 21 and Table 9). A 2-year return flow under regulated conditions is less than or equal to a 1.2-year return flow under unimpaired conditions. A 2-year flow under regulated conditions ranges from 1,040 cfs at Site 1 to 2,800 cfs at Site 5 compared to 3,380 cfs and 5,210 cfs under unimpaired conditions, respectively, which represents a 69 percent reduction in the 2-year flow at Site 1 and a 46 percent reduction at Site 5. The percent reductions in peak flow are much smaller at a 10-year return interval, and for larger peak flow return periods, changes between regulated and unimpaired peak flow series are indeterminate based on the available flow record (33 years) (Table 9, Attachment 3).

7.3 Channel Reach Morphology in the Lower McCloud River

The Lower McCloud River is a mixed bedrock-alluvial channel with high transport capacity and generally low volumes of active sediment storage. Bedrock outcrops intermittently control channel width and gradient throughout the Lower McCloud River between McCloud Dam and the Squaw Valley Creek confluence. Channel reach morphology in the Lower McCloud River



broadly transitions from predominantly step pool upstream of Ah-Di-Na to alternating plane bed and pool riffle downstream of Ah-Di-Na (Figure 12), reflecting an overall decrease in slope and confinement and an increase in mobile sediment supply. Where alluvium is stored within the channel, the cover is typically thin and commonly dominated by coarse deposits (boulder and large cobble) delivered during wetter late Pleistocene climate. These coarse deposits are larger than typical of current bedload material (cobble and gravel) and remain in long-term storage, where they armor the bed surface and, in the case of larger boulders, function like bedrock in controlling channel width and gradient.

The steep (average gradient 1.72 percent)(Figure 10) and confined channel between McCloud Dam and Fitzhugh Creek (located 4.9 km downstream of McCloud Dam) occupies a narrow valley with little floodplain or terrace development. Channel morphology is typically boulder and bedrock dominated step pool, except between Hawkins Creek and Squirrel Creek, where lower channel gradient is distributed in riffle step and boulder cobble plane bed morphology (Figure 12a). Little coarse sediment is delivered to this reach under current conditions due to sediment trapping in McCloud Reservoir. High unit stream power typically limits sediment storage potential, and the relatively small amount of mobile coarse sediment supplied by larger tributaries (Hawkins, Squirrel, and Fitzhugh creeks) is effectively routed to reaches downstream of Fitzhugh Creek.

From Fitzhugh Creek to approximately Ladybug Creek, stream power decreases due to lower channel gradient (average gradient 1.24 percent)(Figure 10) and increased channel width. The frequency of large pools increases, and pools are commonly separated by plane bed morphology (Figure 12a). Coarse sediment supplied to the reach from upstream bedload transport and by erosion of nearby unstable areas (*e.g.*, tributary inner gorges formed in dormant landslides and active landsliding [Figure 28a]), combined with the abrupt decrease in stream power allows for greater sediment storage potential. Alluvial river terraces bounding the channel between Ah-Di-Na and Ladybug Creek suggest a geologically recent history in which the sediment mass balance resulted in deposition, lateral channel migration, and associated floodplain development. This is the reach where any Project's effects on mobile coarse sediment storage or bed surface texture are most likely to be detected.

Between Ladybug Creek and approximately Claiborne Creek, the channel is typically boulder dominated and average gradient channel gradient is 1.10 percent (Figure 10), although gradient is highly variable as a result of increasingly large pools separated by long reaches of plane bed and riffle step morphology (Figure 12b and 12c). The valley is confined by steep slopes with floodplain and terrace development limited to meander bends. The largest and only named tributary in the reach is Bald Mountain Creek, although numerous smaller tributaries supply lesser quantities of water and sediment. Channel gradient decreases in the vicinity of the Claiborne Creek confluence, where alluvial river terraces again occupy broad valley bottom areas. The remaining length of the Lower McCloud River between Claiborne Creek and Squaw Valley Creek is lower gradient (0.83 percent) but more confined, with highly variable channel morphology (large pool riffle sequences, long reaches of boulder and cobble plane bed, and shorter reaches of boulder-dominated riffle step and step pool) (Figure 12c).



7.4 Channel Boundaries and Bed Sediment Composition

The relatively undeformable bedrock and boulder boundary conditions render channel geometry adjustments less sensitive to changes in the hydrologic and sediment supply regimes. Based on surface pebble counts, the D_{84} grain size at 14 of the 15 cross-sections surveyed in this study were > 256 mm (boulder)(Attachment 1). These cross-sections were located in channel segments with the lowest gradient and stream power within their respective response reaches, and represent the finer grain size distributions within the Lower McCloud River. The predominance of coarse, relatively immobile clasts on the Lower McCloud River channel bed has implications for the transport of finer bedload material under current conditions. These large, immobile clasts (*e.g.*, boulders) consume a significant portion of the total shear stress, thereby reducing the stress available for transporting finer mobile sediment (Yager *et al.* 2007). Large boulders and bedrock outcrops also create velocity shadows that induce deposition of finer material and form one of the primary storage elements for mobile sediment within the active channel.

Bulk samples taken from mobile sediment deposits at intensive study sites on the lower mainstem of the McCloud River and bed texture study sites in major tributaries (Hawkins, Claiborne, and Squaw Valley Creeks) indicated similar grain size distributions between study sites and did not exhibit any strong longitudinal trends that would imply systematic sorting or changes in the composition of coarse sediment supply between McCloud Dam and Squaw Valley Creek (Figure 15). Tributary bulk sample distributions fell within a similar range (Figure 21) due in large part to the similar geology and geomorphology (predominantly Eastern Klamath belt) in the lower basin source area. Bulk sample distributions from primary tributary sources of sediment exhibited similar distributions to mainstem bulk samples (Figures 15 and 19). Similarity in the size of coarse sediment supplied by major tributaries and the size of mobile deposits in the mainstem of the Lower McCloud River emphasizes the importance of coarse sediment inputs from major lower basin tributaries in supplying the mobile sediment fraction (including spawning gravel size classes) to the McCloud River downstream of McCloud Dam.

Bulk sample results also indicate that gravel composed the majority of mobile material in both the mainstem (average gravel content of 79 percent, range of 56 to 100 percent, $n = 14$)(Figure 15) and major tributaries (average gravel content of 79 percent, range of 65 to 90 percent, $n = 8$)(Figure 21). The fine sediment fraction (< 2 mm, *i.e.*, sand and finer material) was generally low in both mainstem and tributary bulk samples, with the mean fine sediment fraction measuring 10 percent for mainstem samples and 11 percent for tributary samples. The average D_{50} and D_{84} for mainstem samples was 20 mm and 54 mm, respectively; tributary samples similarly averaged 17 mm and 52 mm, respectively (Attachment 1). Bulk sampling results suggest that major tributary sediment inputs fine the bed, and that the mainstem channel bed coarsens with increasing distance from major tributaries. Two of the three bulk samples from Site 4, the intensive study site located furthest from a major tributary sediment source (Figure 10), had the coarsest distributions of all the mobile deposits sampled (Figure 15). In contrast, mobile size distributions sampled from Site 5 (located 4 km downstream of Site 4 and 1.5 km downstream of Claiborne Creek) were finer than Site 4 and were similar in size distribution to mobile material sampled in Claiborne Creek.



7.5 Sediment Transport

The primary variable controlling differences in bed mobility and transport capacity at intensive study sites is channel slope, which generally follows a downstream decreasing continuum (Table 6). Other variables that can strongly influence bedload transport (channel geometry, surface and subsurface grain size, and discharge) vary little between intensive study sites (Tables 6 and 7). Thus, bedload mobility thresholds and annual average coarse sediment (> 2 mm) transport capacities at the intensive study sites reflect the decreasing downstream slope continuum and have the following trends: (1) bedload transport capacities generally decrease with distance downstream and (2) threshold discharges for bed mobility increase with distance downstream (Figures 24 and 25).

Annual average bedload transport capacities under both regulated and unimpaired flow regimes peak at Site 2 and decline downstream, reaching a minimum at Site 5 where the rates are about half the capacity estimated at Site 2 (Table 10 and Figure 26a). Decreases in transport capacities due to regulated flow reduction are higher at sites near the dam (70 percent at Site 1) and decrease with distance downstream (51 percent at Site 5). Changes in estimated transport capacity are primarily due to increased tributary flow input with downstream distance and do not reflect changes in channel geometry or grain size distribution. Bed mobility thresholds increase in the downstream direction, with mobilization occurring at 1,030 cfs at Site 2 and at 2,060 cfs at Site 5 (Table 10 and Figure 27). Initial mobilization of more mobile sediment patches in most locations occurs at flows > 620 cfs based on tracer observations, and may occur at the lower range of flows indicated in the range of bed mobility shown in Figure 27b.

7.6 Mass Balance

The mass balance between coarse sediment supply and bedload transport capacity is a fundamental relationship governing many morphologic responses in river channels, including channel form, channel aggradation and degradation, sediment storage, and bed surface texture. Mass balance for the Lower McCloud River is developed by relating coarse sediment transport capacities calculated at intensive study sites (Table 10) to coarse sediment supply estimated at subbasin delivery nodes (Table 4, Figure 33). Under unimpaired conditions, the Lower McCloud River was supply-limited (*i.e.*, annual bedload transport capacity exceeded annual coarse sediment supply) from McCloud Dam to approximately Intensive Study Site 3, located 11.3 km downstream of McCloud Dam and immediately downstream of Bald Mountain Creek. Under regulated conditions, the approximate point in the Lower McCloud River where estimates of annual coarse sediment supply balance or exceed estimates of annual bedload transport capacity is shifted 9.5 km downstream to approximately Site 5, located 20.8 km downstream of McCloud Dam and 1.5 km downstream of the Claiborne Creek confluence. Under regulated conditions, excess transport capacity is greater at sites near McCloud Dam. Transport capacity decreases and supply increases with distance downstream.

To aid in evaluating the potential downstream geomorphic response of Project-induced changes to the mass balance between sediment supply and transport capacity, the conceptual framework of Grant *et al.* (2003) was applied, which scales hydrogeomorphic variables by the degree of



change between regulated and unimpaired conditions. Change in the percentage of time (T) that threshold transport conditions are equaled or exceeded is expressed as:

$$T = \frac{\sum t(Q \geq Q_{cr})}{\sum t_Q}$$

where t_Q refers to time at flow Q and Q_{cr} is the discharge necessary to mobilize the channel bed. Changes in the frequency of critical flows are based on the synthesized flow records at each intensive study site (Figure 22) and are compared using a dimensionless ratio (T^*) between regulated (T_{reg}) and unimpaired (T_{unimp}) frequency of flows exceeding Q_{cr} :

$$T^* = \frac{T_{reg}}{T_{unimp}}$$

Changes in sediment supply for each intensive study site are evaluated for the cumulative coarse sediment supply for regulated and unimpaired conditions at the nearest upstream subbasin node (Table 4). For example, sediment supply at Intensive Study Site 3 is evaluated based on the cumulative supply estimated at the Bald Mountain Creek confluence. The relation between regulated (S_{reg}) and unimpaired (S_{unimp}) coarse sediment supply is expressed as a dimensionless supply ratio (S^*):

$$S^* = \frac{S_{reg}}{S_{unimp}}$$

Predicted downstream effects of Project dams were then evaluated in terms of a bivariate plot of T^* and S^* (Grant *et al.* 2003). The conceptual model predicts channel degradation (*e.g.*, loss of sediment storage and surface coarsening) where T^* is high (sediment transport occurs frequently under the regulated flow regime) and S^* is low (sediment supply is low relative to unimpaired conditions). Conversely, channel aggradation (*e.g.*, bar construction and surface fining) is predicted where T^* is low (sediment-transporting flows are infrequent) and S^* is high (sediment supply is high relative to unimpaired conditions). Downstream channel adjustments are expected to be unpredictable or indeterminate where changes in T^* and S^* are proportional (note that T^* and S^* values near 1 indicate little to no change between regulated and unimpaired conditions).

T^* and S^* values for the five intensive study sites indicate substantial reduction in both coarse sediment supply and frequency of bedload transporting events, as both dimensionless variables are < 0.20 at all sites (Figure 34a). However, the reduction in coarse sediment supply and frequency of bedload transporting events is roughly proportional (*i.e.*, T^* and S^* have similar values at most of the sites). This indicates comparable magnitudes of reduction in supply and transport as well as indeterminate changes under the proposed conceptual model of Grant *et al.* (2003). Based on the conceptual framework of Grant *et al.* (2003), Site 1 is potentially the most degradational (S^* is 0.01) due to low regulated sediment supply (Site 1 is upstream of any tributary sediment inputs). T^* is also low at Site 1, however, due to the absence of tributary flow



input. T^* and S^* generally increase at a similar rate with distance downstream of McCloud Dam (Figure 34b), implying that reductions in coarse sediment supply and frequency of bedload transport associated with Project operations are decreasing at a proportional rate with distance downstream of the dam.

7.7 Relation between Regulated Mass Balance and Mobile Sediment Storage

In the Lower McCloud River, where the channel bed is comprised of a relatively undeformable boundary and sediment transport capacity is high, a Project-induced coarse sediment deficit downstream of McCloud Dam will be expressed as coarsening of the bed surface (*e.g.*, loss of gravel from the interstices of larger framework grains) and changes in the frequency and size of mobile sediment deposits. The *area* of mobile sediment in flatwater (*e.g.*, pocketwater, run, step-run, and glide) is most responsive to Project operation because (1) these deposits are patchy and primarily associated with large roughness, (2) the thickness of these deposits is typically less than the depth of scour during a large bed mobilizing flood event, and (3) a shift in mass balance toward supply limitation in these reaches reduces the size and frequency of mobile sediment patches. Pool tail deposits may coarsen or change thickness, and therefore volume in response to Project operation, but the Project is unlikely to influence the planform area of mobile coarse sediment stored in pools.

Trends in (1) sediment storage *area* and *patch size* in flatwater reaches (Figure 29 and Figure 31), (2) sediment storage *volume* in pools (Figure 30), and (3) percent transitory mobile bed (Figure 32) indicate a peak in mobile sediment storage approximately 8 km downstream of McCloud Dam near Ladybug Creek. These longitudinal patterns in sediment storage and sediment storage potential (*i.e.*, stream power) suggest that the Project forces or at least exacerbates supply limitation (deficit of coarse sediment supply relative to bedload transport capacity) in responsive reaches in the first 7 or 8 km downstream of McCloud Dam. Although storage is lowest in the first 5.2 km downstream of McCloud Dam, where coarse sediment has been reduced most by impoundment in McCloud Reservoir, there is little responsive reach length with storage potential and the relatively small quantity of coarse sediment supplied by larger tributaries (*i.e.*, Hawkins Creek, Squirrel Creek, Fitzhugh Creek) is efficiently routed downstream (Figure 28 and Figure 29). Downstream of about 8 km, sediment supply appears to be in approximate equilibrium with unit stream power and the amount of sediment in storage fluctuates in response to local changes in channel morphology (slope, width, and confinement) that influence storage potential, as well as local variability in coarse sediment supply. The reach of the Lower McCloud River most likely to experience degradation (*e.g.*, bed surface coarsening and reduction in the frequency and size of mobile sediment deposits) related to a Project-induced coarse sediment deficit is therefore, from about 5 km to 8 km downstream of McCloud Dam. Mass balance relations between unimpaired coarse sediment supply and bedload transport at intensive study sites imply that the system was trending toward equilibrium through this reach and achieved an approximate equilibrium by about Bald Mountain Creek (*i.e.*, Intensive Study Site 3 located about 11.3 km downstream of McCloud Dam). Mass balance relations and results of the mobile sediment storage analysis indicate the reach has become more strongly supply limited under regulated conditions, potentially resulting in coarsening of the bed surface (*i.e.*,



armoring) and less frequent and smaller mobile sediment deposits. Comparison of historical cross sections at the MC-1 gaging cableway, located approximately 5.5 km downstream of McCloud Dam, indicates negligible net change in channel geometry or mean bed elevation. Total variation in thalweg elevation (0.8 ft) and total variation in the maximum elevation in the low-flow wetted channel (1.1 ft) are within expected error ranges given the sampling method applied to a coarse grained channel bed and represent a feasible scour depth during a typical bed-mobilizing flow.

8 REFERENCES

- Ambers, R. 2001. Using the sediment record in a western Oregon flood-control reservoir to assess the influence of storm history and logging on sediment yield. *Journal of Hydrology* 244:181–200.
- Brown, C.B. 1943. Discussion of sedimentation in reservoirs. *Proceedings of the American Society of Civil Engineers* 69:1,493–1,500.
- Brune, G.M. 1953. Trap efficiency of reservoirs. *Transactions of the American Geophysical Union* 34:407–418.
- Buffington, J.M., and D.R. Montgomery. 1999. A procedure for classifying textural facies in gravel-bed rivers. *Water Resources Research* 35:1,903–1,914.
- Bunte, K. and S.R. Abt. 2001. Sampling surface and subsurface particle size distributions in wadable gravel and cobble bed streams for analyses in sediment transport, hydraulics, and streambed monitoring. General Technical Report RMRS-GTR-74. Rocky Mountain Research Station, Fort Collins, CO.
- California Department of Forestry and Fire Protection. 2000. Timber Harvest Plans. January Geospatial Data Presentation Form: Computer file. Updated periodically.
- Childs, J.R., N.P. Snyder, and M.A. Hampton. 2003. Bathymetric and geophysical surveys of Englebright Lake, Yuba-Nevada Counties, California. Open-file report 03-383. U.S. Geological Survey, Santa Cruz, CA.
- Christiansen, R.L., F.J. Kleinhampl, R.J. Blakely, E.T. Tuck, F.L. Johnson, M.D. Conyac. 1977. Resource appraisal of the Mount Shasta Wilderness Study Area, Siskiyou County, California. Open-file report 77-250. U.S. Geological Survey.
- Churchill, M.A. 1948. Discussion of analyses and use of reservoir sedimentation data, by L.C. Gottschalk. In: *Proceedings of the Federal Interagency Sedimentation Conference*, Denver, Colorado. U. S. Geological Survey, Washington DC.
- Cover, M., C. May, V. Resh, and W. Dietrich. 2006. Technical report on quantitative linkages between sediment supply, streambed fine sediment, and benthic macroinvertebrates in streams of the Klamath National Forest. Prepared for the United States Forest Service, Pacific Southwest Region and Klamath National Forest, Prepared by the University of California, Berkeley. July.



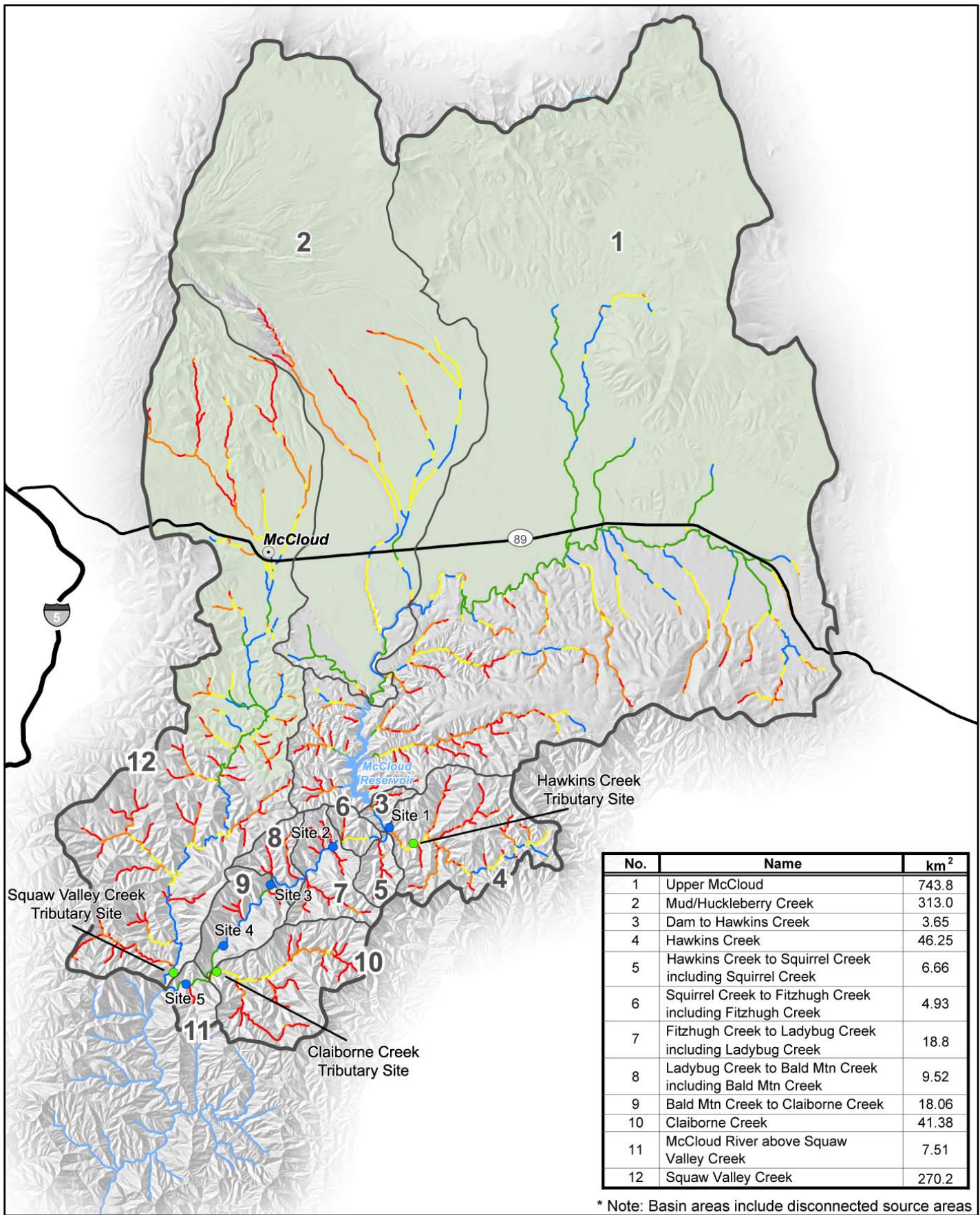
- Curtis, J.A., L.E. Flint, C.N. Alpers, and S.M. Yarnell. 2005. Conceptual model of sediment processes in the upper Yuba River watershed, Sierra Nevada, California. *Geomorphology* 68:149–166.
- Davidson, M.L. and T.P. Rose. September 1997. Comparative Isotope Hydrology Study of Groundwater Sources and Transport in the Three Cascade Volcanoes of Northern California. Isotope Science Division, Lawrence Livermore National Laboratory.
- Freeman, Gary J. 2001. “The Impacts of Current and Past Climate on Pacific Gas & Electric’s 2001 Hydroelectric Outlook”. 2001 PACLIM Conference Proceedings, p. 21-38.
- Grant, G. E., J. C. Schmidt, and S. L. Lewis. 2003. A geological framework for interpreting downstream effects of dams on rivers. Pages 209-225 in J. E. O’Connor and G. E. Grant, editors. *A peculiar river: geology, geomorphology, and hydrology of the Deschutes River, Oregon*. Water Science and Application Series No. 7. American Geophysical Union. Washington D. E.
- Harrelson, C.C., C.L. Rawlins, and J.P. Potyondy. 1994. Stream channel reference sites: an illustrated guide to field technique. General Technical Report RM-245. U.S. Forest Service, Rocky Mountain Forest and Range Experiment Station, Fort Collins, CO.
- Haschenburger, J.K., and P.R. Wilcock. 2003. Partial transport in a natural gravel bed channel. DOI:10.1029/2002WR001532. *Water Resources Research* 39:1,020.
- Irwin, W.P. 2003. Correlation of the Klamath Mountains and Sierra Nevada with map showing accreted terranes and plutons of the Klamath Mountains and Sierra Nevada. U.S. Geological Survey Open File Report 02-490.
- Irwin, W.P. 1966. Geology of the Klamath Mountains Province. Pages 19-38 in E.H. Bailey, editor. *Geology of Northern California*. California Division of Mines and Geology Bulletin 190.
- Irwin, W.P. and J.L. Wooden. 1999. Plutons and accretionary episodes of the Klamath Mountains, California and Oregon. U.S. Geological Survey Open File Report 99-374.
- Kelsey, H.M., R. Lamberson, and M.A. Madej. 1987. Stochastic model for the long-term transport of stored sediment in a river channel. *Water Resource Research* 23:1,738–1,750.
- Lara, J.M., and E.L. Pemberton. 1963. Initial Unit Weight of deposit sediments. Proceedings of the Federal Inter-Agency Sedimentation Conference, Paper No. 82. U.S. Forest Service.
- McBain and Trush. 2002. Sediment yield analysis for the Oak Grove Fork and upper mainstem Clackamas River above North Fork Reservoir. Technical report. Prepared by McBain and Trush, Arcata, California for Clackamas River Hydroelectric Project Relicensing Fish and Aquatics Workgroup, Portland General Electric, Portland, OR.
- Montgomery, D.R., and J.M. Buffington. 1998. Channel processes, classification, and response. In: *River Ecology and Management*. R. Naiman and R. Bilby (eds.). Springer-Verlag, Inc., New York, NY. pp. 13–42.



- Montgomery, D.R., and J.M. Buffington. 1997. Channel-reach morphology in mountain drainage basins. *GSA Bulletin* 109:596–611.
- Morris, G. L., and J. Fan. 1998. *Reservoir sedimentation handbook: design and management of dams, reservoirs, and watersheds for sustainable use*. McGraw-Hill, New York, NY.
- Mueller, E.R., J. Pitlick, and J.M. Nelson. 2005. Variation in the reference Shields stress for bed load transport in gravel-bed streams and rivers. DOI: 10.1029/2004WR003692. *Water Resources Research* 41:W04006.
- Osterkamp, W.R., C.R. Hupp, and J.C. Blodgett. 1986. Magnitude and frequency of debris flows, and areas of hazard on Mount Shasta, Northern California. U.S. Geological Survey Professional Paper 1396-C.
- Parker, G. 1990a. Surface-based bedload transport relation for gravel rivers. *Journal of Hydraulic Research* 28:417–436.
- Parker, G. 1990b. The Acronym Series of PASCAL program for computing bedload transport in gravel rivers. External Memorandum M-220. St. Anthony Falls Laboratory, University of Minnesota, Minneapolis, MN.
- PG&E (Pacific Gas and Electric Company). 2009a. Unimpaired Hydrology Development (WR-S1), Technical Memo 46. McCloud-Pit Project, FERC Project No. 2106. San Francisco, CA. In progress.
- PG&E. 2009b. Assess Potential Ongoing Project Effects on Riparian Vegetation Community Types in the Project Area (BR-S4), Technical Memo 65. McCloud-Pit Project, FERC Project No. 2106. San Francisco, CA. In progress.
- PG&E. 2008. McCloud-Pit Hydroelectric Project, FERC Project No. 2106: Licensee’s Initial Study Report, McCloud-Pit Project, FERC Project No. 2106. Pacific Gas and Electric, San Francisco, CA. June.
- Roering, J.J., and M. Gerber. 2005. Fire and the evolution of steep, soil-mantled landscapes. *Geology* 33:349–352.
- Snyder, N.P., D.M. Rubin, C.N. Alpers, J.R. Childs, J.A. Curtis, L.E. Flint, and S.A. Wright. 2004. Estimating accumulation rates and physical properties of sediment behind a dam: Engebright Lake, Yuba River, northern California. *Water Resource Research* 40.
- Snyder, N.P., S.A. Wright, C.N. Alpers, L.E. Flint, C.W. Holmes, and D.M. Rubin. 2006. Reconstructing depositional processes and history from reservoir stratigraphy: Engebright Lake, Yuba River, northern California. *Water Resource Research* 40.
- Stillwater Sciences. 2003. Appendix 2-1: Sediment budget for the North Umpqua River basin. North Umpqua Cooperative Watershed Analysis. In: *Synthesis Report for the North Umpqua Hydroelectric Project, FERC Project No. 1927, Douglas County, Oregon*. Prepared for PacifiCorp, Portland, OR. Prepared by Stillwater Sciences, Berkeley, CA.
- Swanson, F.J. 1981. Fire and geomorphic processes. Pages 410-420 in H. Mooney, editor. *Fire regimes and ecosystem properties: proceedings of the conference*. General technical



- report WO-26. U.S. Forest Service, Pacific Northwest Forest and Range Experiment Station, Portland, OR.
- U.S. Bureau of Reclamation. 1987. Design of Small Dams. Attachment A. U.S. Department of Interior. pp 529–564.
- USFS (U.S. Forest Service). 2005. Shasta-Trinity CWE 2005—cumulative watershed effects analysis. Quantitative models for surface erosion, mass-wasting and ERA/TOC. Analysis by D. Elder and M. Reichert, ACT2 Enterprise Team. U.S. Forest Service, Shasta-Trinity National Forest, Redding, CA.
- USFS. 1998. Lower McCloud River watershed analysis. Shasta-Trinity National Forest, Shasta-McCloud Management Unit, U.S. Forest Service, McCloud, CA.
- Wagner, D.L., and G.J. Saucedo. 1987. Geologic map of the Weed quadrangle. California Division of Mine and Geology, scale 1:250,000.
- Wilcock, P.R., and J. C. Crowe. 2003. Surface-based transport model for mixed-size sediment. *Journal of Hydraulic Engineering*, 129, 120-128.
- Wolman, G.M. 1954. A method of sampling coarse river-bed material. *Transactions of the American Geophysical Union* 35:951–956.
- WRCC. 2009. Western Regional Climate Center: database of historical climate information. <http://www.wrcc.dri.edu/>. Accessed on January 7, 2009.
- Wondzell, S.M., and J.G. King. 2003. Postfire erosional processes in the Pacific Northwest and Rocky Mountain regions. *Forest Ecology and Management* 178:75–87.
- Vanoni, V.A., 1977. *Sedimentation Engineering*. ASCE Publications, New York, NY. 745 pp.
- Yager, E. M., J. W. Kirchner, and W. E. Dietrich. 2007. Calculating bed load transport in steep boulder bed channels. DOI:10.1029/2006WR005432. *Water Resources Research*, 43, W07418.



* Note: Basin areas include disconnected source areas

Study Sites

- Intensive Study Sites on the Lower McCloud River
- Tributary Bed Texture Study Sites



GS-S2 Sub-basins



Disconnected Source Areas

Channel Gradient

- 0-1 %
- 1-2 %
- 2-4 %
- 4-8 %
- >8 %

McCloud-Pit Project
FERC Project No. 2106



* GS-S2 Sub-basin delineations modified from CalWater Ver 2.2.1

0 1.25 2.5 5
Kilometers



Figure 1. GS-S2 Study Area and study sites

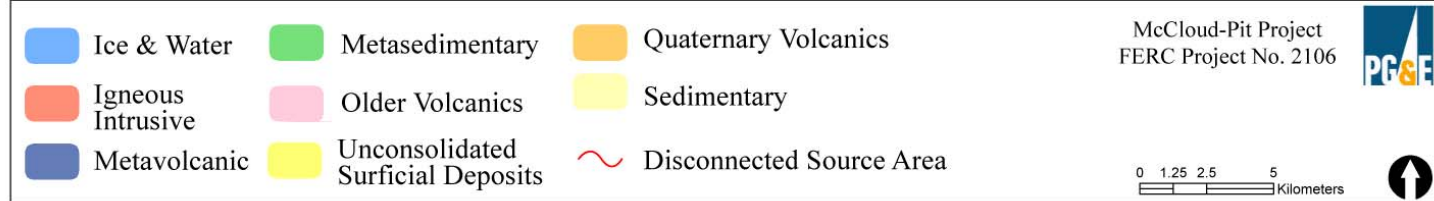
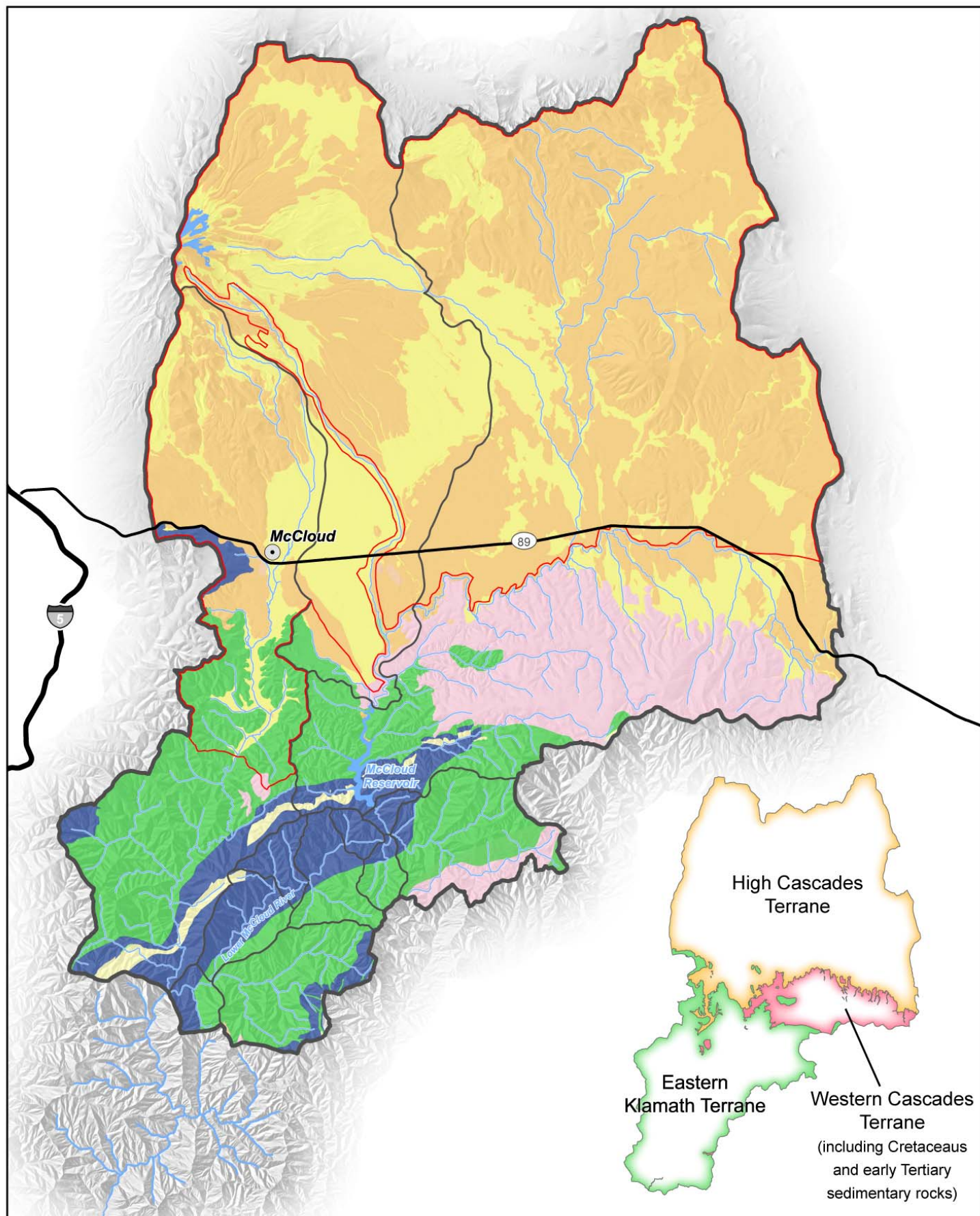


Figure 2. Geology in the GS-S2 Study Area

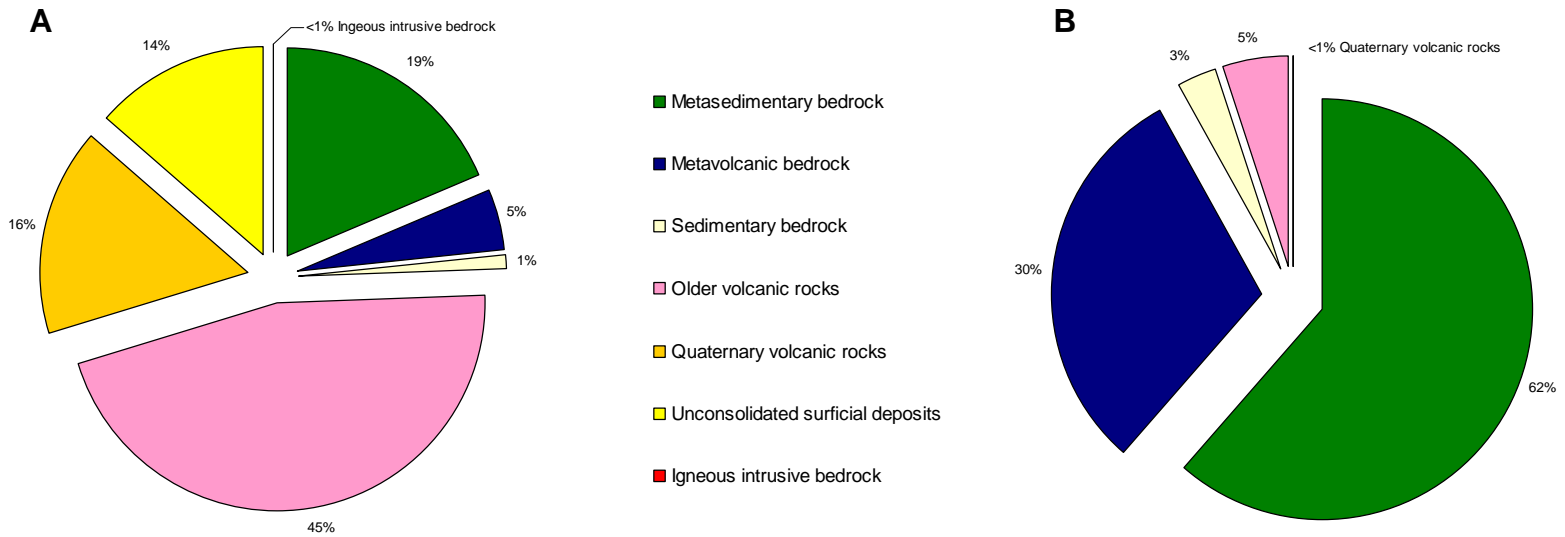


Figure 3. Geology of sediment source areas (A) upstream and (B) downstream of McCloud Dam

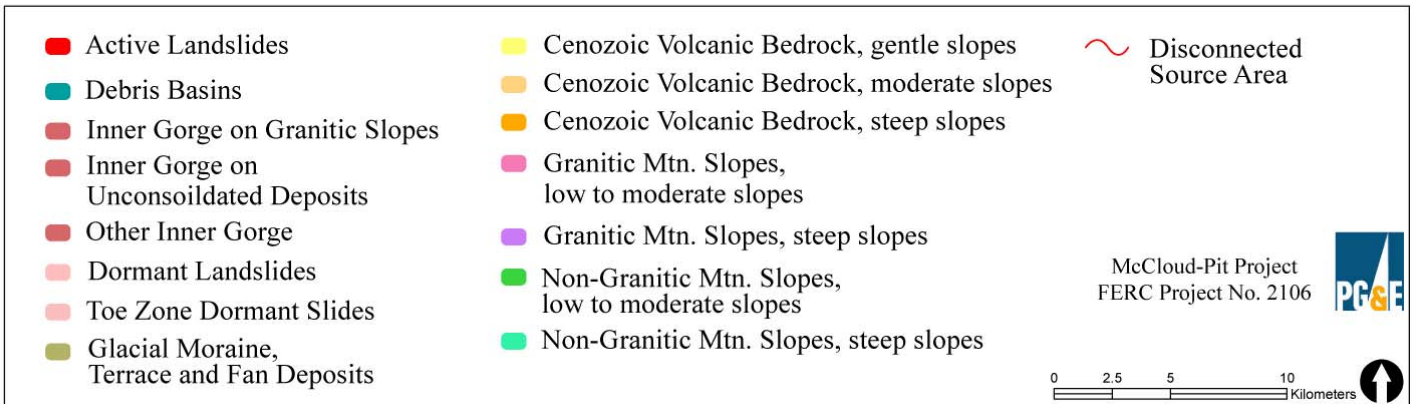
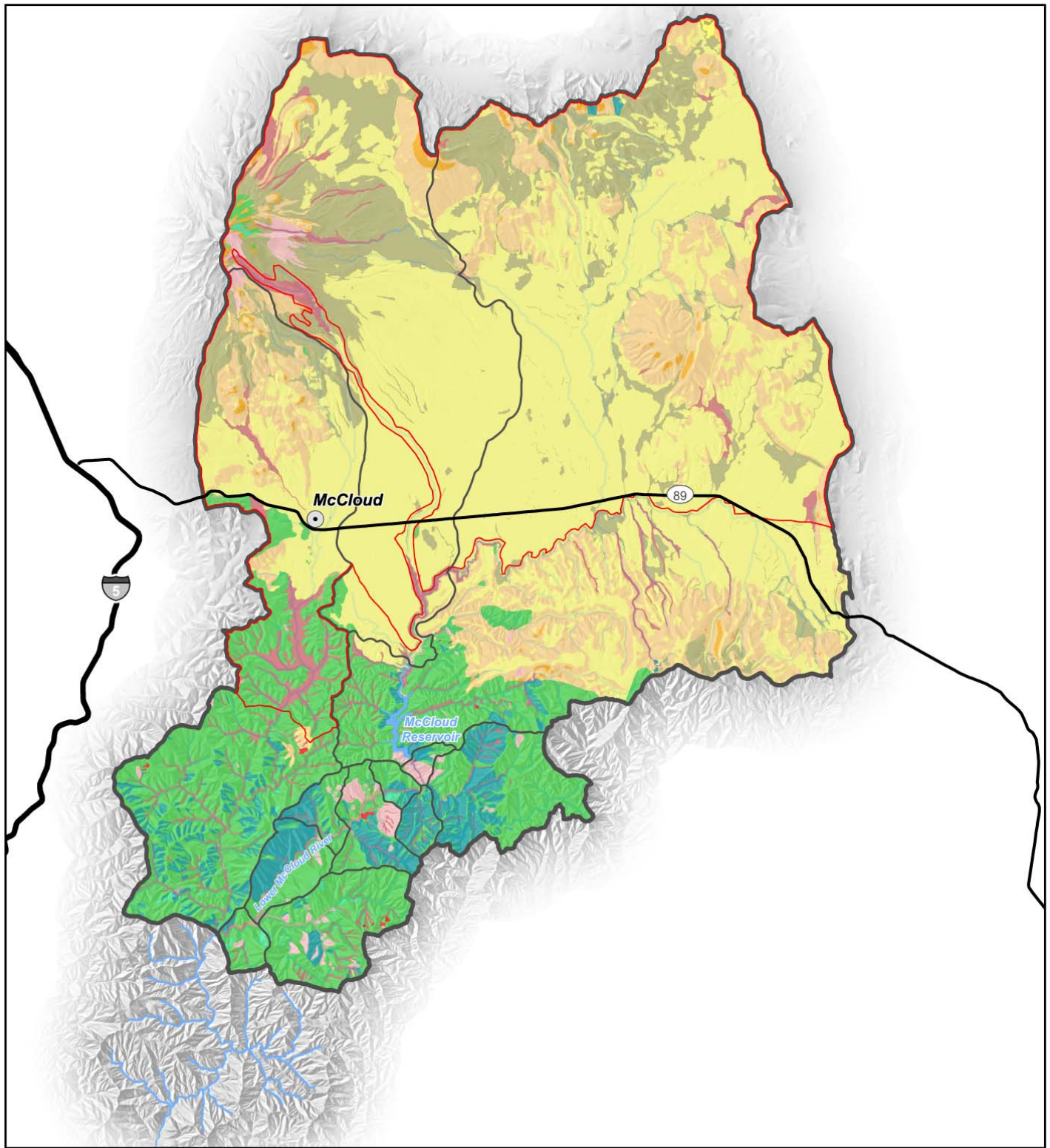


Figure 4. Geomorphology in the GS-S2 Study Area, defined by the USFS Geo 13 geomorphic terrane coverage

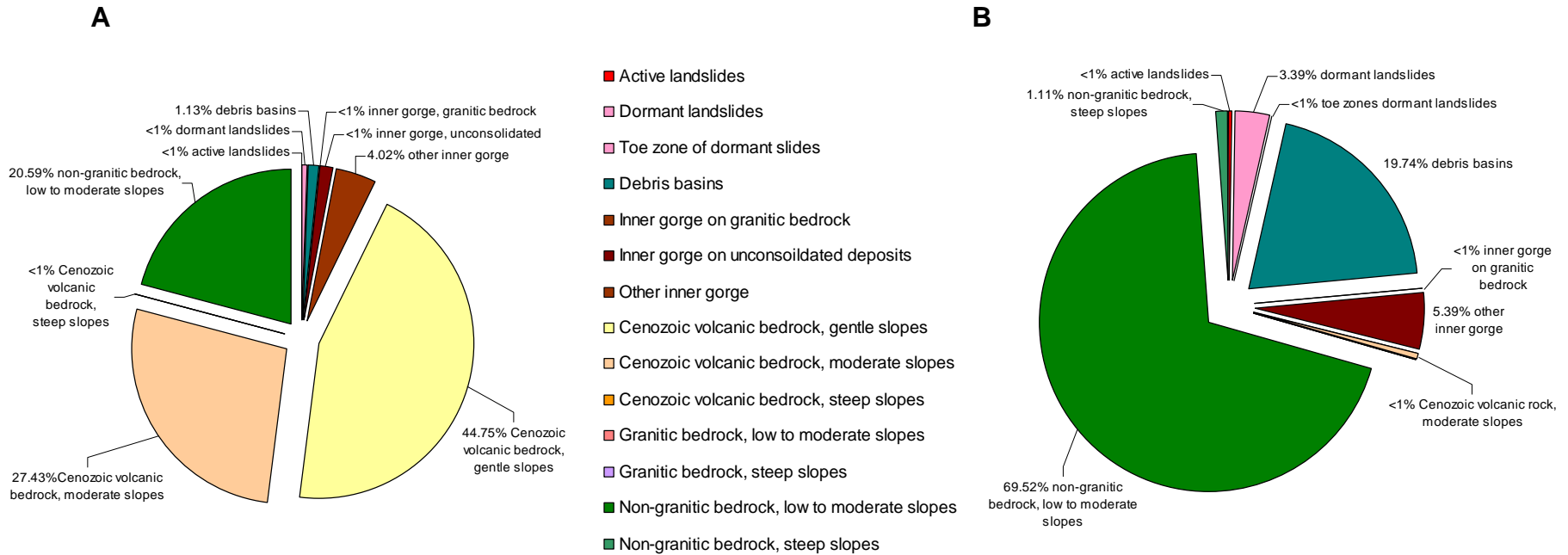


Figure 5. Geomorphic terranes in sediment source areas (A) upstream and (B) downstream of McCloud Dam

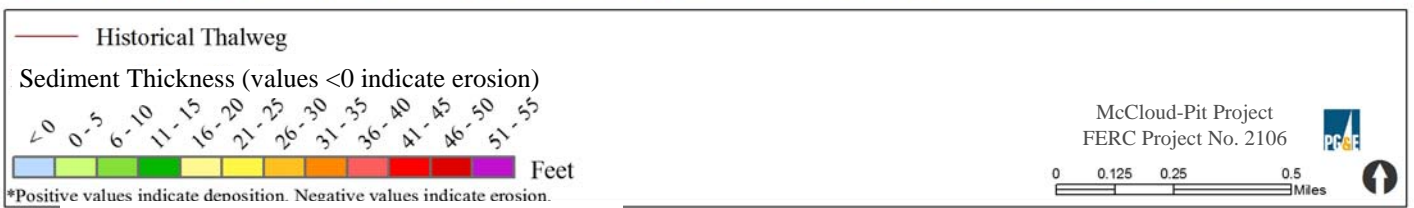
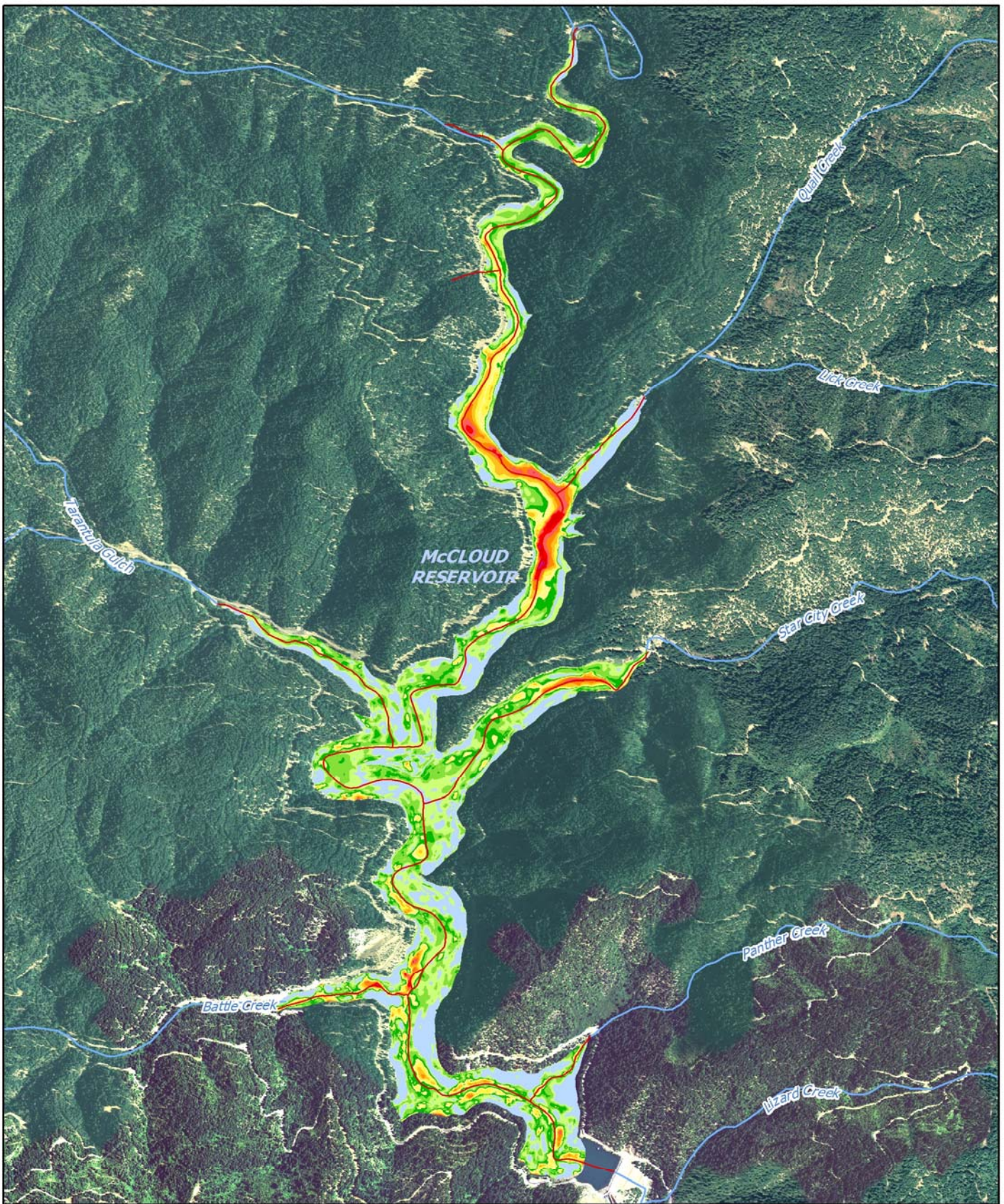


Figure 6. Sediment thickness in McCloud Reservoir

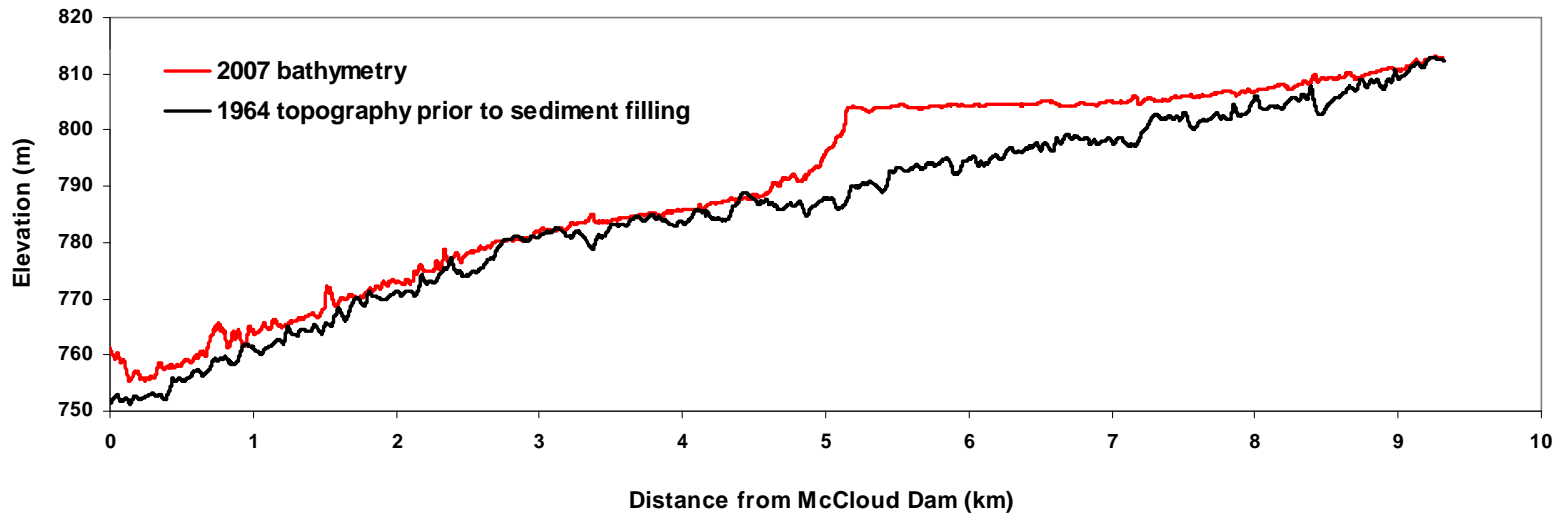


Figure 7. Longitudinal profile of the McCloud River arm of McCloud Reservoir

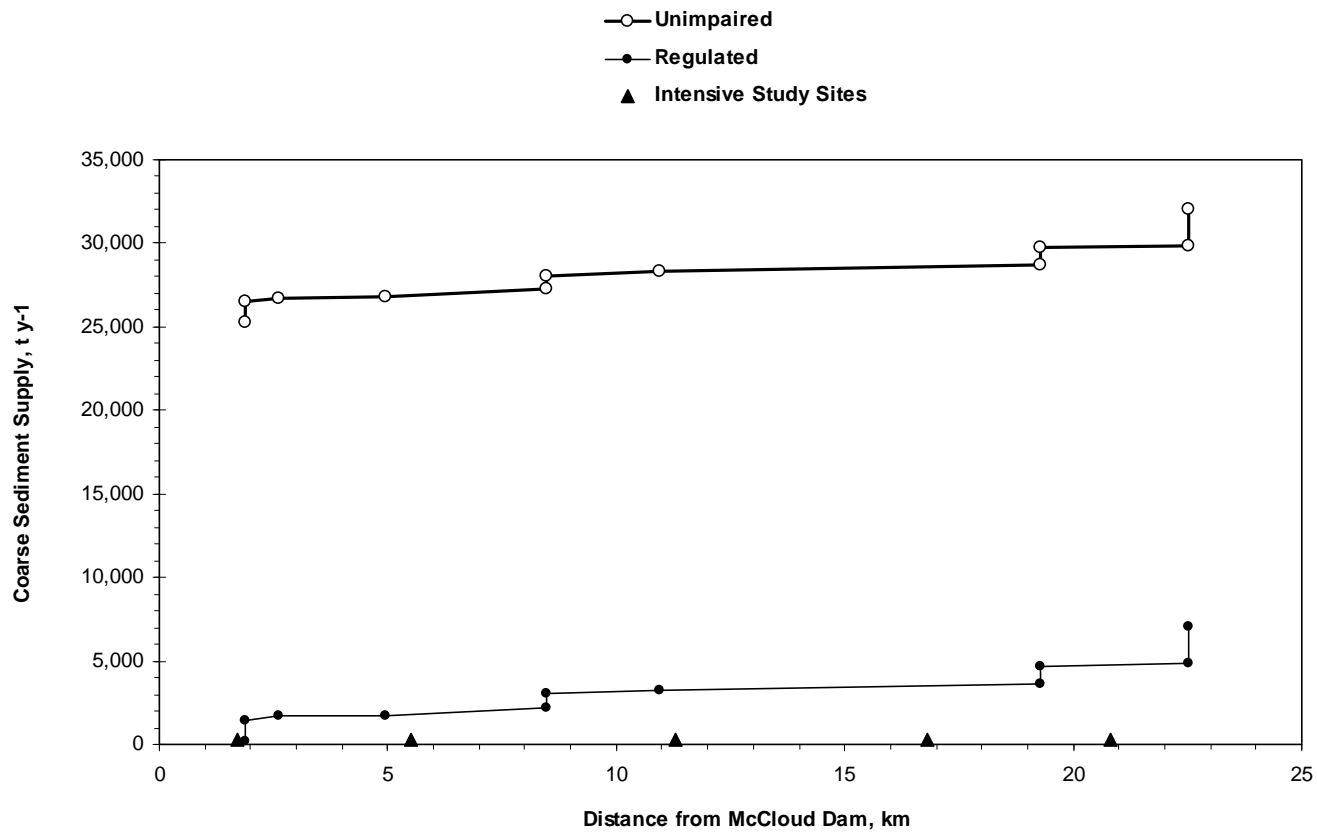


Figure 8. Sediment delivery estimates in the Lower McCloud River

Typical Mass Balance	Typical Slope	Basic Reach Types	Transitional Reach Types
Transport Limited ↑ ↓ Supply Limited	<2%	Pool Riffle (PR)	Riffle Bar (RB) Riffle Step (RS)
	<3%	Plane Bed (BP)	
	3-5%	Step Pool (SP)	
	>5%	Cascade (CS)	

Definitions:

Pool Riffle: Undulating bed defining a sequence of riffles and pools; bar and pool topography formed by either cross-stream flow and sediment transport or forced by channel bends and obstructions.

Riffle Bar: Poorly defined (low amplitude) pool riffle sequences with long sections of plane bed morphology.

Plane Bed: Relatively featureless bed lacking rhythmic bedforms.

Riffle Step: Poorly organized steps (without well-defined pools) separated by predominantly plane bed morphology; commonly steeper and coarser than plane bed.

Step Pool: Longitudinal steps formed by large grains organized into discrete channel-spanning accumulations that separate pools containing finer material.

Cascade: Continuous tumbling flow over and around large grains.

Figure 9. Channel reach types in the Lower McCloud River (modified from Montgomery and Buffington 1998)

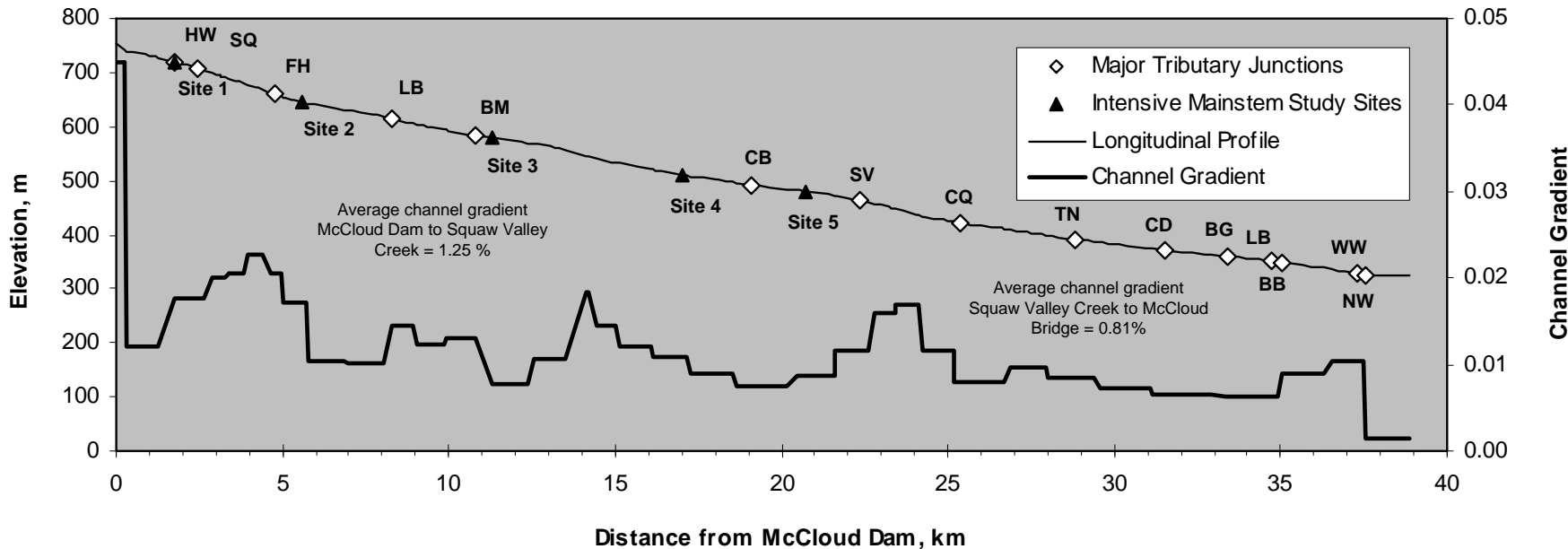


Figure 10. Longitudinal profiles of bed elevation and channel gradient for Lower McCloud River. Major tributaries are Hawkins Creek (HW), Squirrel Creek (SQ), Fitzhugh Creek (FH), Ladybug Creek (LB), Bald Mountain Creek (BM), Claiborne Creek, (CB), Squaw Valley Creek (SV), Chiquito Creek (CQ), Tuna Creek (TN), Chatterdown Creek (CD), Big Gray Creek (BG), Little Bollibokka Creek (LB), Big Bollibokka Creek (BB), Wittawaket Creek (WW), and Nawtawaket Creek (NW)

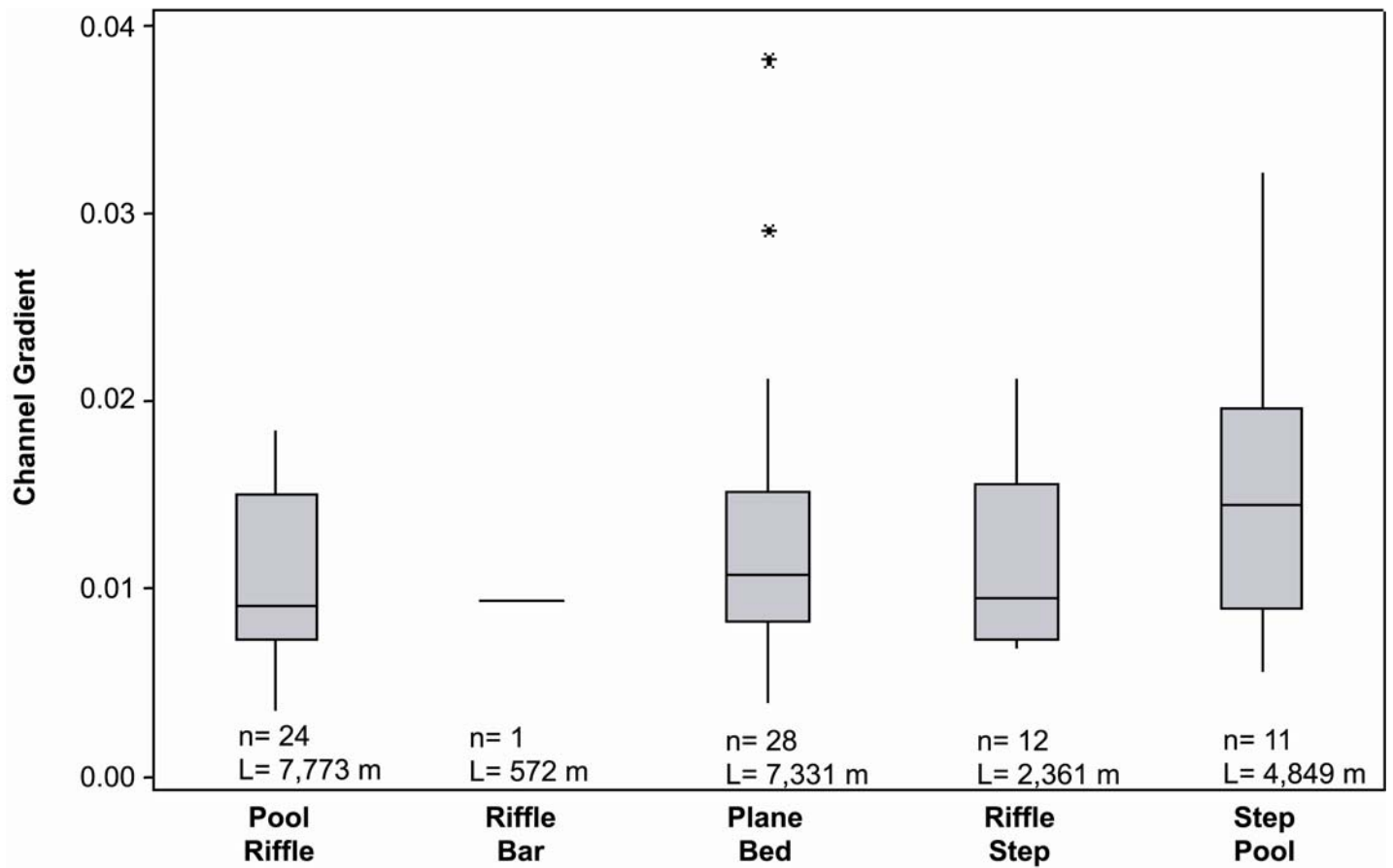
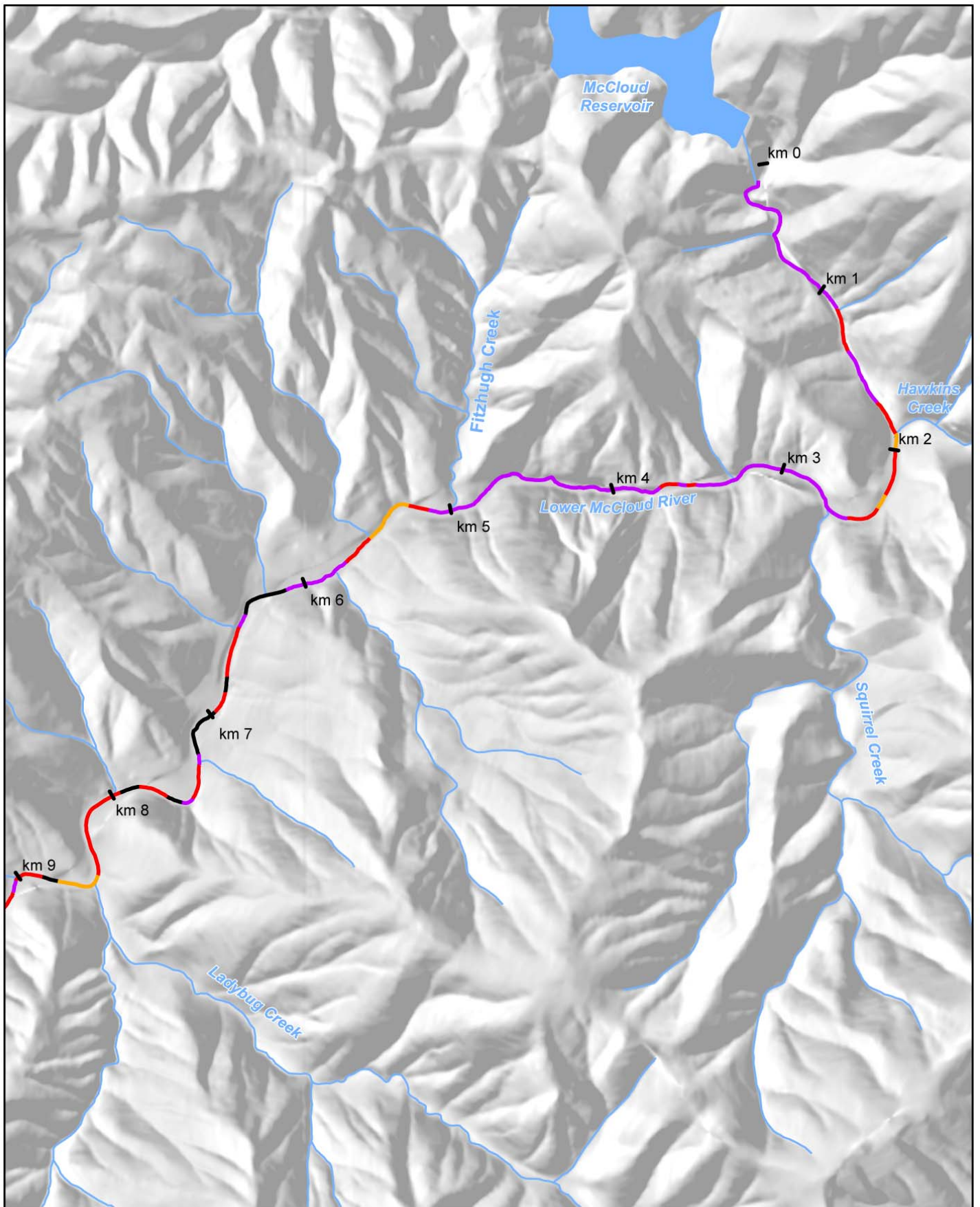


Figure 11. Boxplots comparing channel gradient for channel reach types on the Lower McCloud River, McCloud Dam to Squaw Valley Creek; N= number of reaches, L = total length of channel

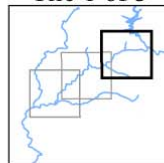


Reach Types

- ~ Pool Riffle (PR)
- ~ Riffle Bar (RB)
- ~ Plane Bed (PB)
- ~ Riffle Step (RS)
- ~ Step Pool (SP)

*There were no occurrences of cascade reach

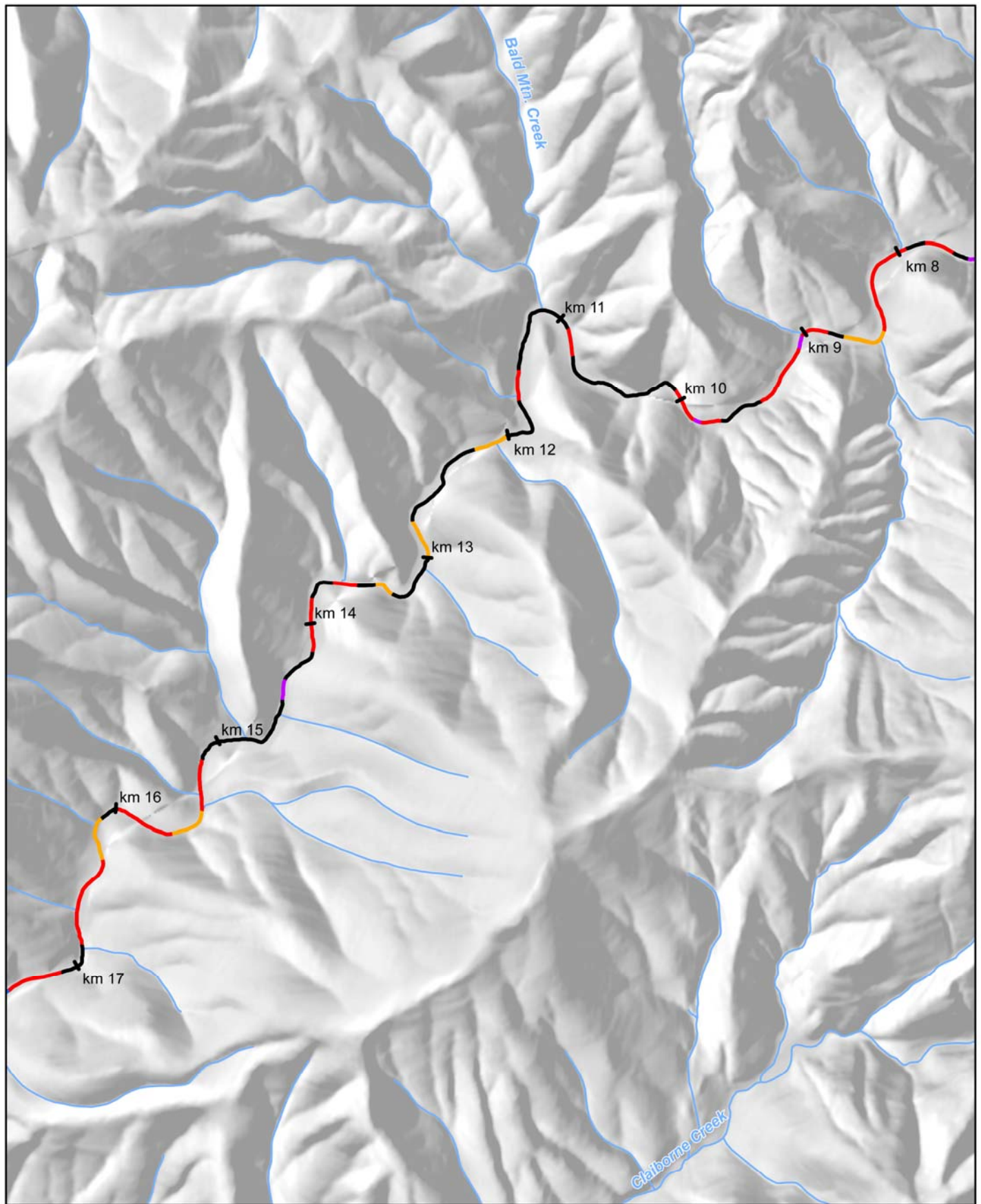
Tile 1 of 3

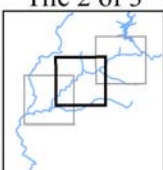


McCloud-Pit Project
FERC Project No. 2106



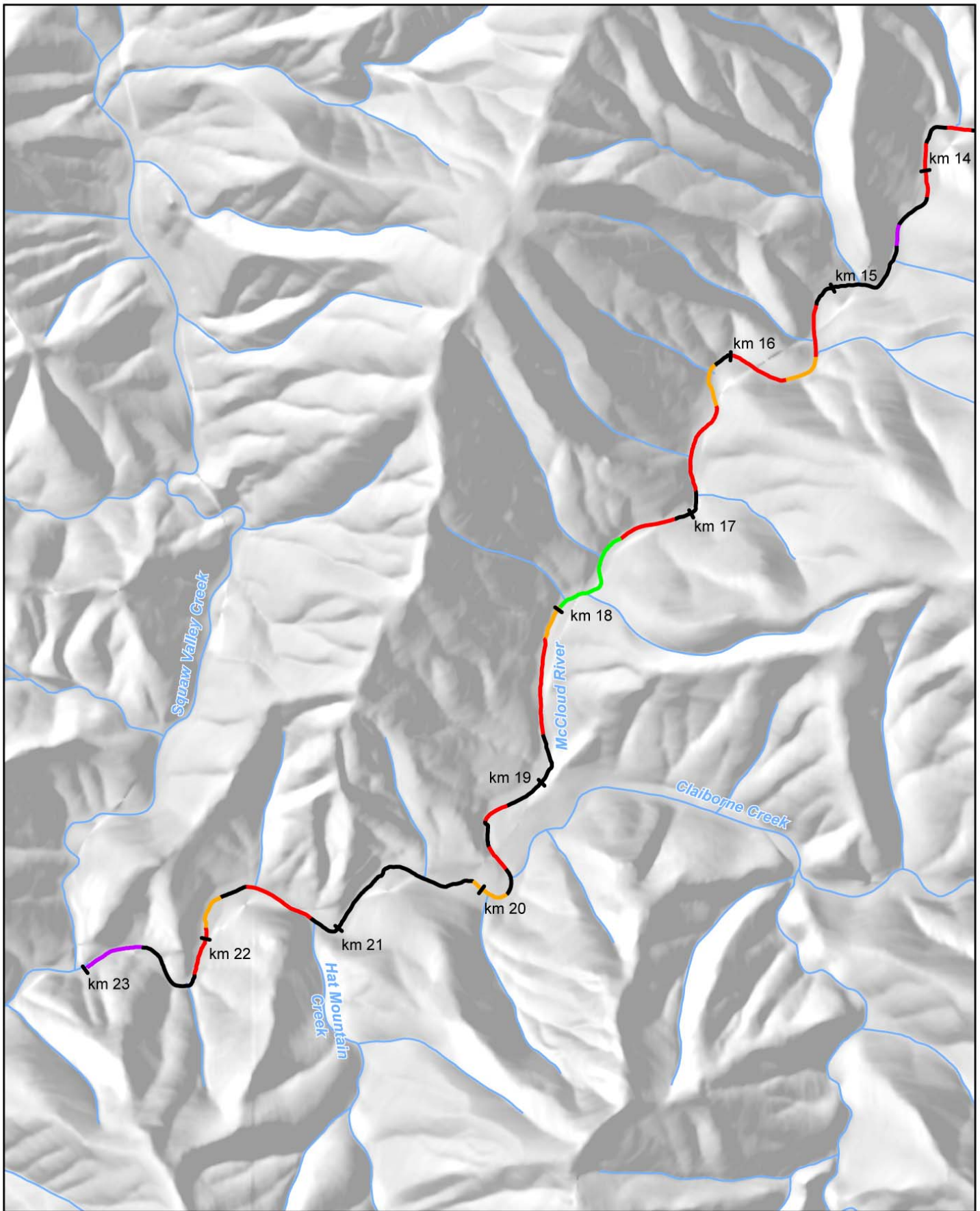
Figure 12a. Channel reach morphology on the Lower McCloud River from McCloud Dam to Squaw Valley Creek



Reach Types		Tile 2 of 3 	McCloud-Pit Project FERC Project No. 2106 
 Pool Riffle (PR)  Plane Bed (PB)  Step Pool (SP)	 Riffle Bar (RB)  Riffle Step (RS)		

*There were no occurrences of cascade reach

Figure 12b. Channel reach morphology on the Lower McCloud River from McCloud Dam to Squaw Valley Creek



Reach Types		<p>Tile 3 of 3</p>	<p>McCloud-Pit Project FERC Project No. 2106</p>
Pool Riffle (PR) Plane Bed (PB) Step Pool (SP)	Riffle Bar (RB) Riffle Step (RS)		

*There were no occurrences of cascade reach

Figure 12c. Channel reach morphology on the Lower McCloud River from McCloud Dam to Squaw Valley Creek

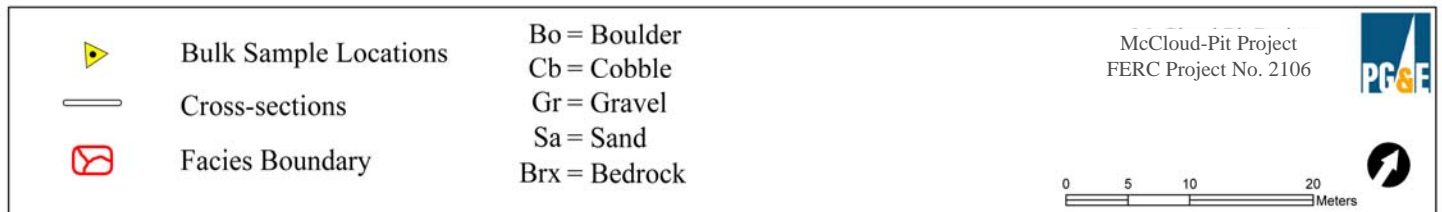
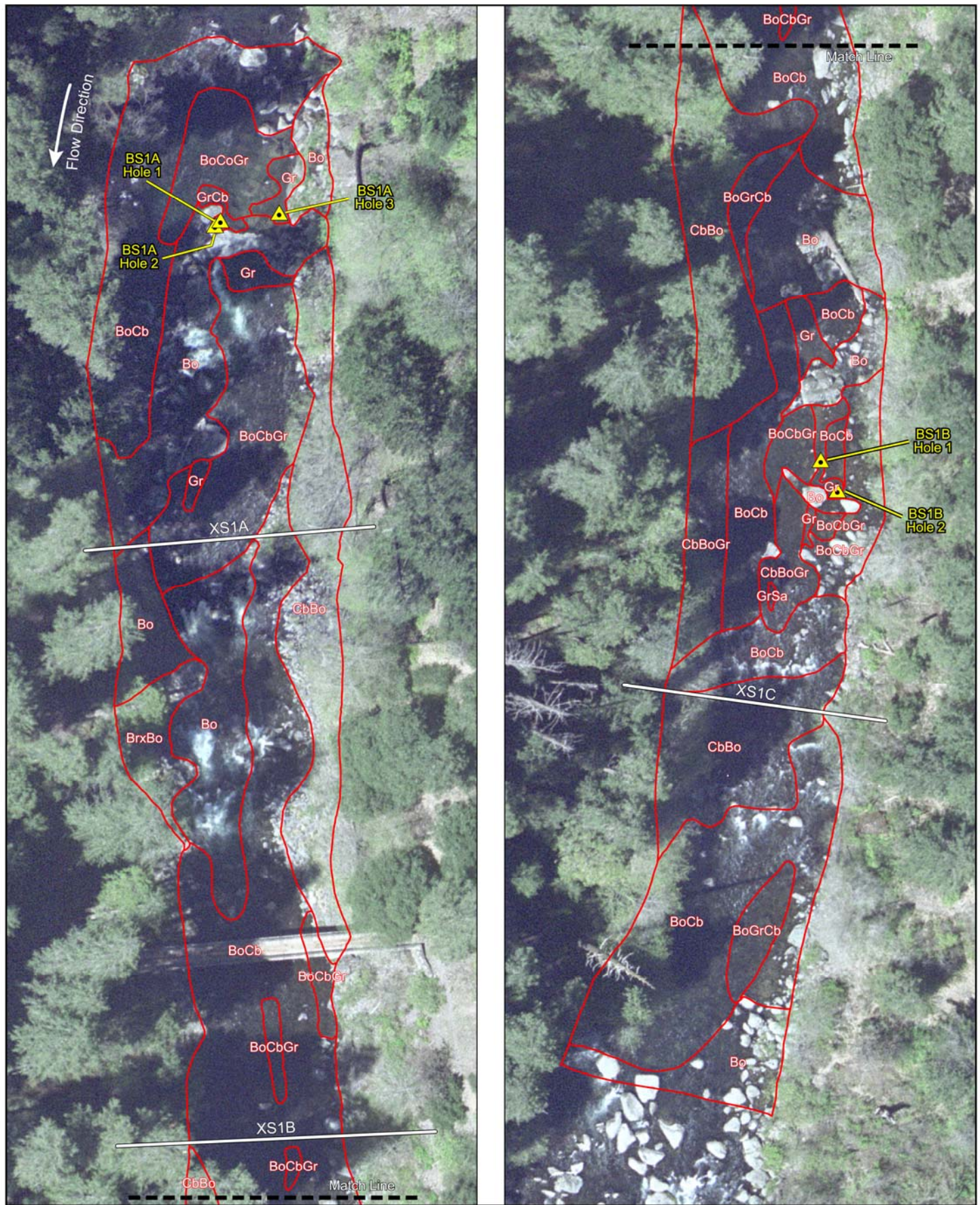
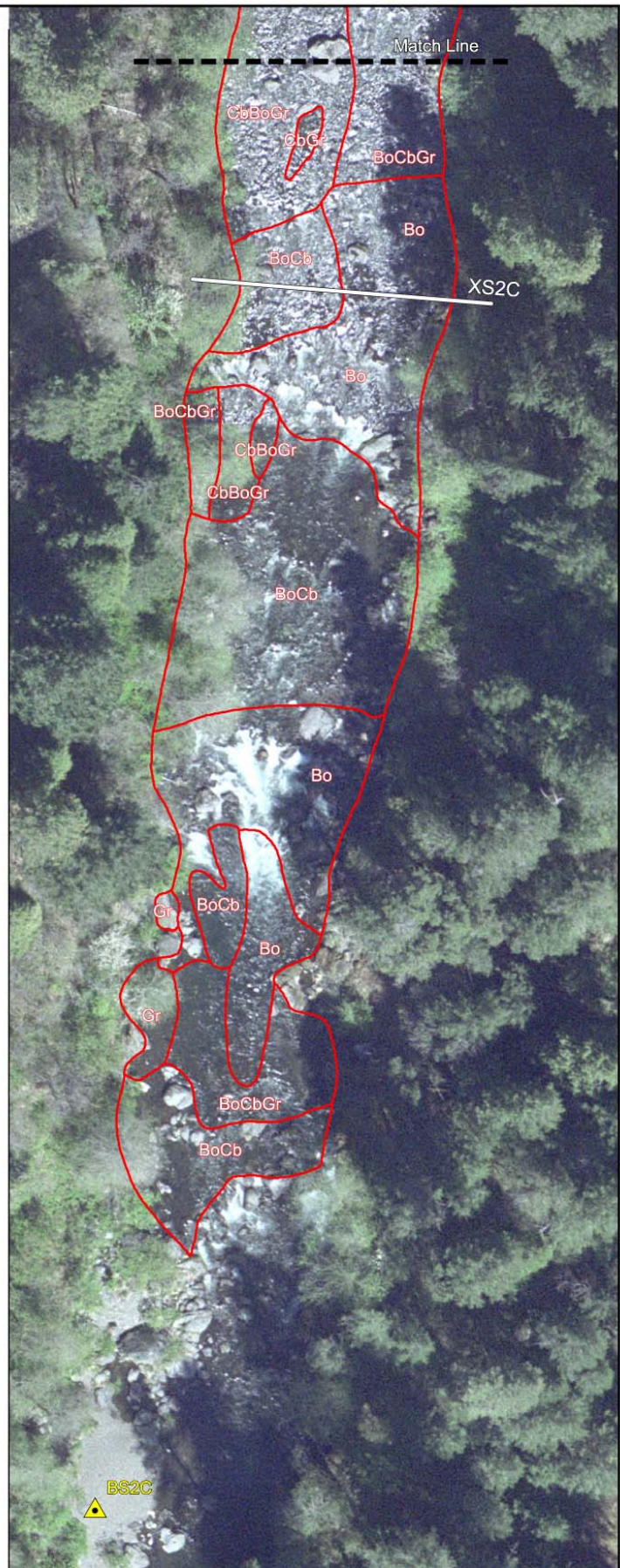
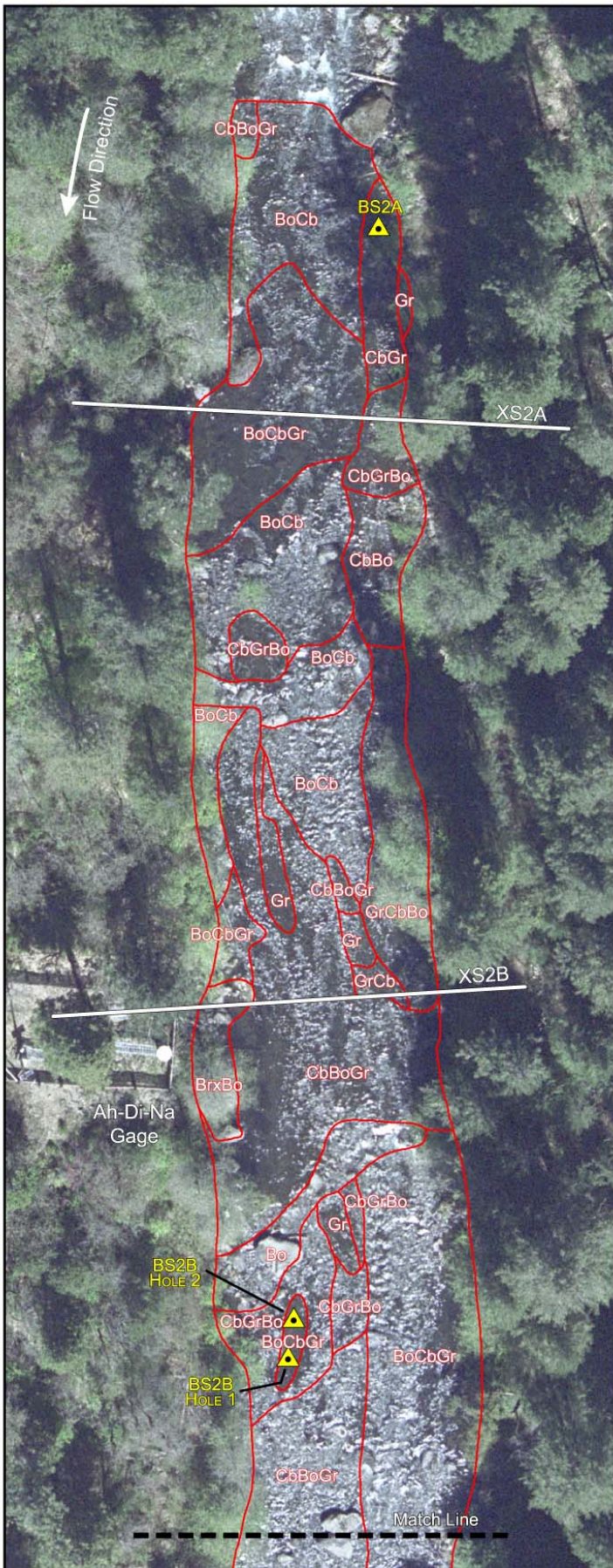


Figure 13. Intensive Study Site 1, located upstream of the Hawkins Creek confluence



	Bulk Sample Locations	Bo = Boulder
	Cross-sections	Cb = Cobble
	Facies Boundary	Gr = Gravel
		Sa = Sand
		Brx = Bedrock

McCloud-Pit Project
FERC Project No. 2106



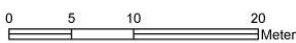



Figure 14. Intensive Study Site 2, located at Ah-Di-Na

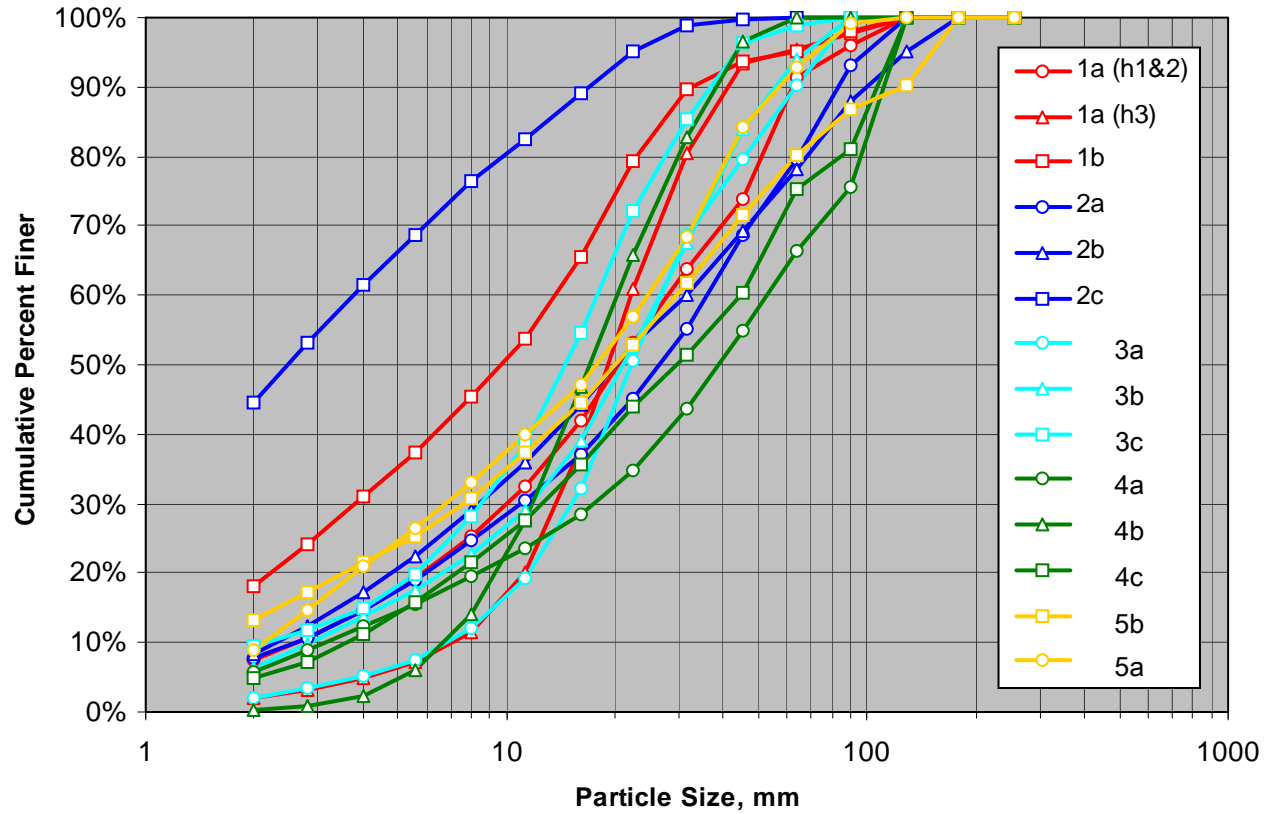


Figure 15. Particle size distributions of bulk samples collected at mainstem intensive study sites. Numeric ID of each sample denotes the intensive study site where the bulk sample was collected

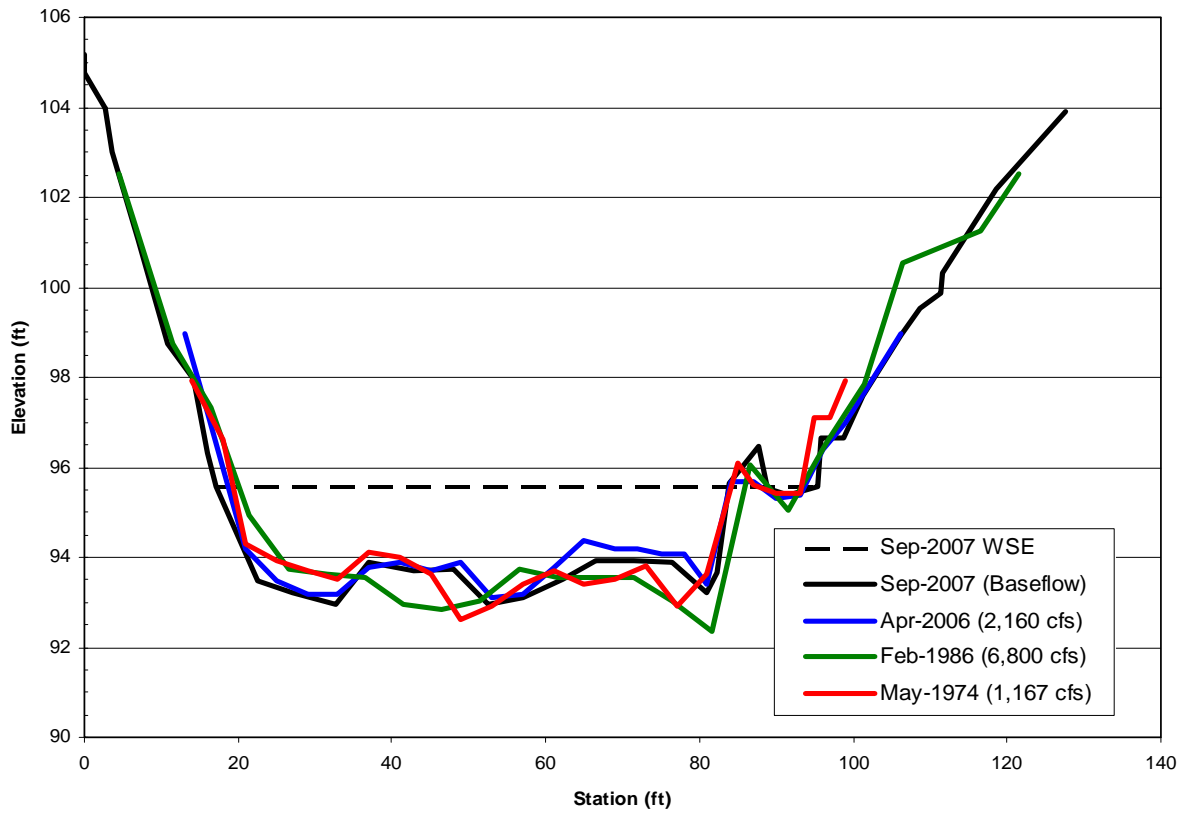


Figure 16. Comparison of historical cross-sections at the MC-1 gaging cableway (1974-2007)

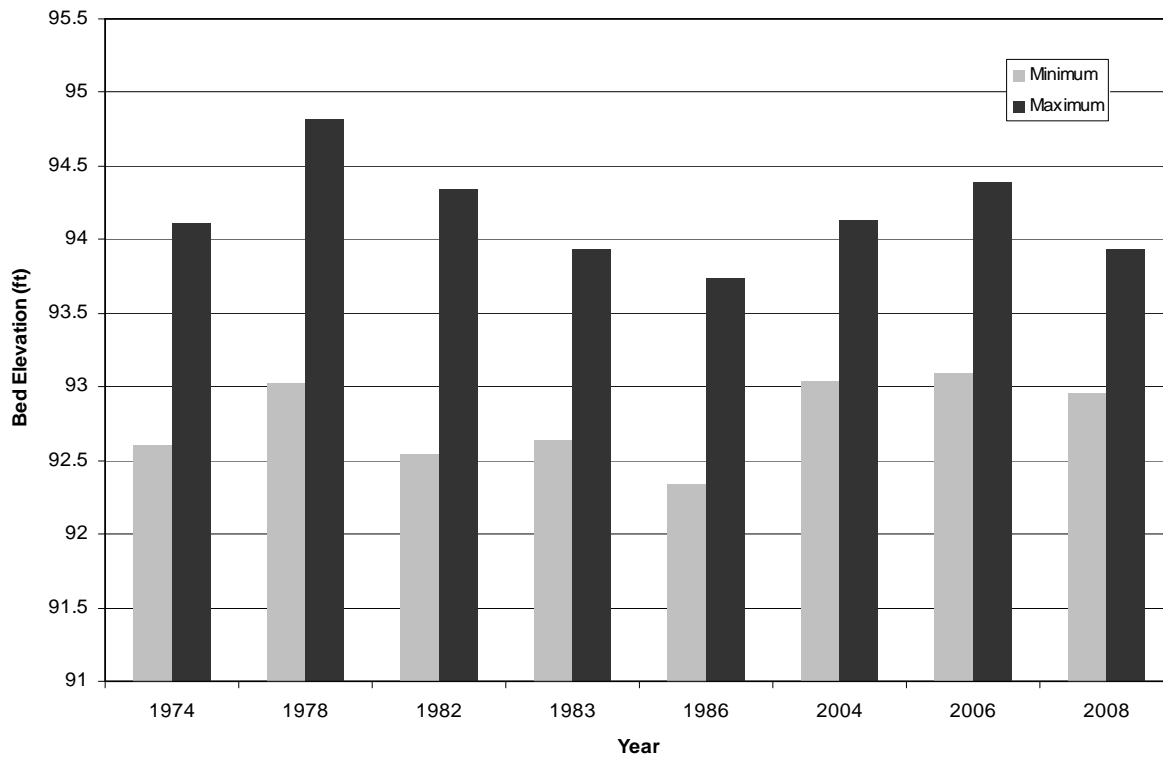
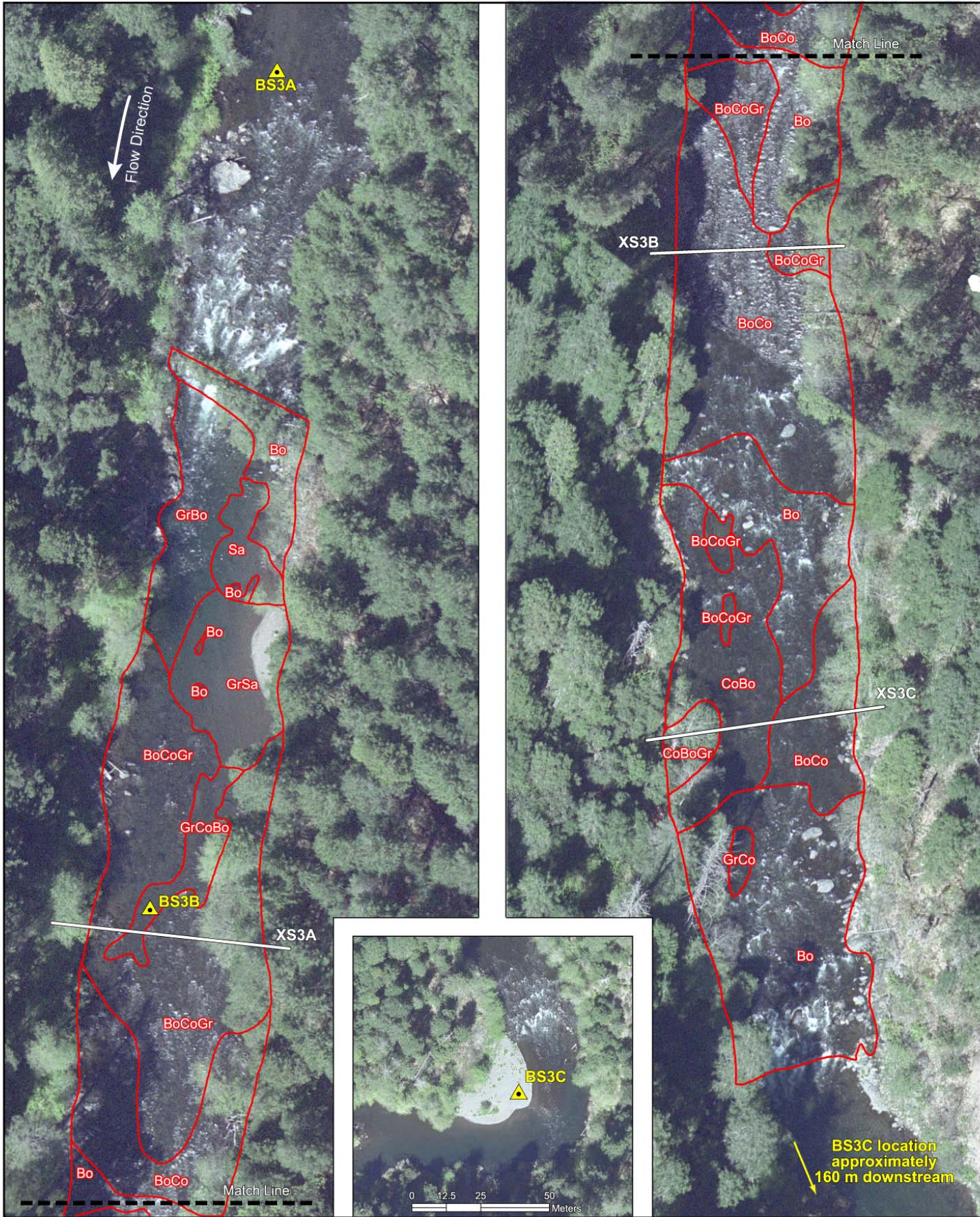


Figure 17. Variation in minimum (thalweg) and maximum bed elevations within the low-flow wetted channel width at the MC-1 gaging cableway (1974-2008)



	Bulk Sample Locations	Bo = Boulder
	Cross-sections	Cb = Cobble
	Facies Boundary	Gr = Gravel
		Sa = Sand
		Brx = Bedrock

McCloud-Pit Project
FERC Project No. 2106



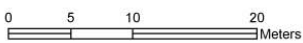
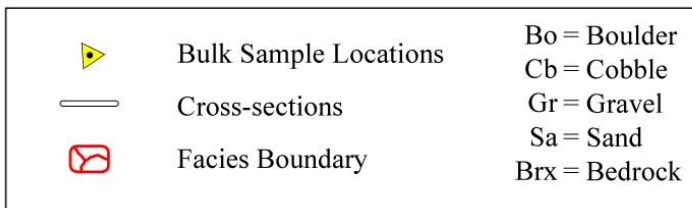
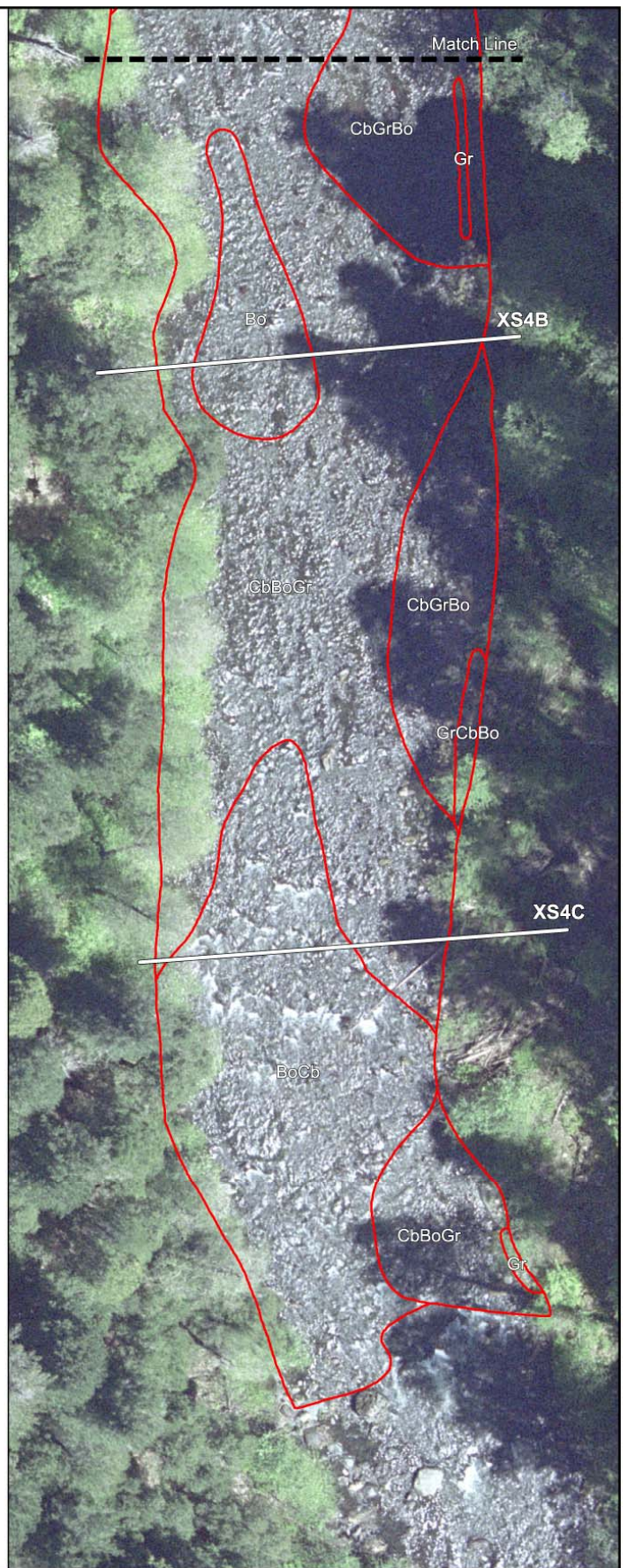
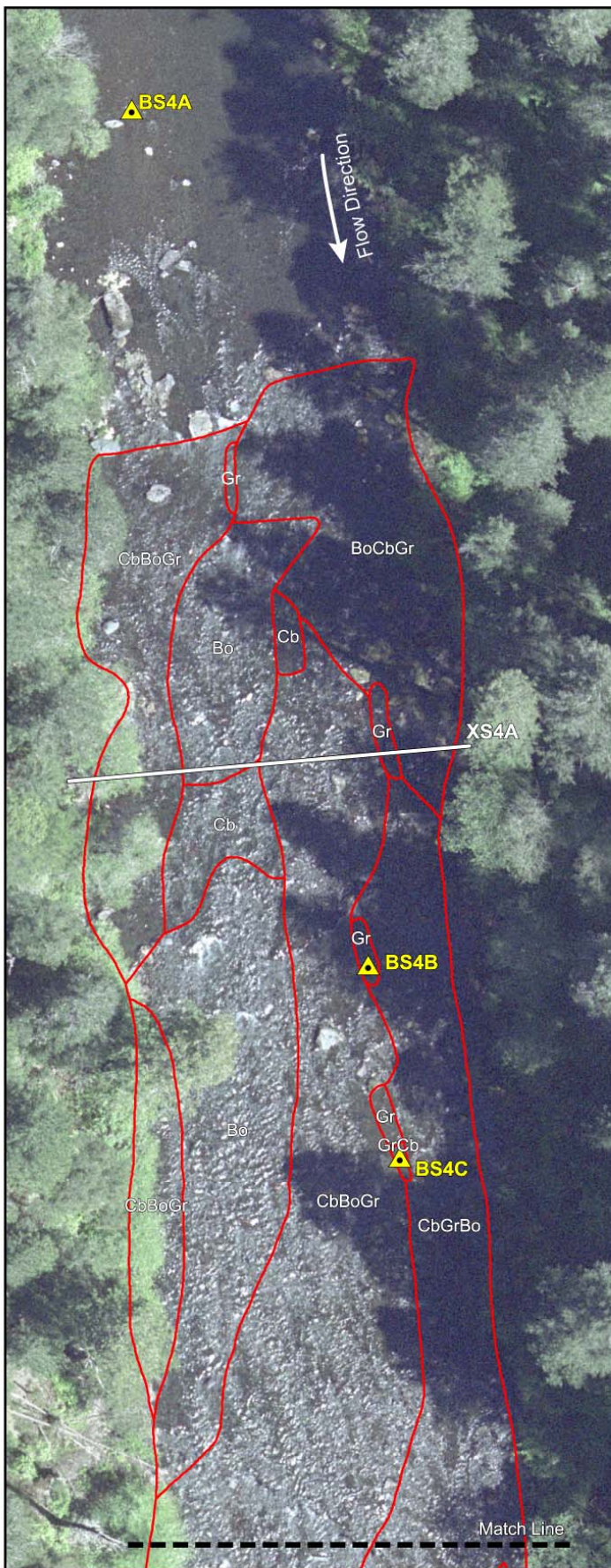



Figure 18. Intensive Study Site 3, located downstream of Bald Mountain Creek



McCloud-Pit Project
FERC Project No. 2106

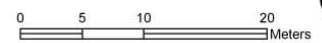
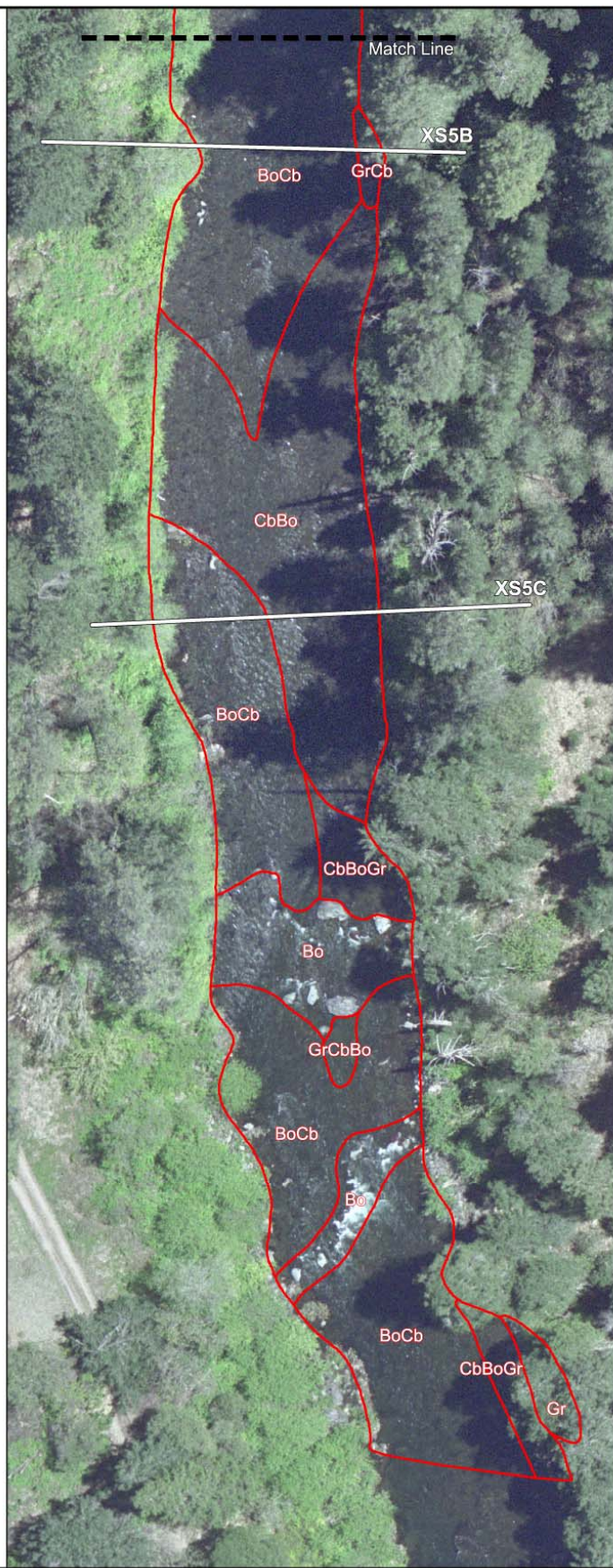
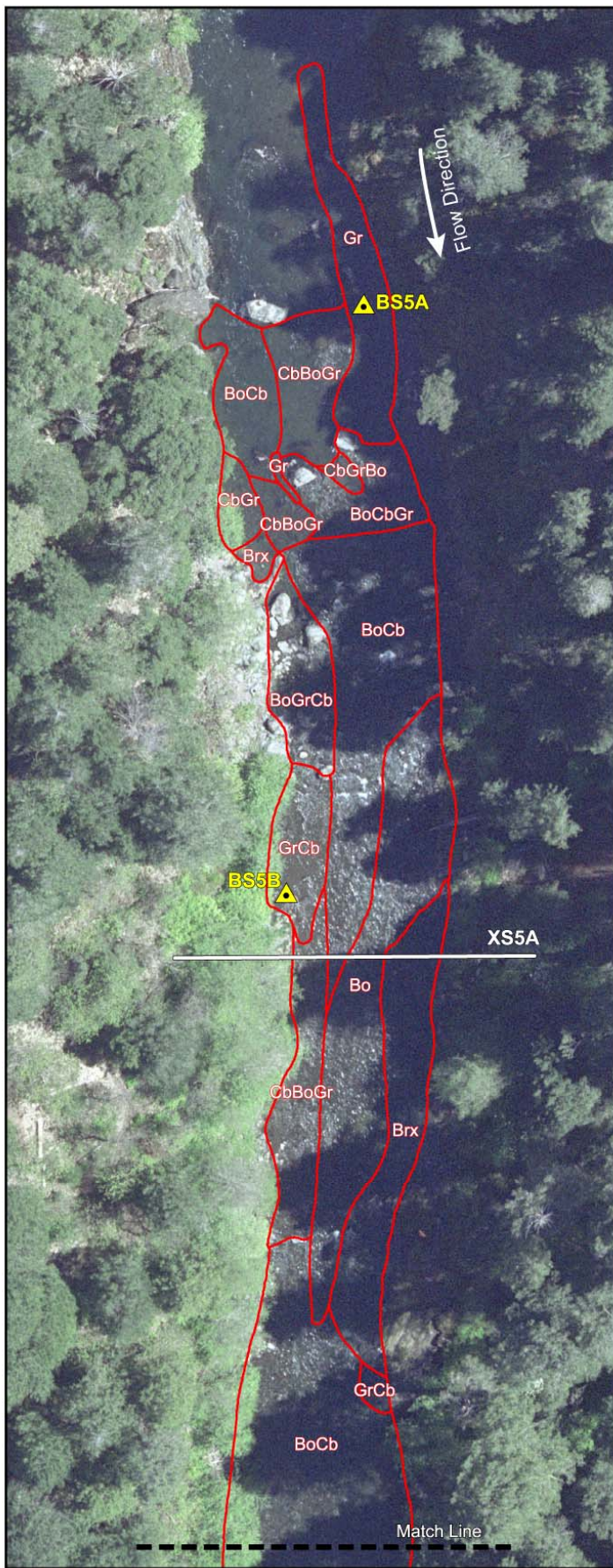


Figure 19. Intensive Study Site 4, located in the vicinity of T37N, R3W, Sec. 14



	Bulk Sample Locations	Bo = Boulder
	Cross-sections	Cb = Cobble
	Facies Boundary	Gr = Gravel
		Sa = Sand
		Brx = Bedrock

McCloud-Pit Project
FERC Project No. 2106



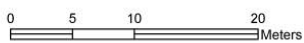



Figure 20. Intensive Study Site 5, located upstream of Hamilton Bend

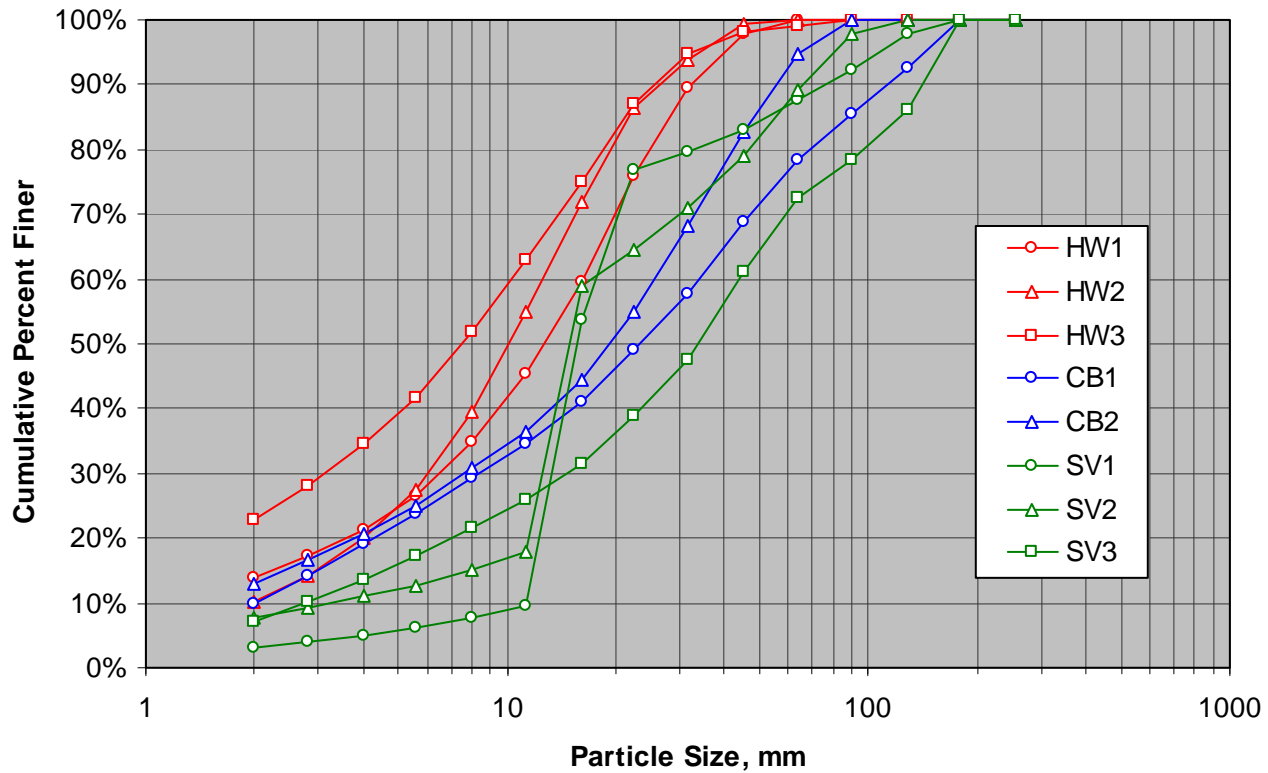


Figure 21. Particle size distributions of bulk samples collected at tributary bed texture study sites. Tributary samples include: Hawkins Creek (HW), Claiborne Creek (CB), and Squaw Valley Creek (SV)

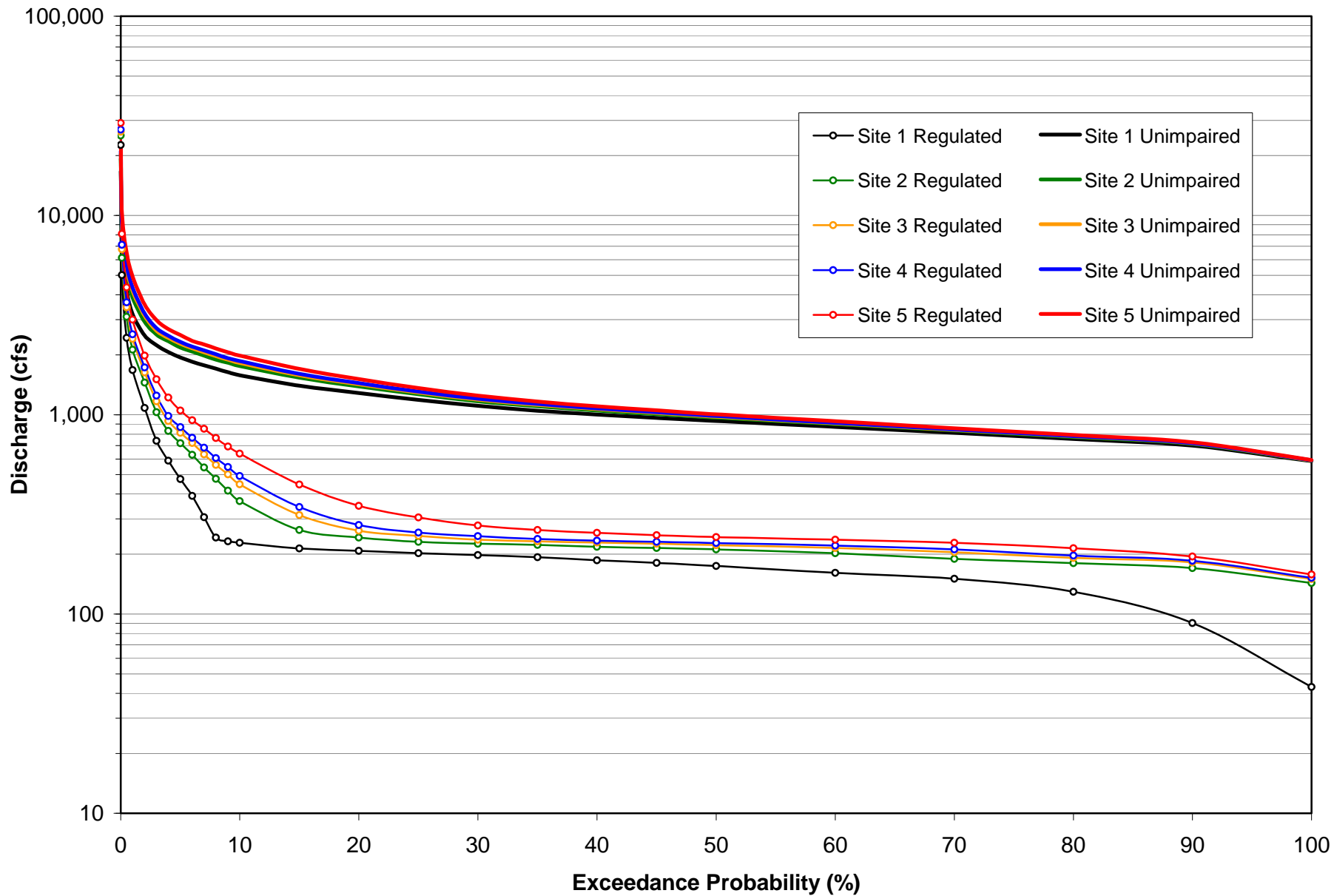


Figure 22. (A) Annual flow exceedance curves for regulated and unimpaired synthetic hydrology from WY 1974 to 2006 at the five intensive study sites

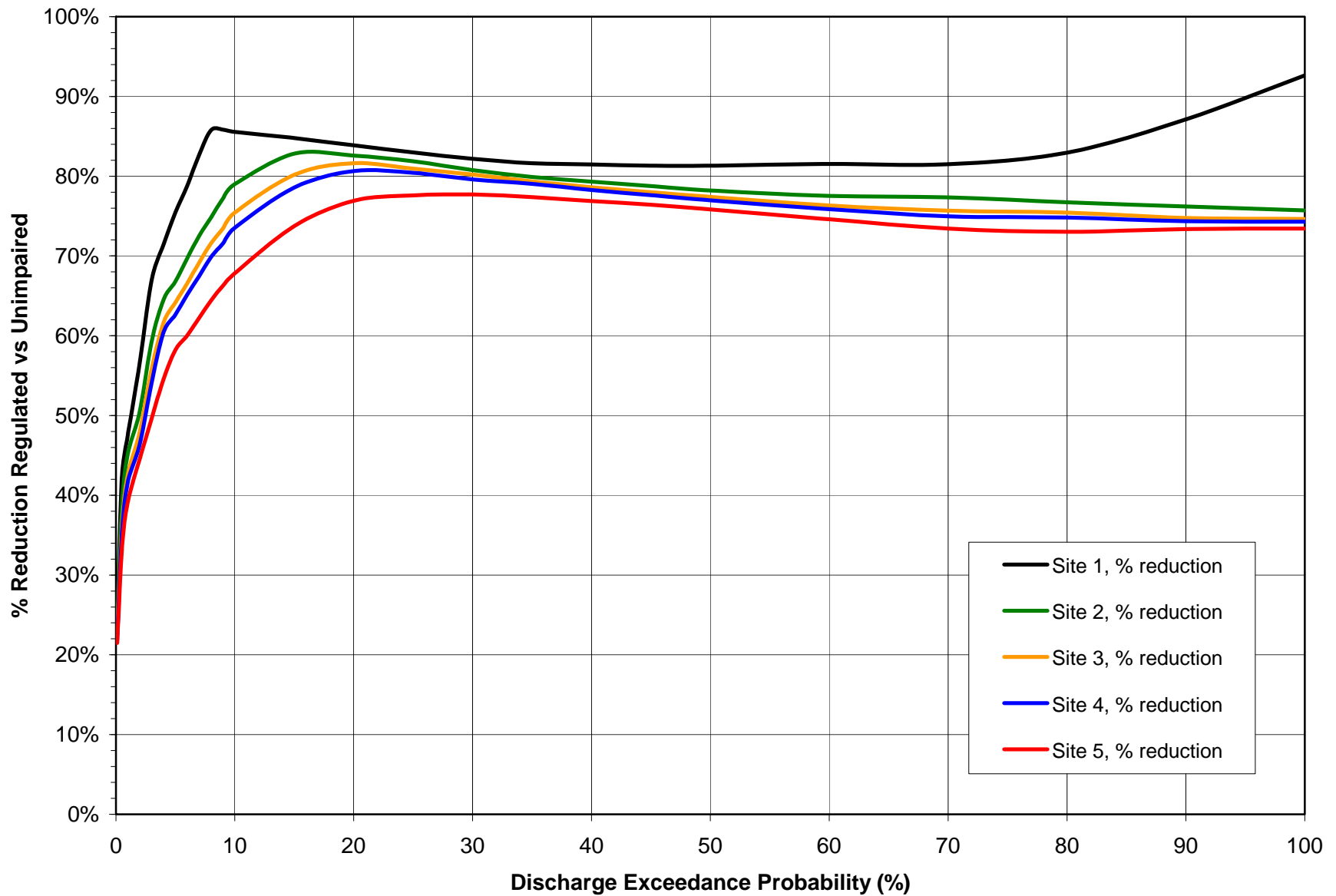


Figure 23. The percent flow reduction from unimpaired to regulated synthetic hydrologies for annual flow exceedance curves

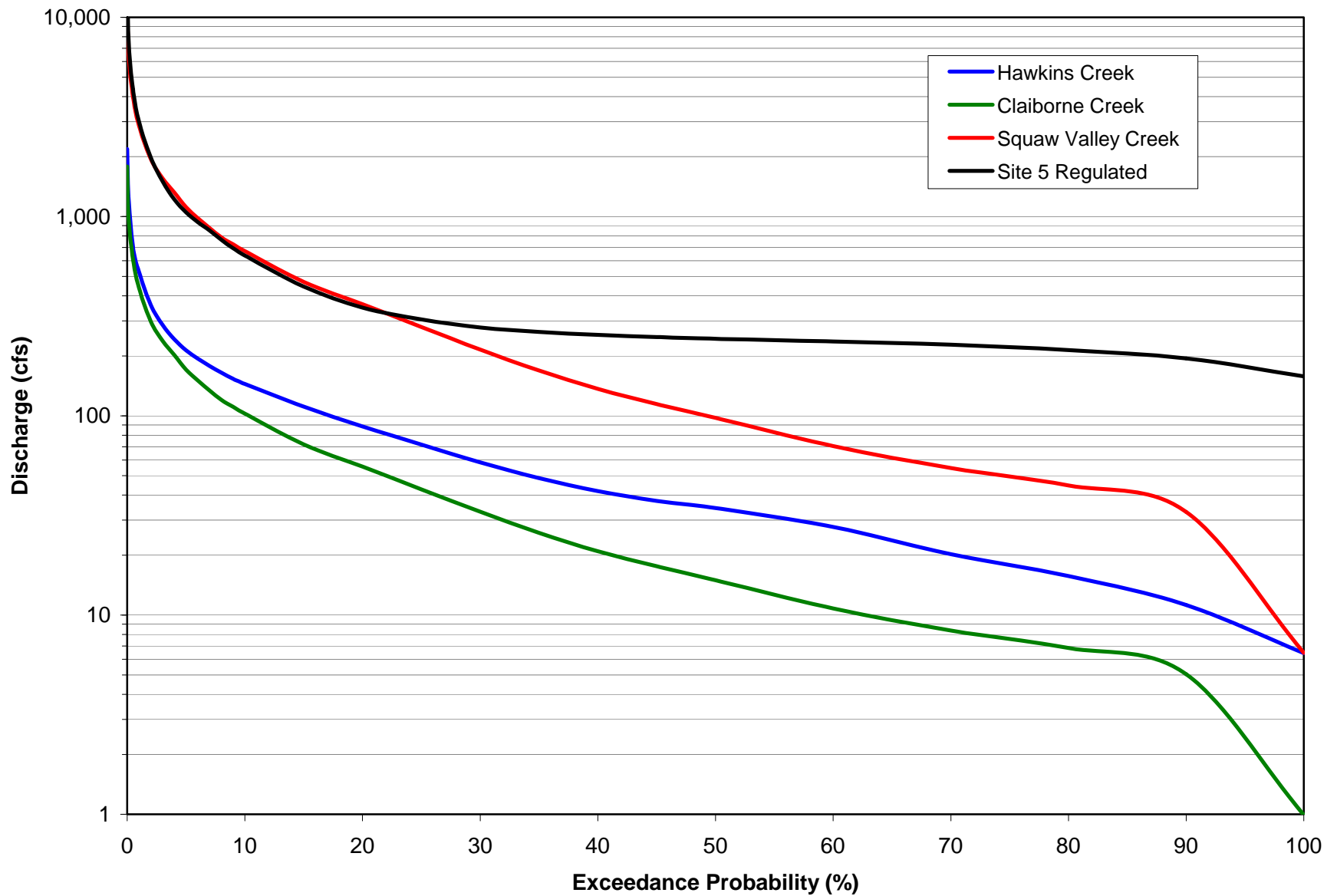


Figure 24. Annual flow exceedance curves for primary tributaries to the Lower McCloud River in the GS-S2 Study Area

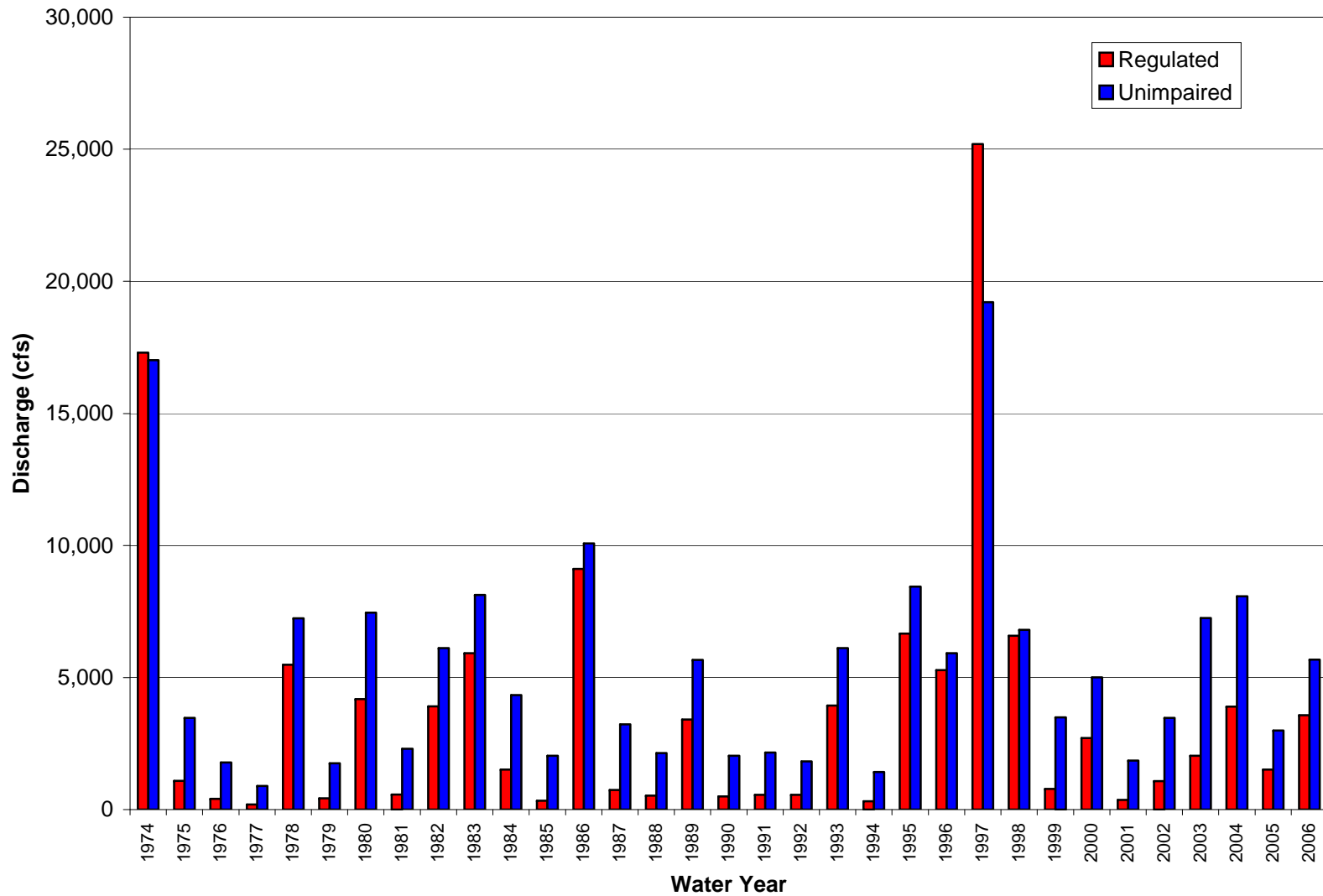


Figure 25. Annual maximum daily discharge at Intensive Study Site 2 (Gage MC-1) based on gage data for the regulated conditions and synthetic hydrology for unimpaired conditions

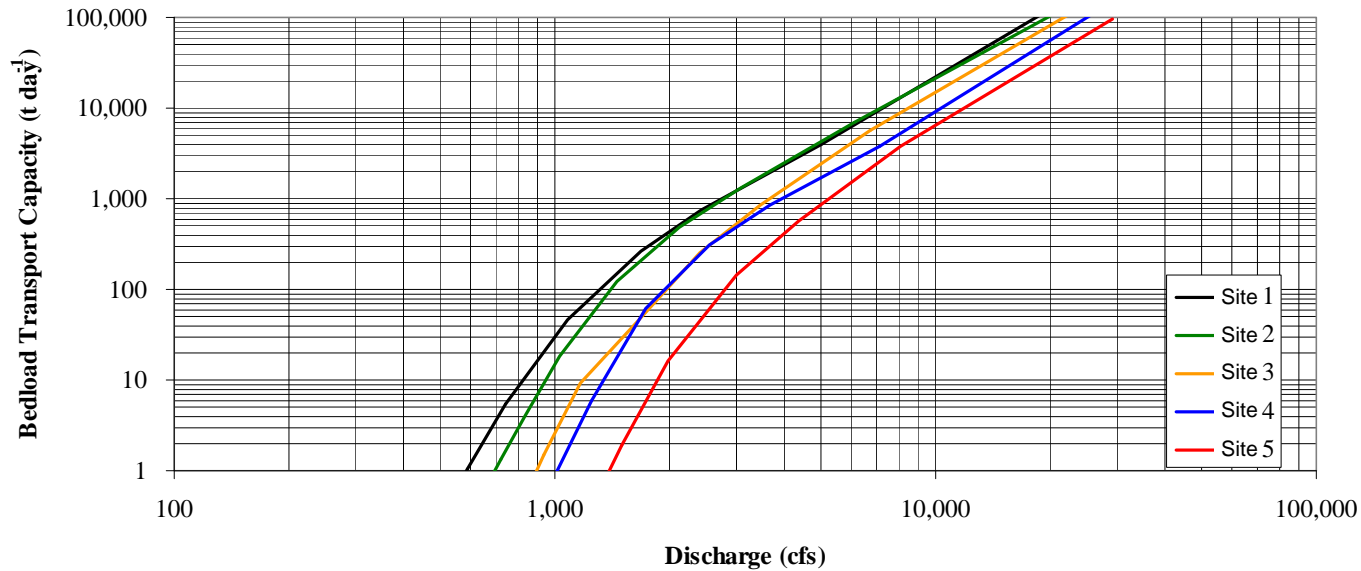
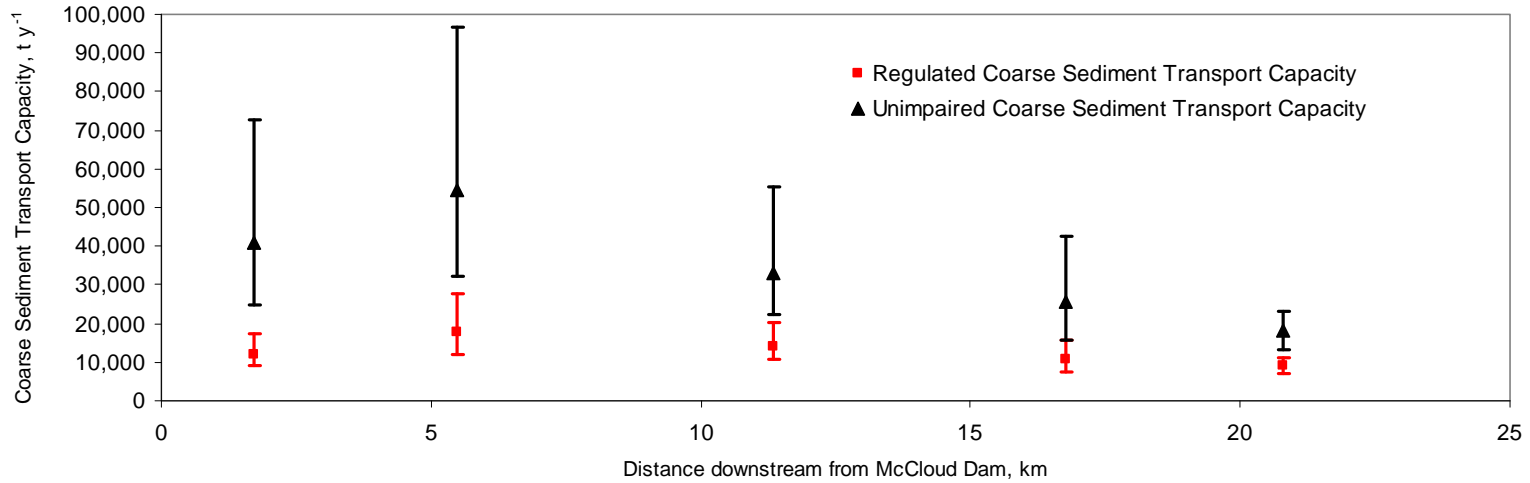


Figure 26. (A) Average annual bedload transport capacity under regulated and unimpaired flow conditions at the five intensive study sites plotted by distance downstream of McCloud Dam; and (B) bedload transport capacities by discharge

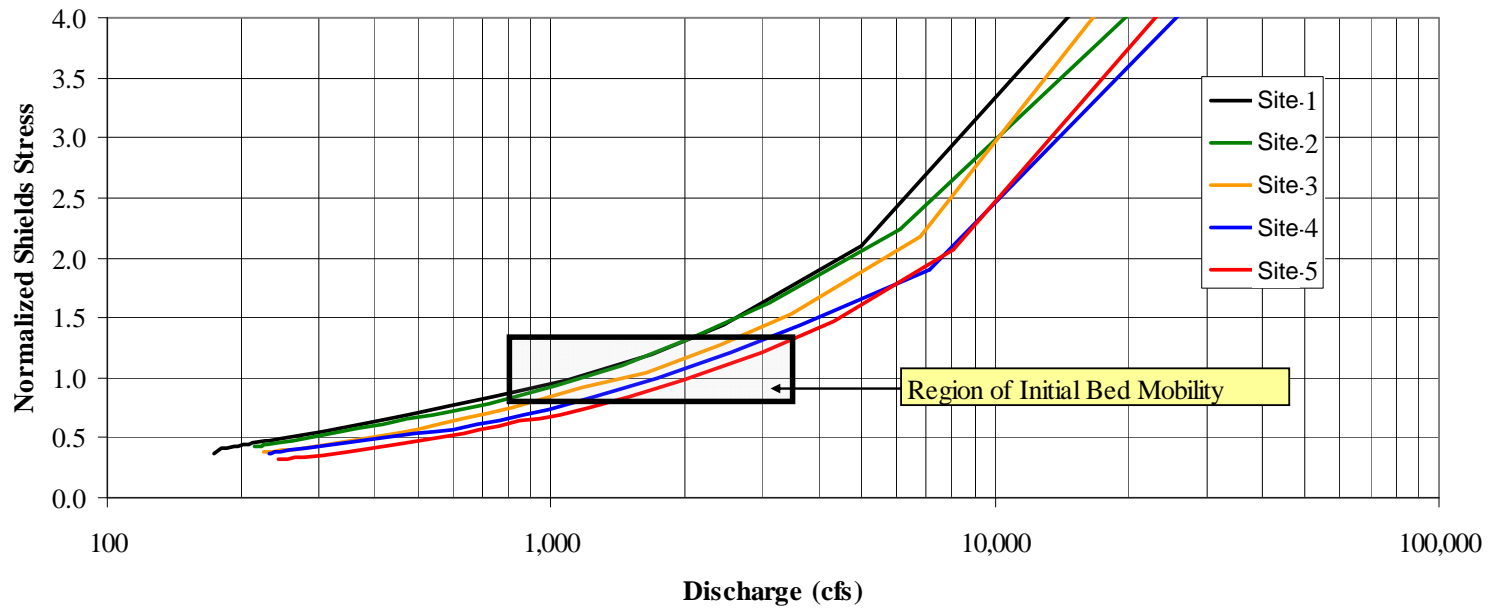
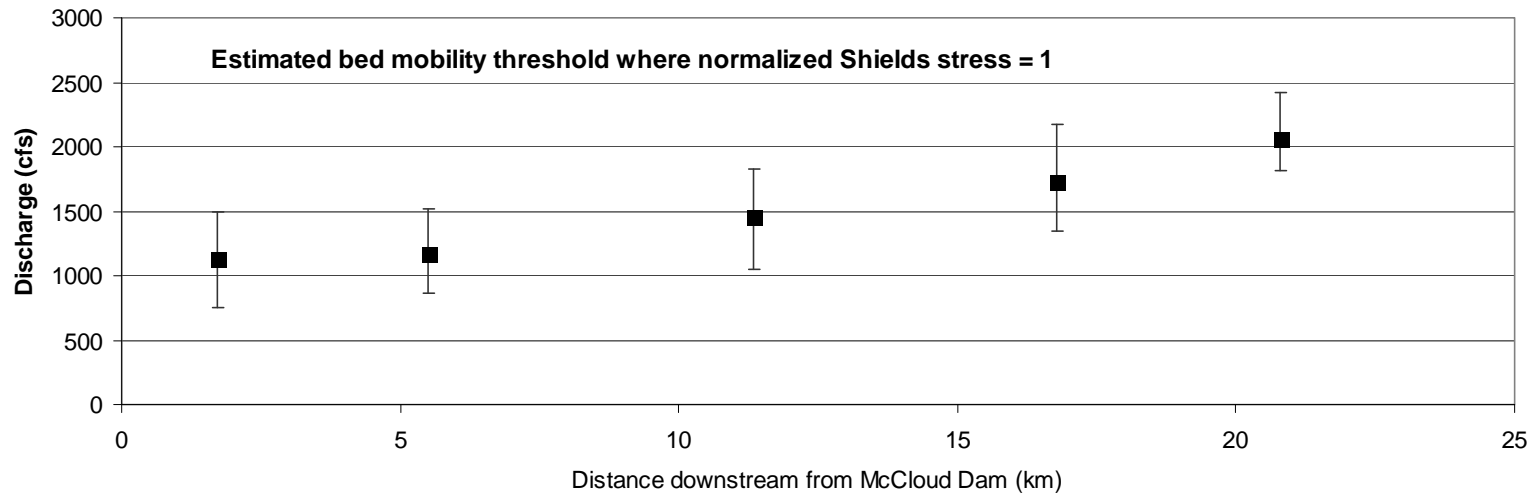
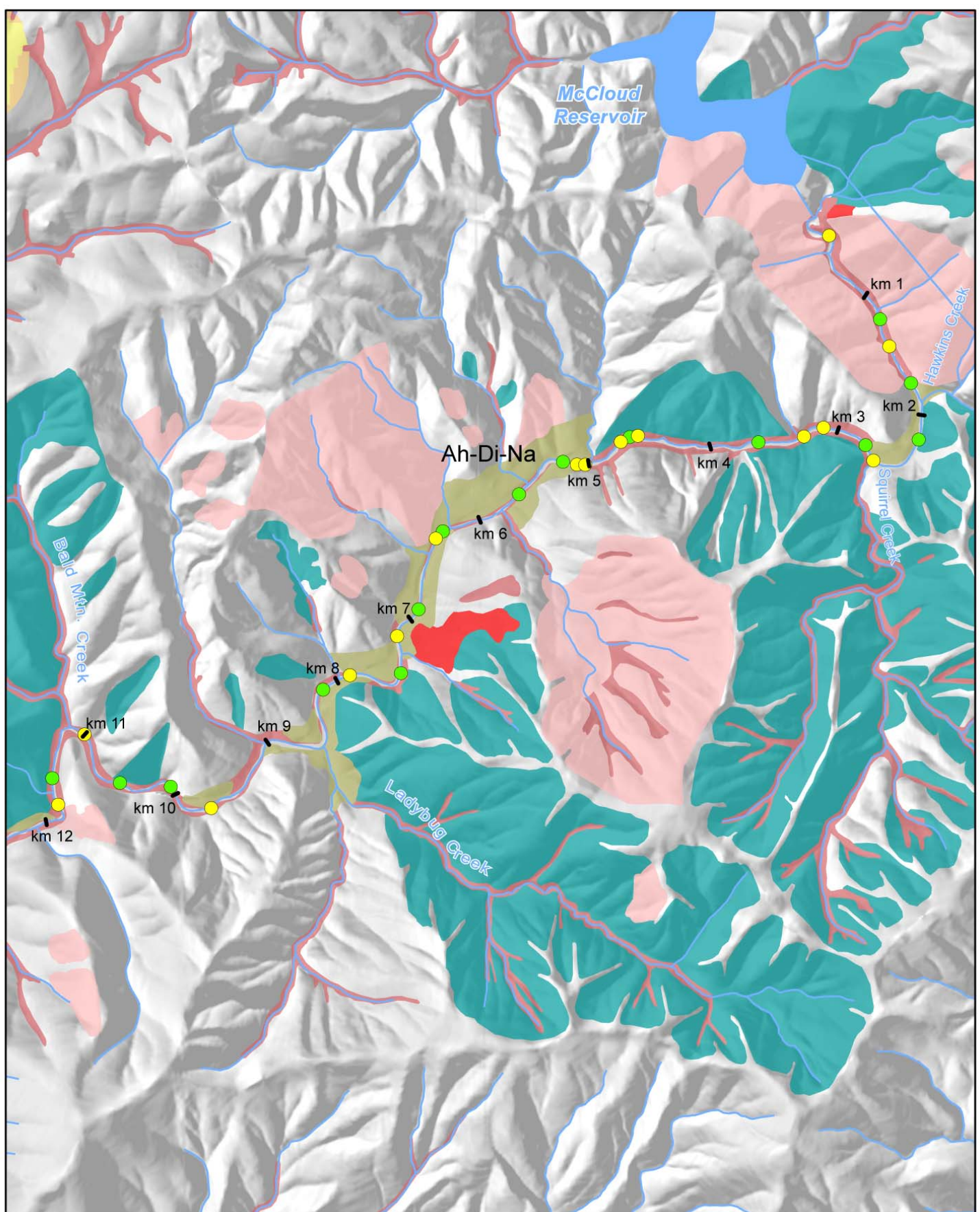


Figure 27. (A) Estimated bed mobility thresholds at the five intensive study sites plotted by distance downstream of McCloud Dam; and (B) normalized Shields stress by discharges for five intensive study sites



DFG Level I
Habitat Type

- Flatwater
- Pool

● Active Landslides

● Debris Basins

● Other Inner Gorge

● Glacial Moraine,
Terrace and Fan Deposits

● Dormant Landslides

● Toe Zone Dormant Slides

McCloud-Pit Project
FERC Project No. 2106



Figure 28a. Sample reaches for characterizing coarse sediment storage in the Lower McCloud River from McCloud Dam to Bald Mountain Creek

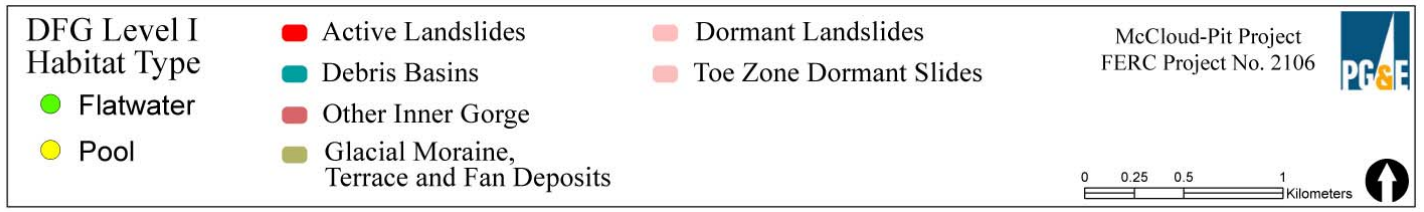
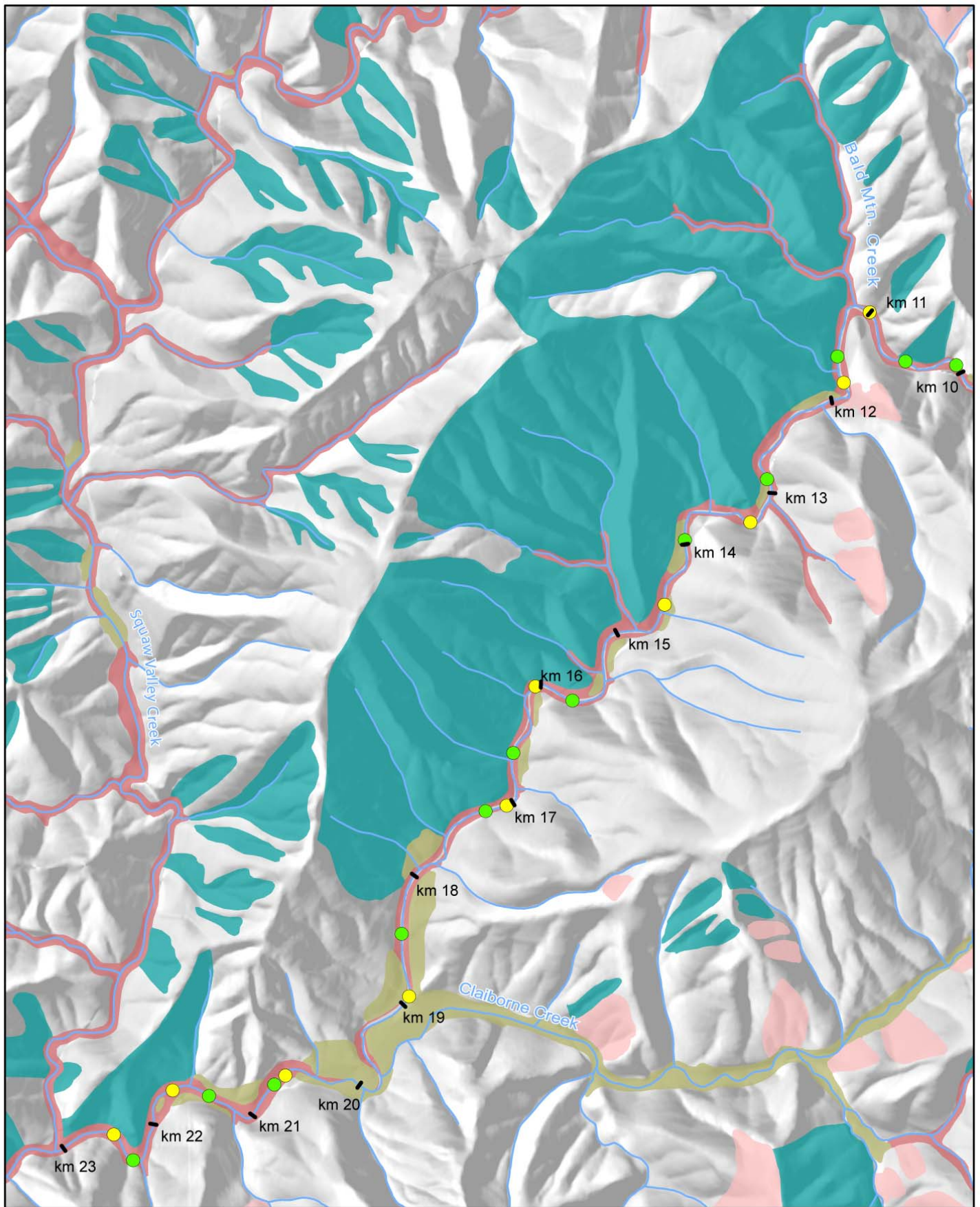


Figure 28b. Sample reaches for characterizing coarse sediment storage in the Lower McCloud River from Bald Mountain Creek to Squaw Valley Creek

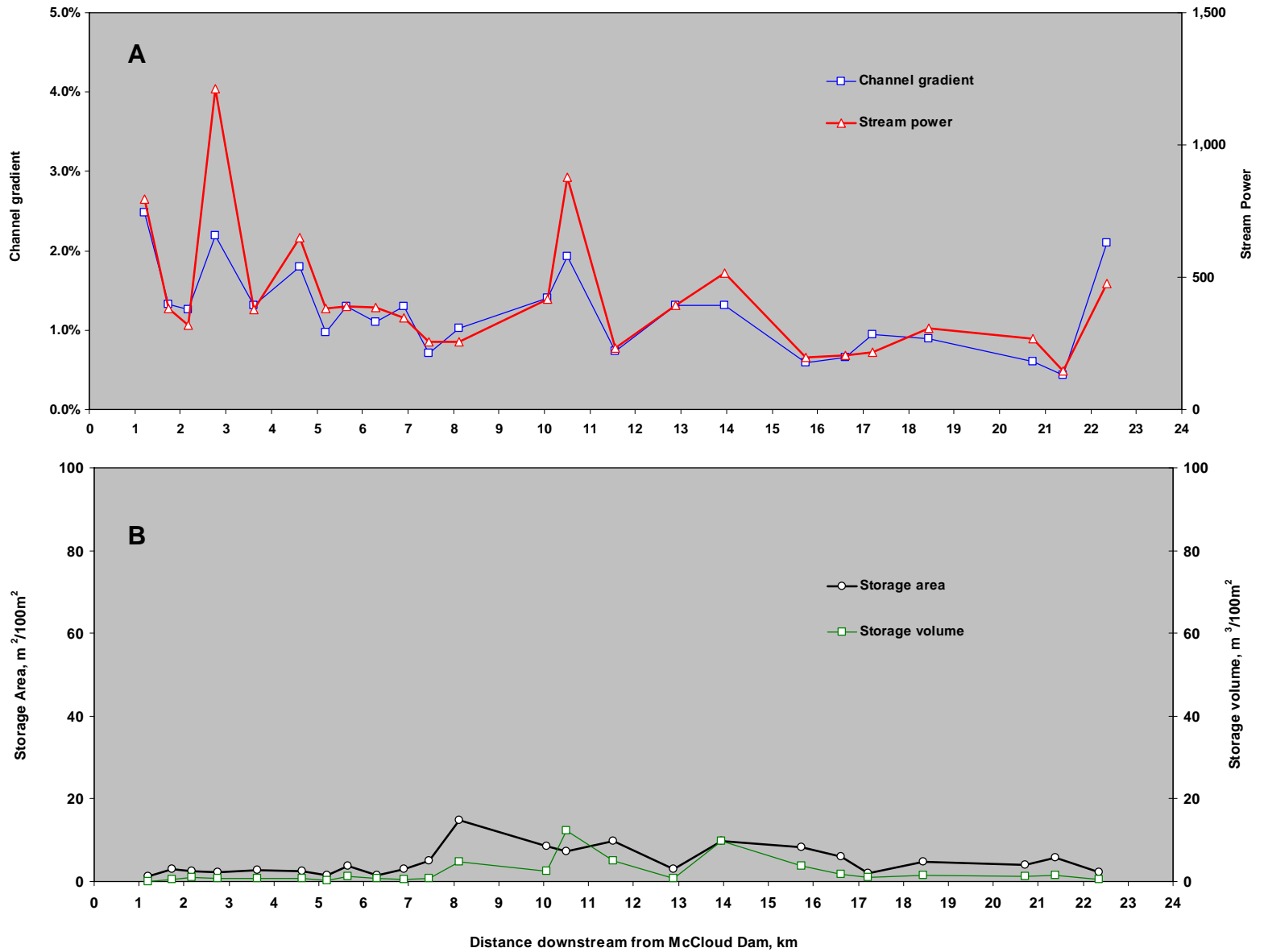


Figure 29. (A) Channel gradient and stream power; and (B) sediment storage area and volume in flatwater sampled for sediment storage

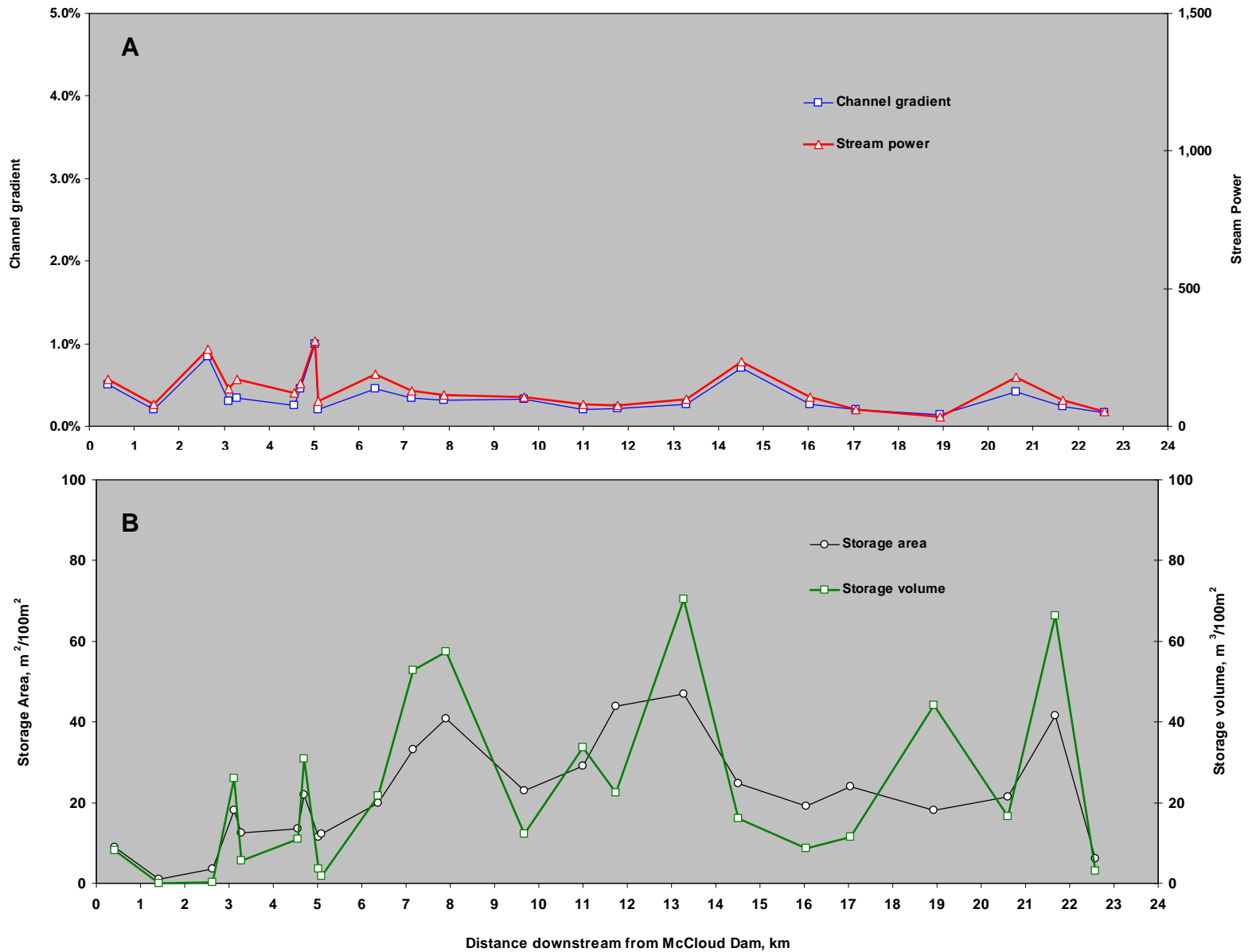


Figure 30. (A) Channel gradient and stream power; and (B) sediment storage area and volume in pools sampled for sediment storage

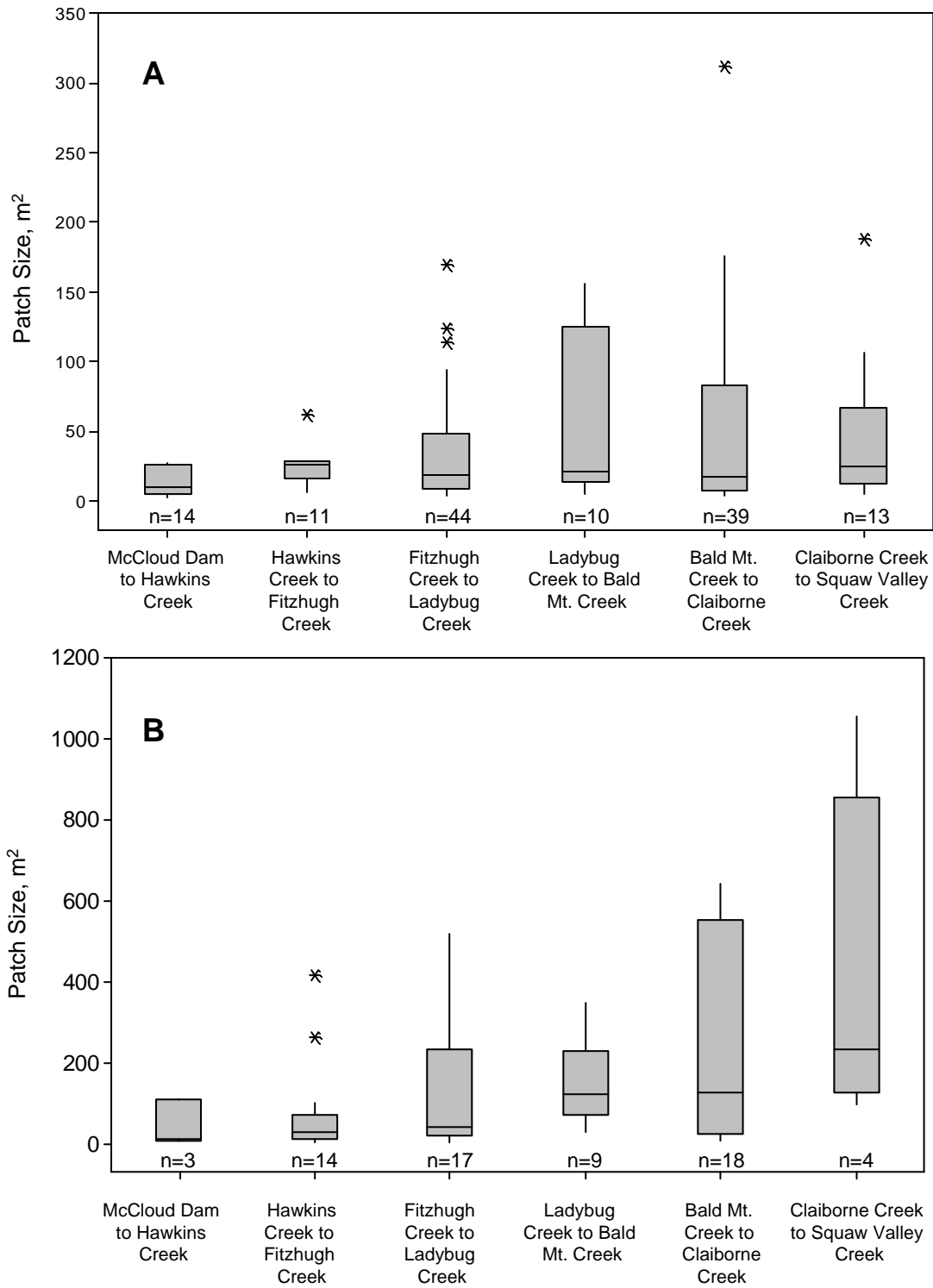


Figure 31. Boxplots illustrating mobile patch size with increasing distance downstream of McCloud Dam in (A) flatwater and (B) pools. Patch sample size indicated by n

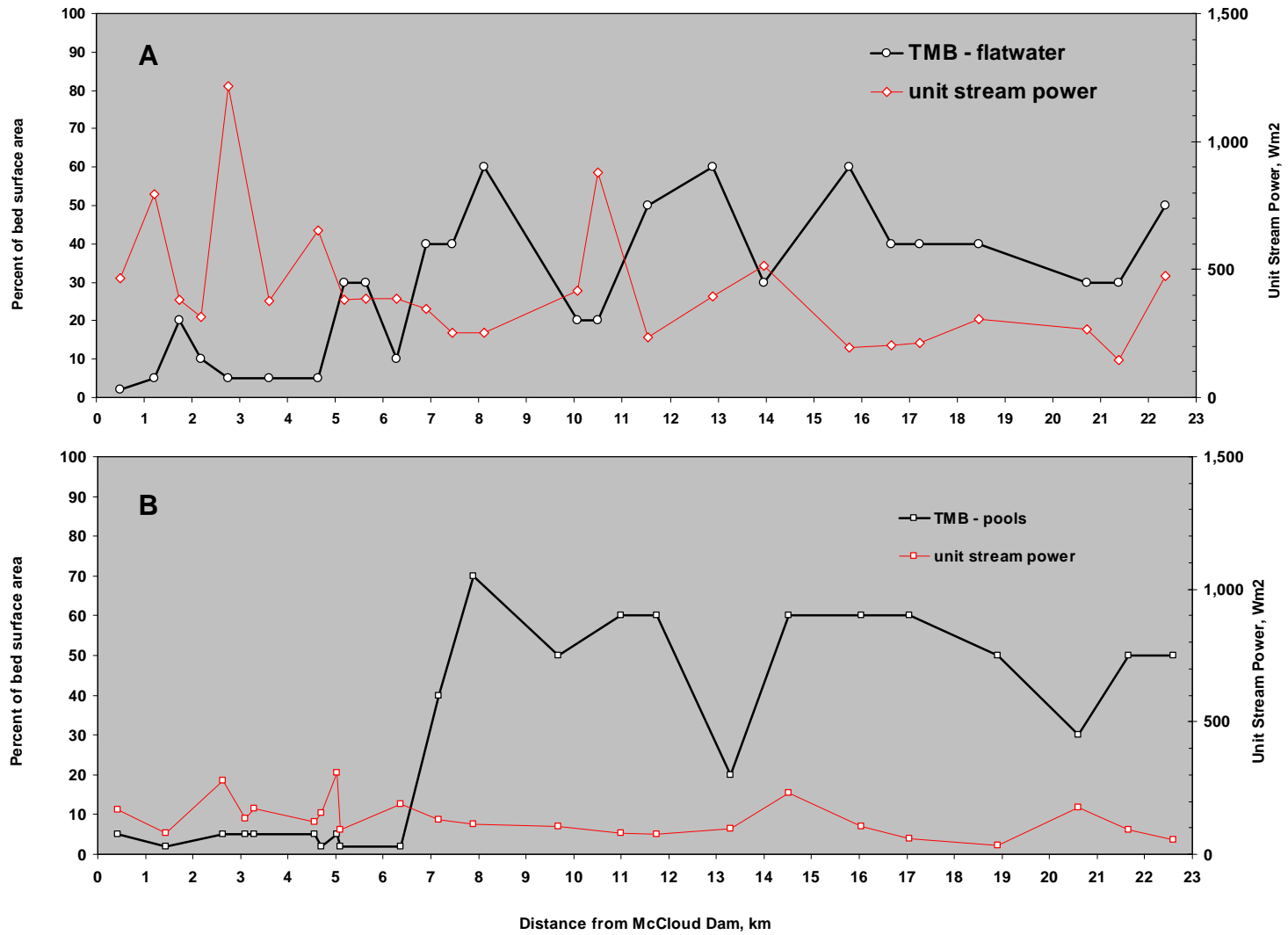


Figure 32. Percent area of transitory mobile bed (TMB) in (A) flatwater and (B) pools sampled for sediment storage

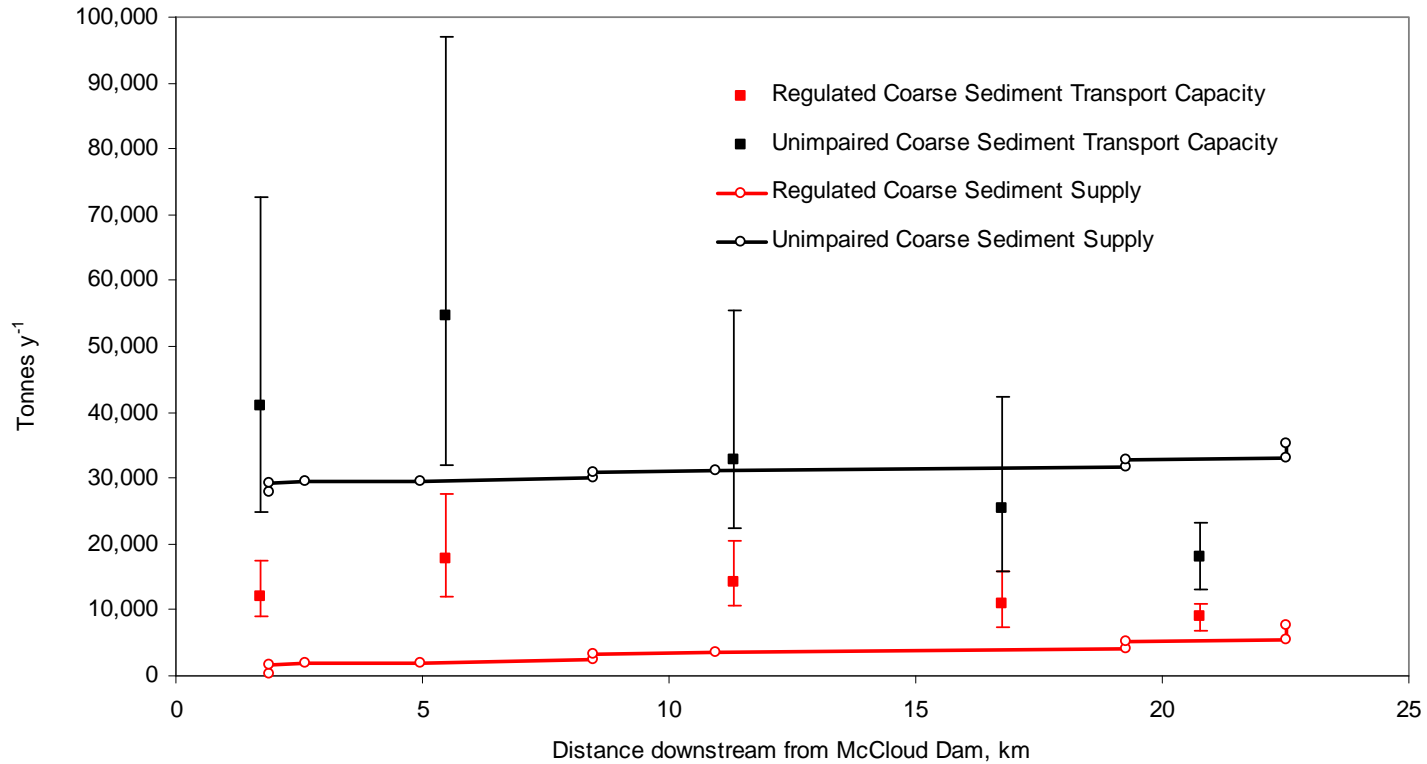


Figure 33. Comparison of regulated and unimpaired coarse sediment transport capacity at the five intensive study sites and coarse sediment supply plotted by distance downstream of McCloud Dam. Error bars on transport capacity estimates represent high and low estimates

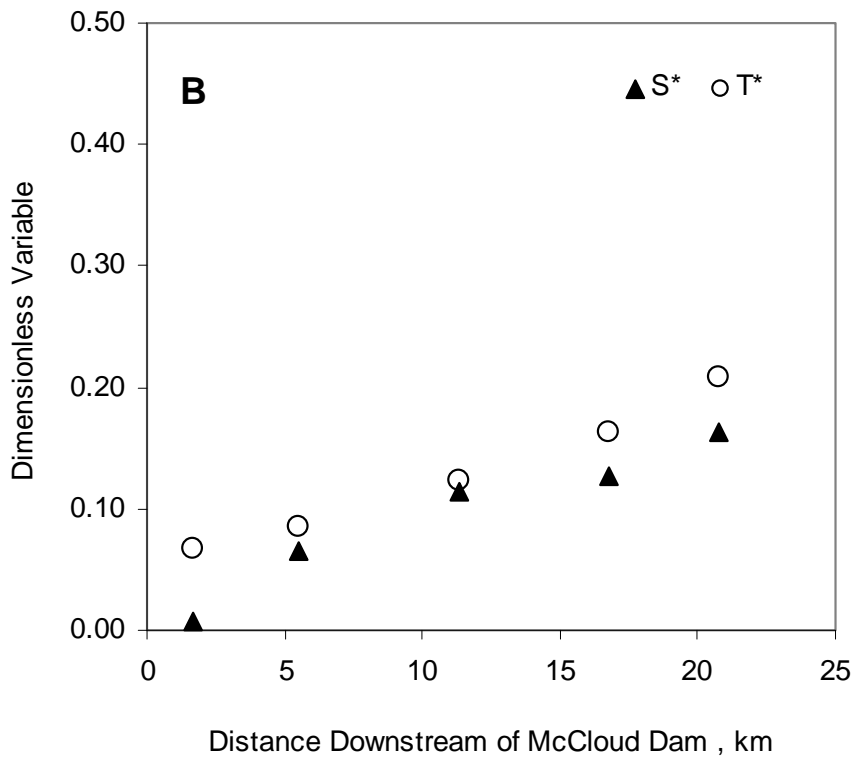
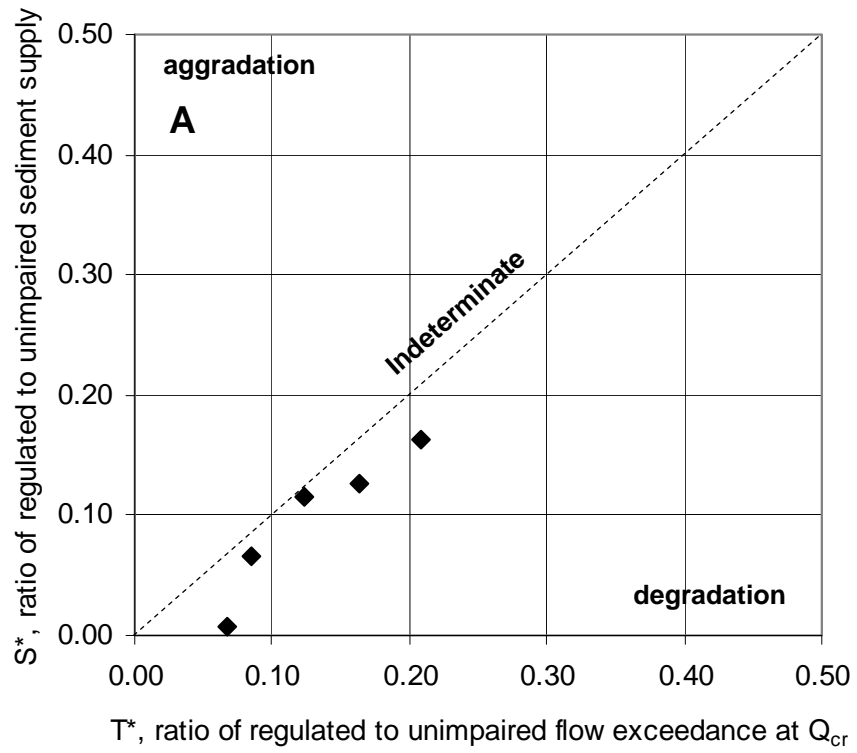


Figure 34. (A) Comparison of T^* (dimensionless ratio of frequency of bed mobilizing flows for regulated and unimpaired conditions) to S^* (dimensionless ratio of regulated and unimpaired sediment supply) at the five intensive study sites; and (B) comparison of T^* and S^* with distance downstream of McCloud Dam

ATTACHMENT 1

Results from Surveys and Sediment Sampling at Intensive Study Sites and Tributary Bed Texture Sites

This page intentionally left blank.

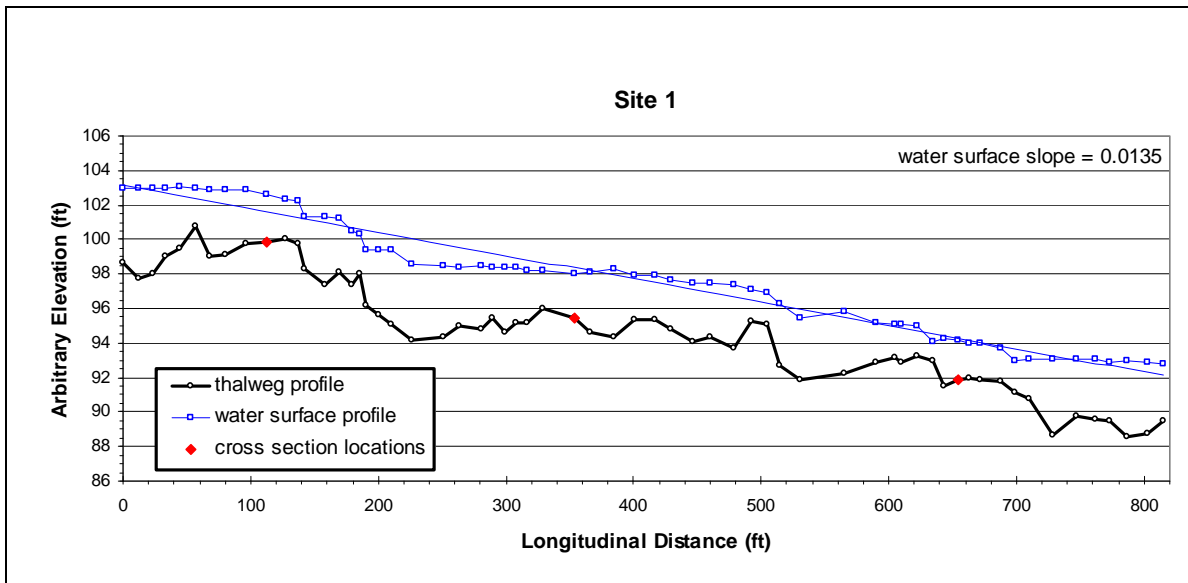


Figure A1-1. Long profile and water surface slope at Intensive Study Site 1, located near Hawkins Creek

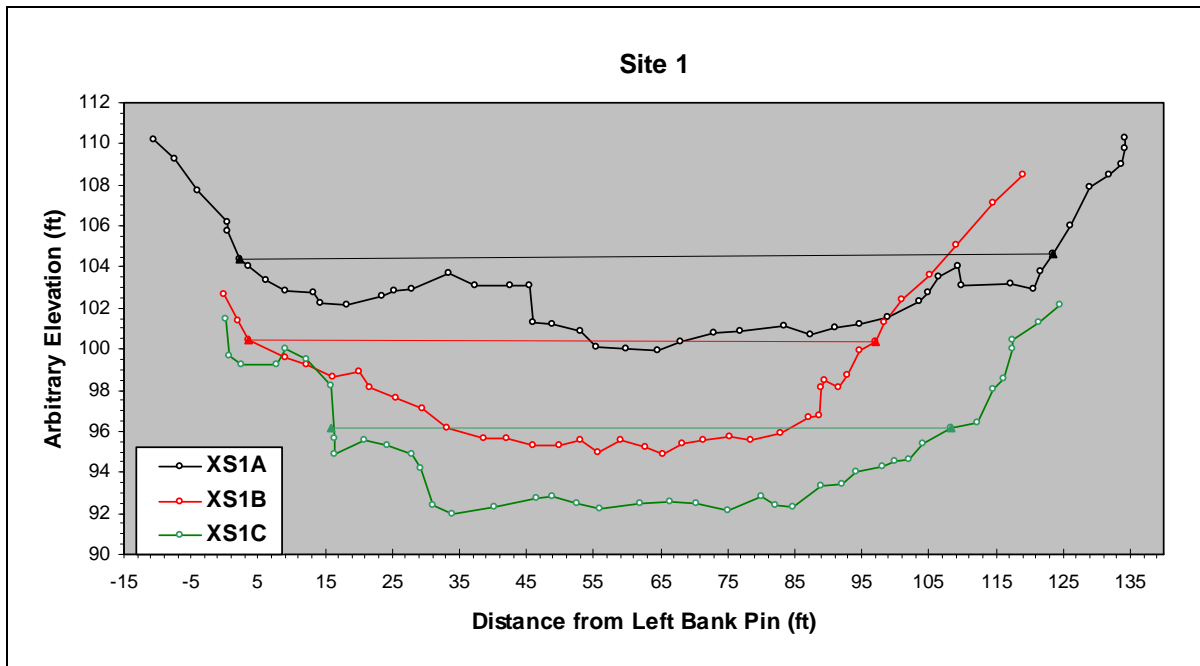


Figure A1-2. Cross-section plots at Intensive Study Site 1; horizontal lines depict bankfull elevations

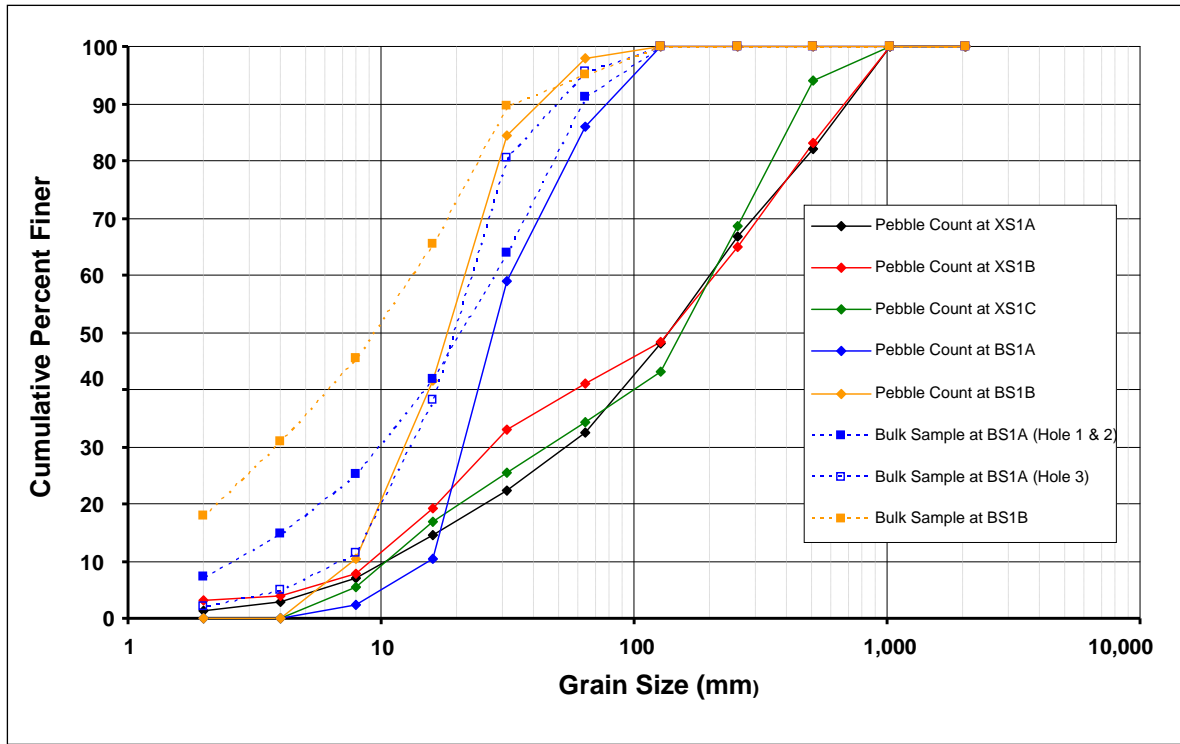


Figure A1-3. Cumulative particle-size distributions for samples collected at Intensive Study Site 1

Table A1-1. Grain-size parameters for pebble counts and bulk samples at Intensive Study Site 1

Summary Statistics	Pebble Count (mm)					Bulk Samples (mm)		
	XS1A	XS1B	XS1C	BS1A	BS1A	BS1A (holes 1&2)	BS1A (hole 3)	BS1B
D ₉₀	513	513	400	69	35	62	41	33
D ₈₄	513	513	380	60	32	55	35	26
D ₅₀	140	130	150	27	19	20	19	10
D ₁₆	20	14	15	17	10	4	10	2
D ₁₀	11	9	10	15	8	3	7	< 2
D _g	99	80	92	29	17	NA	NA	NA
σ _g	4.1	4.8	3.9	1.8	1.8	NA	NA	NA

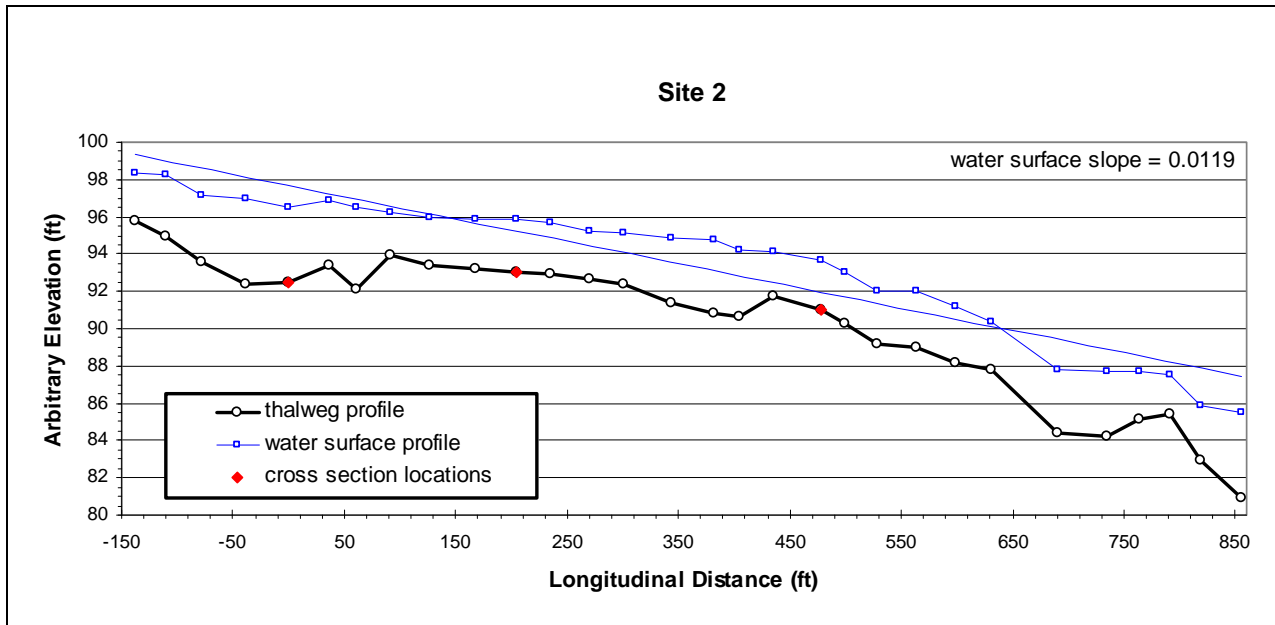


Figure A1-5. Long profile and water surface slope at Intensive Study Site 2 located near Ah-Di-Na

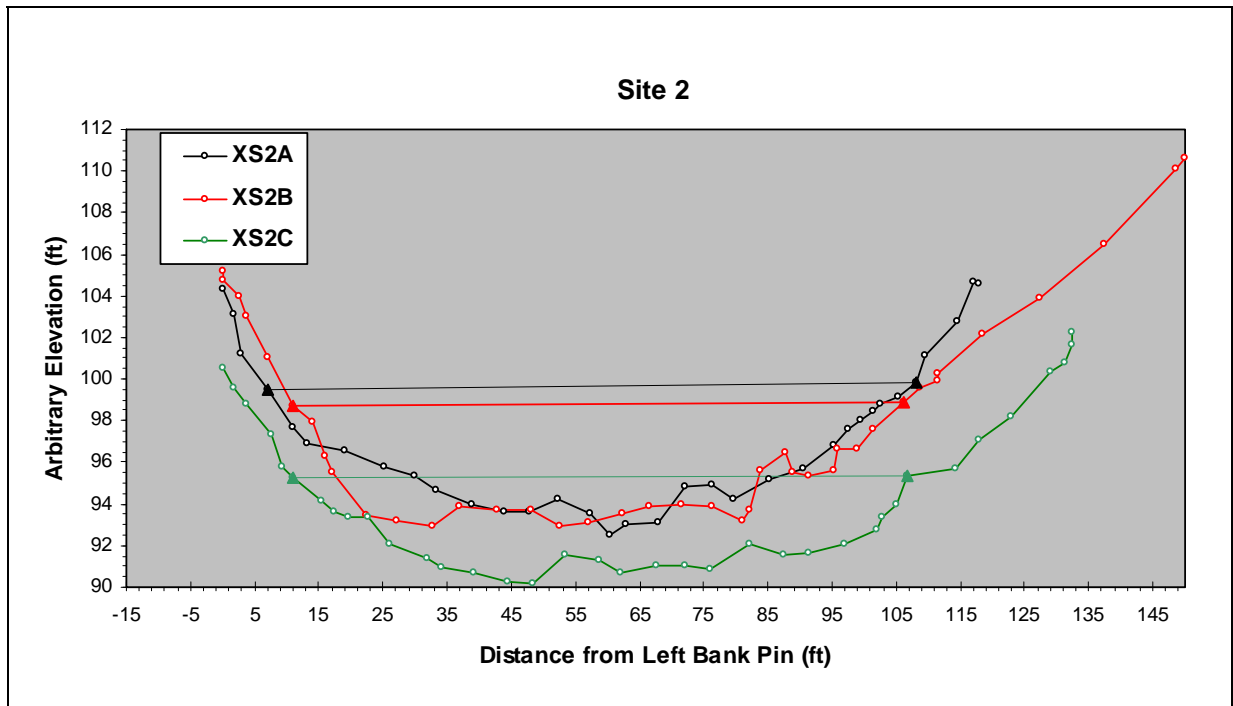


Figure A1-6. Cross-section plots at Intensive Study Site 2; horizontal lines depict bankfull elevations

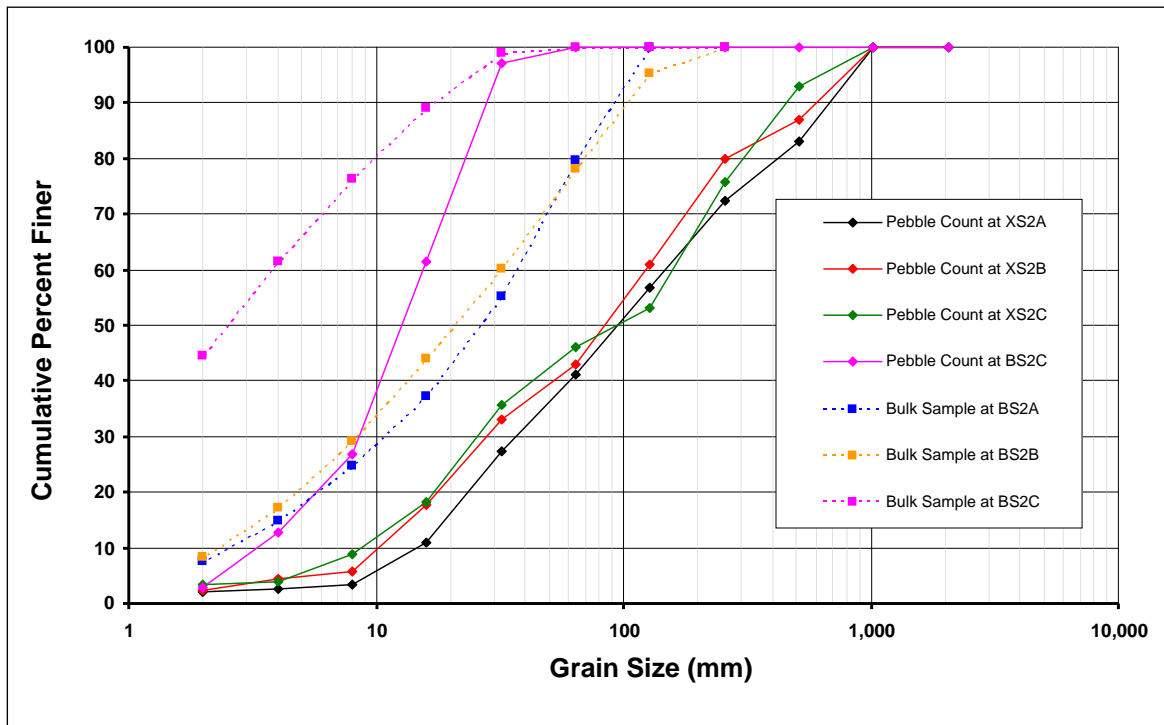


Figure A1-7. Cumulative particle size distributions for samples collected at Intensive Study Site 2

Table A1-2. Grain-size parameters for pebble counts and bulk samples at Intensive Study Site 2

Summary Statistics	Pebble Count (mm)				Bulk Samples (mm)		
	XS2A	XS2B	XS2C	BS2C	BS2A	BS2B	BS2C
D ₉₀	513	513	480	26	83	100	17
D ₈₄	513	410	325	24	71	79	12
D ₅₀	105	87	92	12	27	20	2
D ₁₆	18	15	15	5	4	4	< 2
D ₁₀	15	12	10	3	3	2	< 2
D _g	86	68	67	11	NA	NA	NA
σ _g	3.9	4.0	4.4	2.1	NA	NA	NA

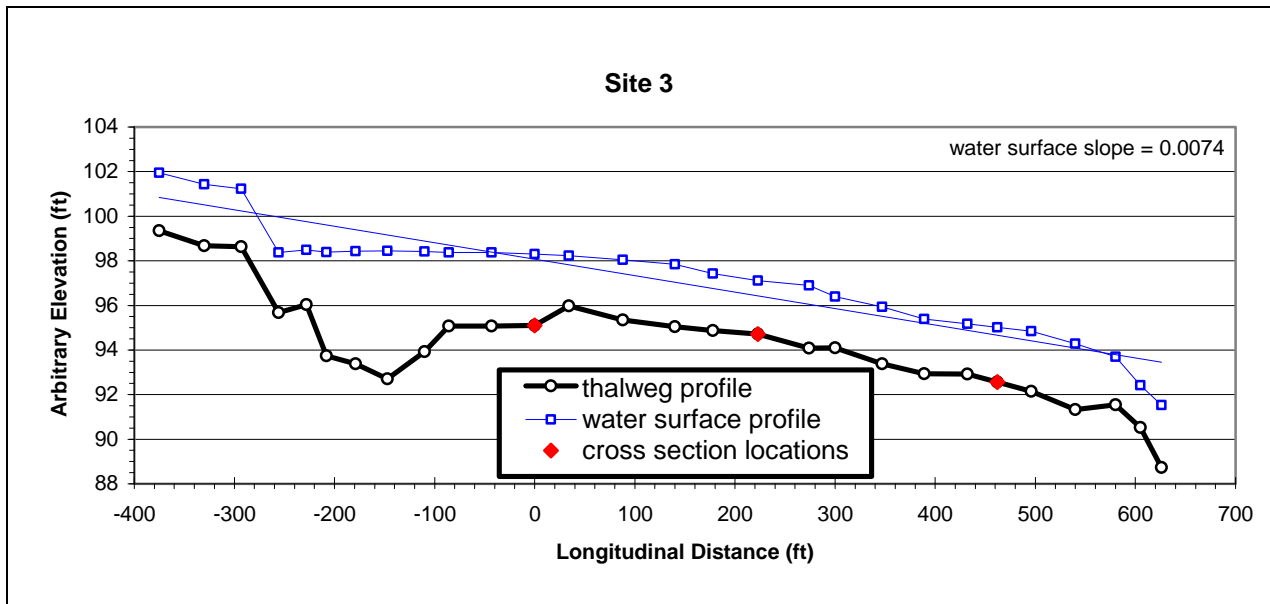


Figure A1-8. Long profile and water surface slope at Intensive Study Site 3, located near Bald Mountain Creek

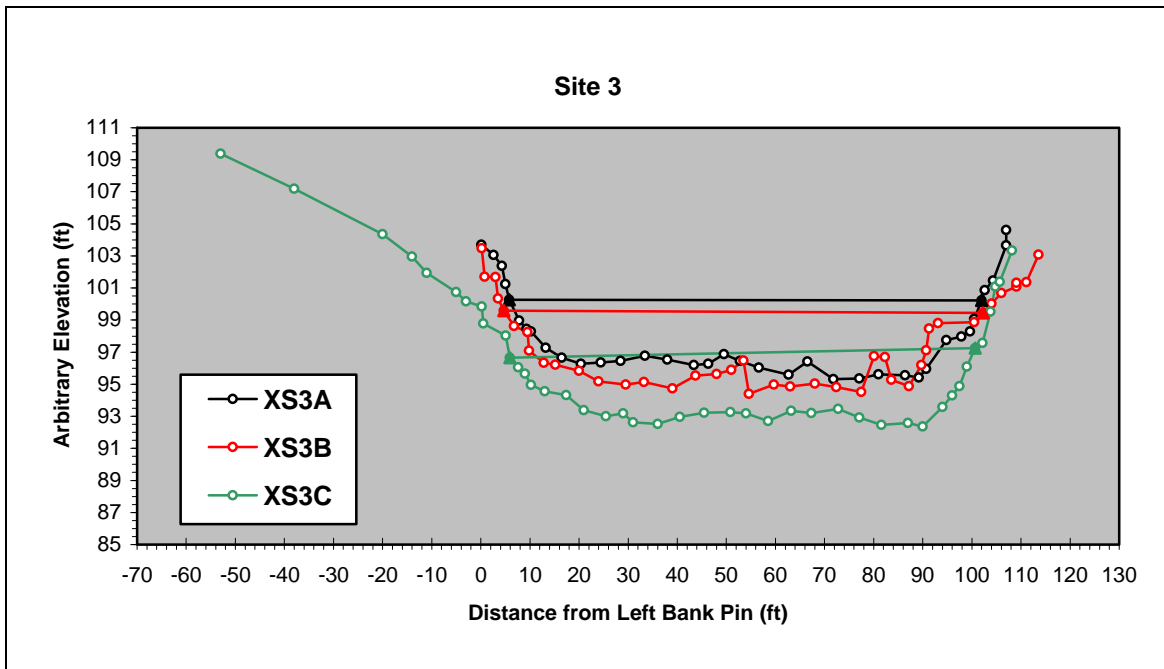


Figure A1-9. Cross-section plots at Intensive Study Site 3; horizontal lines depict bankfull elevations

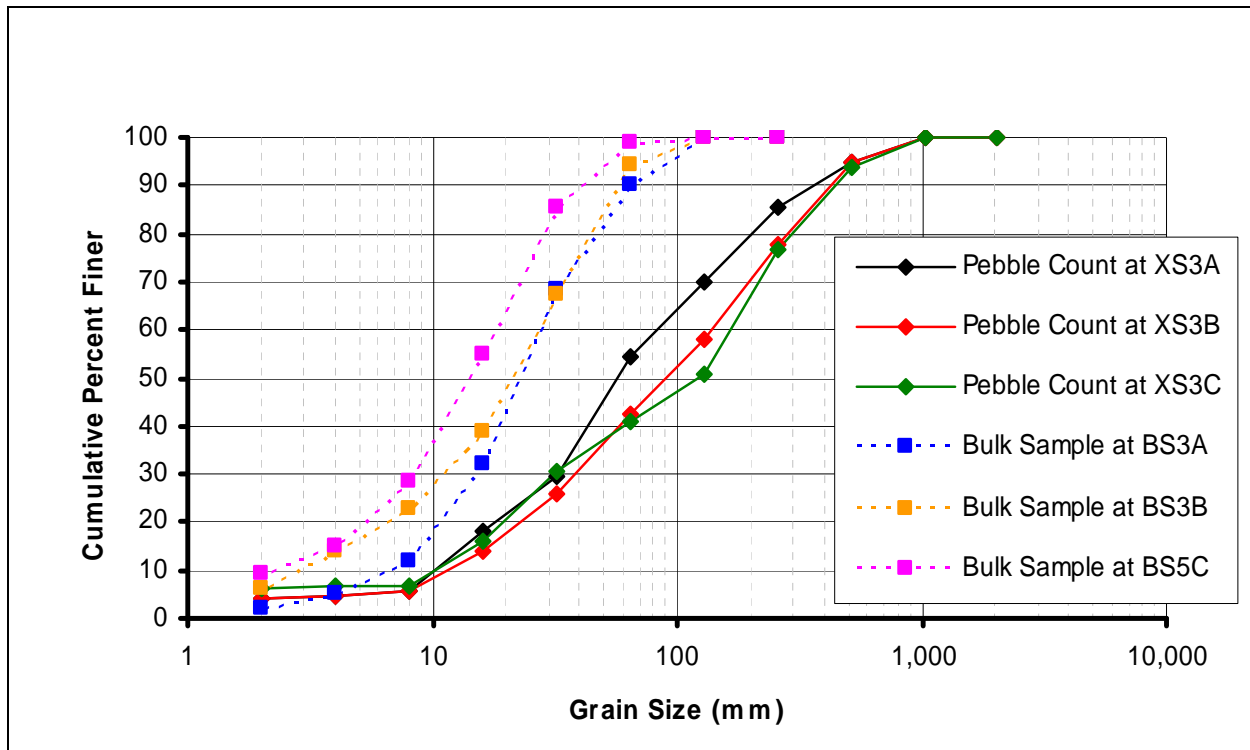


Figure A1-10. Cumulative particle size distributions for samples collected at Intensive Study Site 3

Table A1-3. Grain-size parameters for pebble counts and bulk samples at Intensive Study Site 3

Summary Statistics	Pebble Count (mm)			Bulk Samples (mm)		
	XS3A	XS3B	XS3C	BS3A	BS3B	BS3C
D ₉₀	350	450	380	64	55	37
D ₈₄	235	310	300	52	45	31
D ₅₀	50	90	125	22	21	14
D ₁₆	14	20	15	10	5	4
D ₁₀	9	12	10	7	3	2
D _g	53	73	70	NA	NA	NA
σ _g	3.7	4.0	4.5	NA	NA	NA

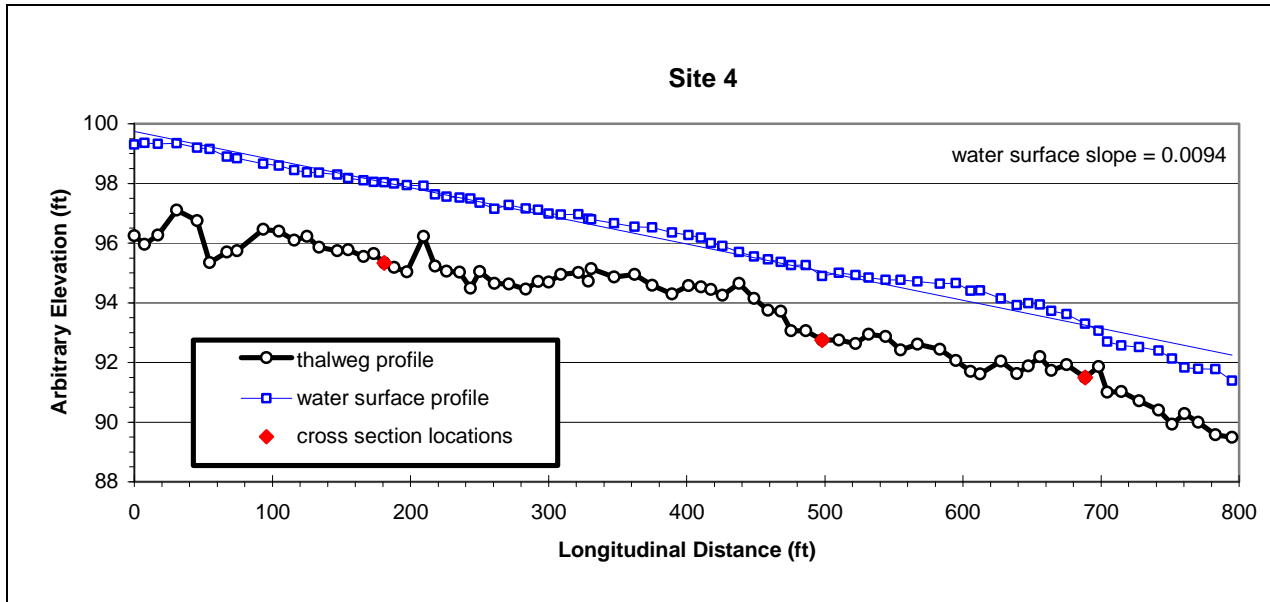


Figure A1-11. Long profile and water surface slope at Intensive Study Site 4, located near T37N R3W, Sec 14

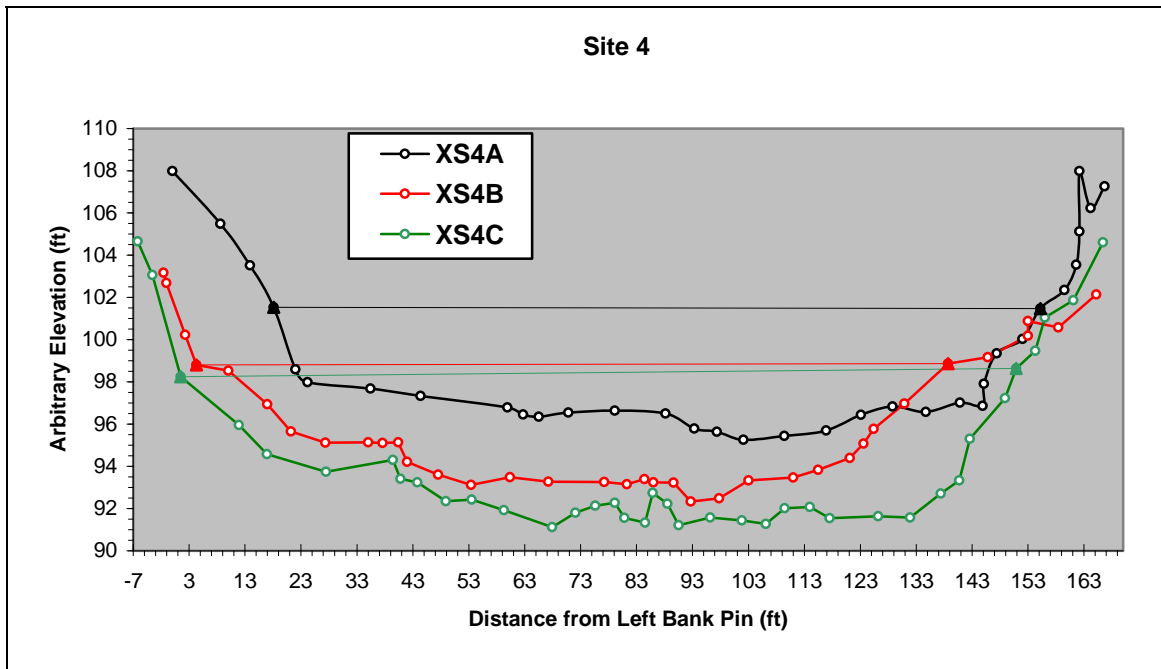


Figure A1-12. Cross-section plots at Intensive Study Site 4; horizontal lines depict bankfull elevations

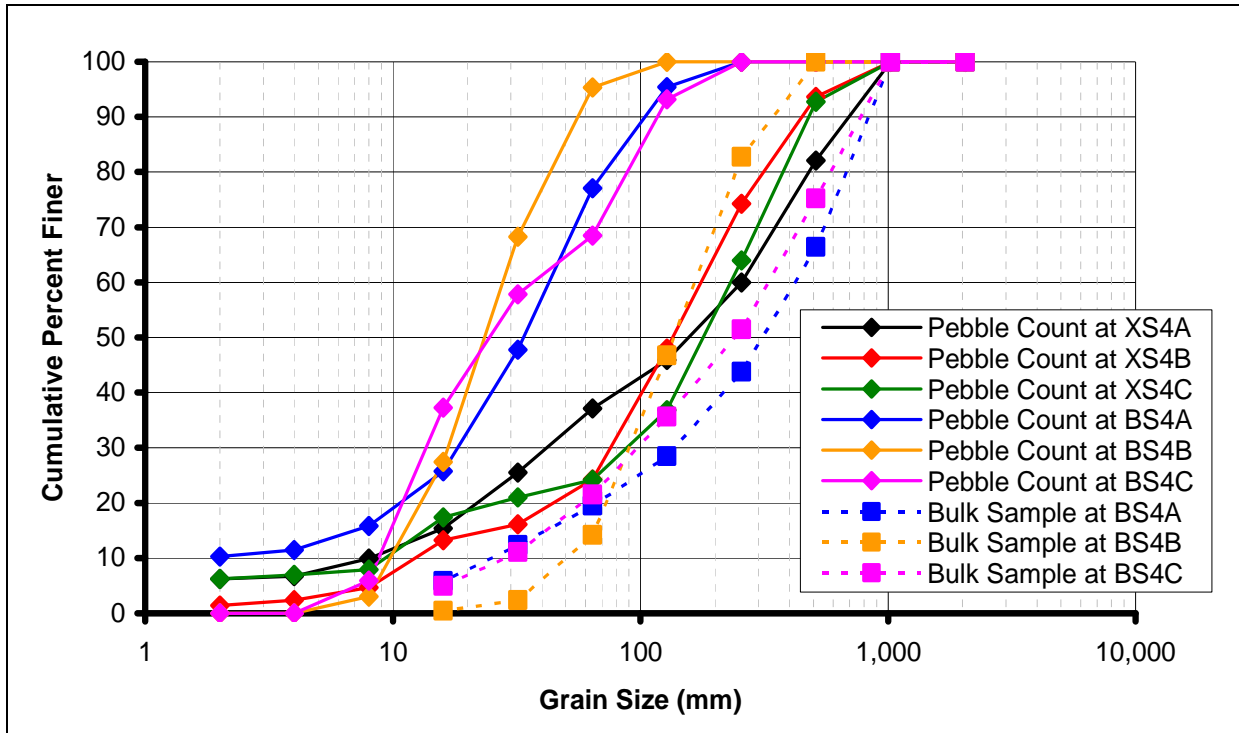


Figure A1-13. Cumulative particle-size distributions for samples collected at Intensive Study Site 4

Table A1-4. Grain-size parameters for pebble counts and bulk samples at Intensive Study Site 4

Summary Statistics	Pebble Count (mm)						Bulk Samples (mm)		
	XS4A	XS4B	XS4C	BS4A	BS4B	BS4C	BS4A	BS4B	BS4C
D ₉₀	513	418	470	104	46	111	111	38	106
D ₈₄	513	332	430	80	41	92	102	33	95
D ₅₀	160	137	180	35	24	25	39	17	30
D ₁₆	17	27	12	8	14	10	6	8	6
D ₁₀	8	12	8	2	10	8	3	7	4
D _g	91	102	102	25	22	26	NA	NA	NA
σ _g	5.2	3.3	4.8	3.4	1.7	2.6	NA	NA	NA

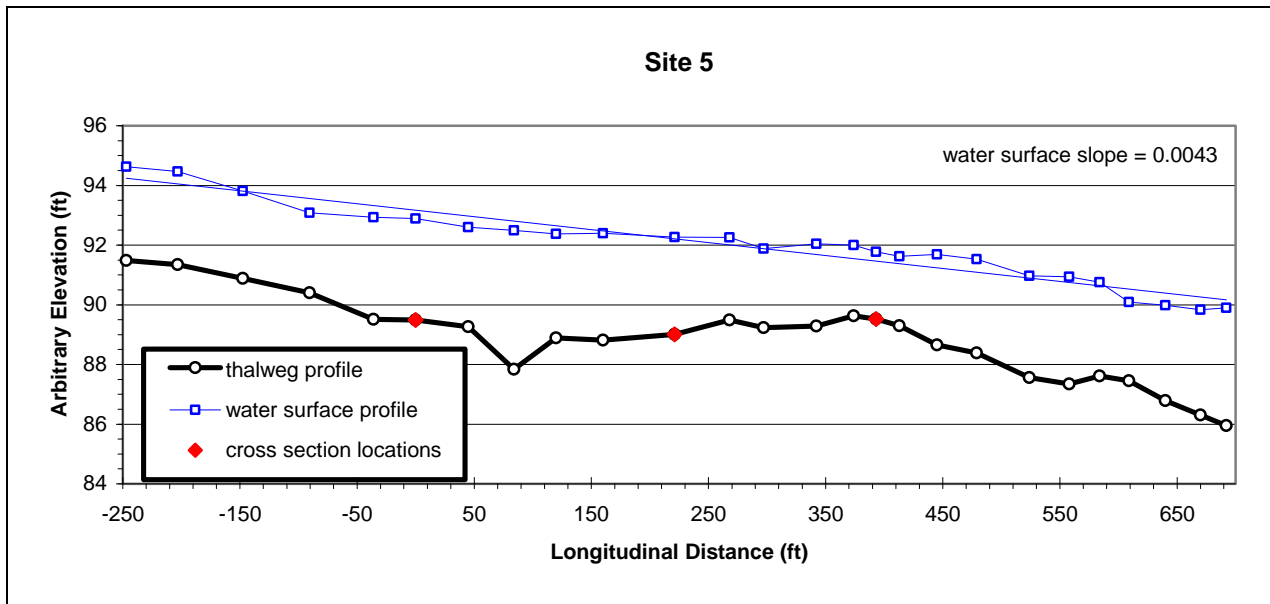


Figure A1-14. Long profile and water surface slope at Intensive Study Site 5, located near Hamilton Bend

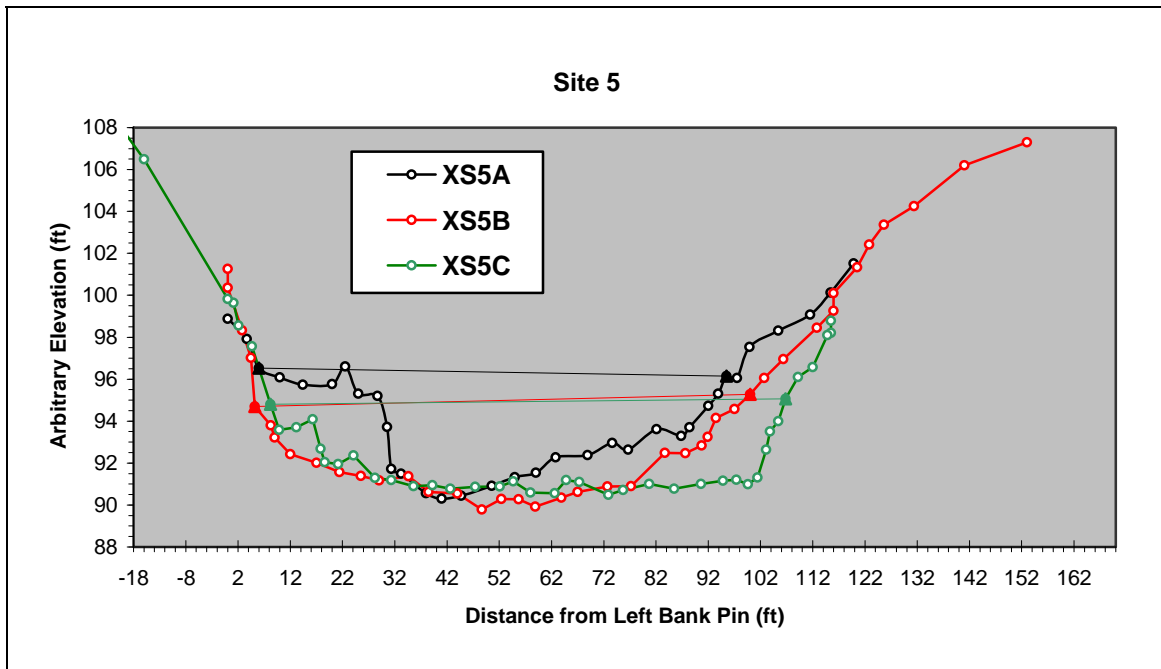


Figure A1-15. Cross-section plots at Intensive Study Site 5; horizontal lines depict bankfull elevations

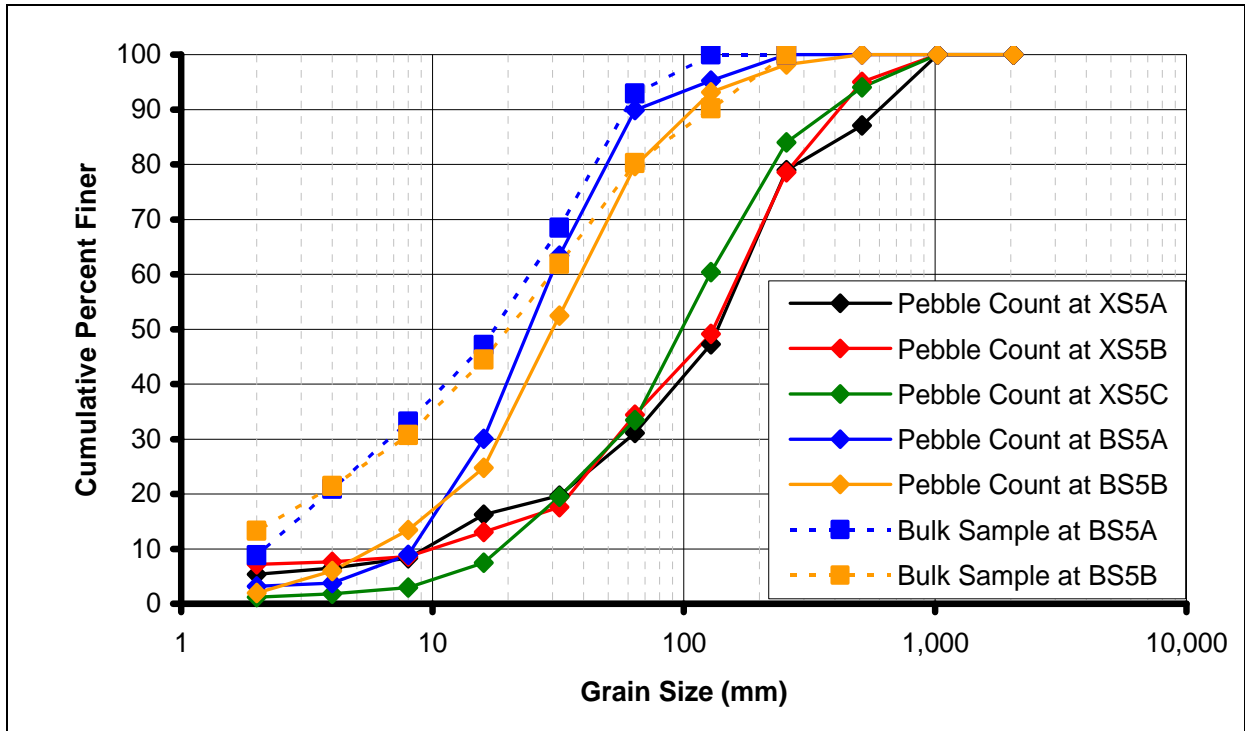


Figure A1-16. Cumulative particle-size distributions for samples collected at Intensive Study Site 5

Table A1-5. Grain-size parameters for pebble counts and bulk samples at Intensive Study Site 5

Summary Statistics	Pebble Count (mm)					Bulk Samples (mm)	
	XS5A	XS5B	XS5C	BS5A	BS5B	BS5A	BS5B
D ₉₀	513	380	420	66	115	57	125
D ₈₄	430	300	260	50	77	45	78
D ₅₀	135	130	113	28	30	18	20
D ₁₆	15	22	27	11	9	3	3
D ₁₀	10	10	20	10	6	2	< 2
D _g	87	79	86	23	27	NA	NA
σ _g	4.4	4.2	2.9	2.3	2.8	NA	NA

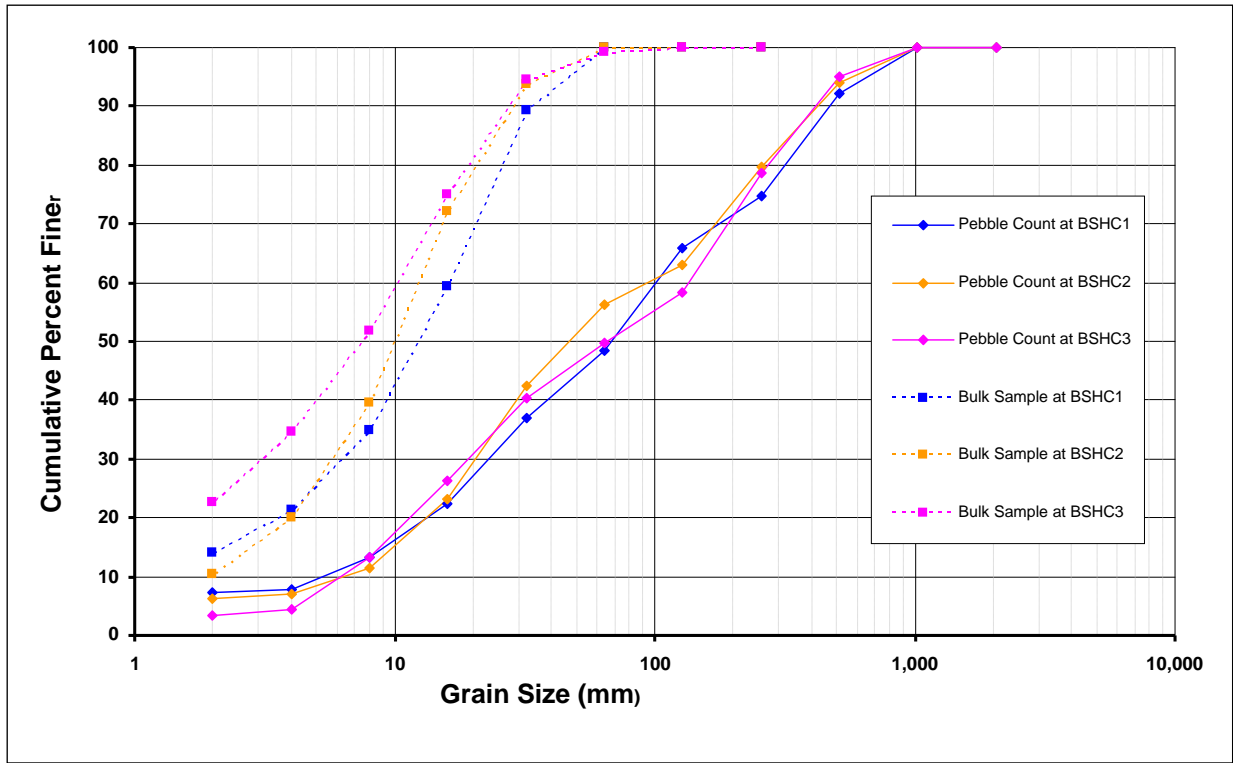


Figure A1-17. Cumulative particle-size distributions for samples collected at Lower McCloud River tributary site Hawkins Creek

Table A1-6. Grain-size parameters for pebble counts and bulk samples at Lower McCloud River tributary site Hawkins Creek

Summary Statistics	Pebble Count (mm)			Bulk Samples (mm)		
	BSHC1	BSHC2	BSHC3	BSHC1	BSHC2	BSHC3
D90	400	390	400	33	27	26
D84	380	320	380	28	21	21
D50	70	40	62	13	10	7
D16	10	12	10	2	3	< 2
D10	6	5	6	< 2	< 2	< 2
Dg	56	48	56	NA	NA	NA
σg	5.1	4.7	4.8	NA	NA	NA



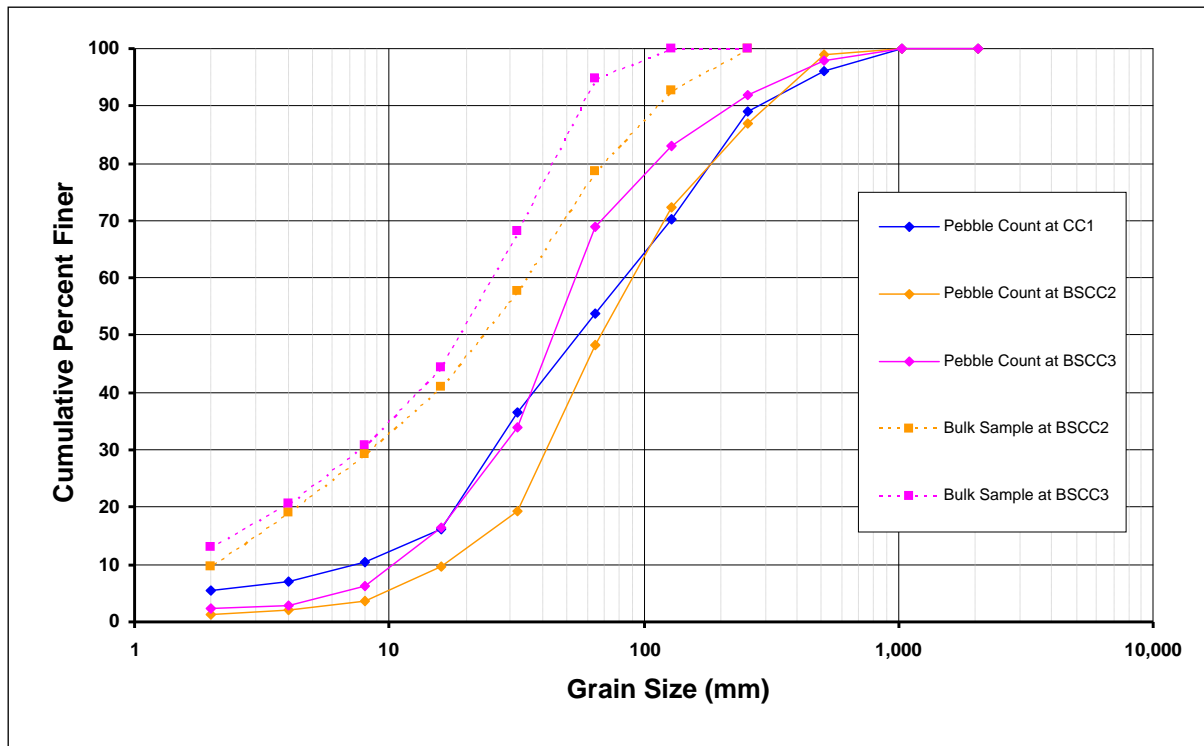


Figure A1-18. Cumulative particle-size distributions for samples collected at Lower McCloud River tributary site Claiborne Creek

Table A1-7. Grain-size parameters for pebble counts and bulk samples at Lower McCloud River tributary site Claiborne Creek

Summary Statistics	Pebble Count (mm)			Bulk Samples (mm)	
	CC1	BSCC2	BSCC3	BSCC2	BSCC3
D90	270	360	200	112	56
D84	190	200	130	84	47
D50	50	68	42	23	19
D16	15	28	15	3	3
D10	5	18	11	< 2	< 2
Dg	48	66	43	NA	NA
σ_g	3.9	2.9	2.9	NA	NA

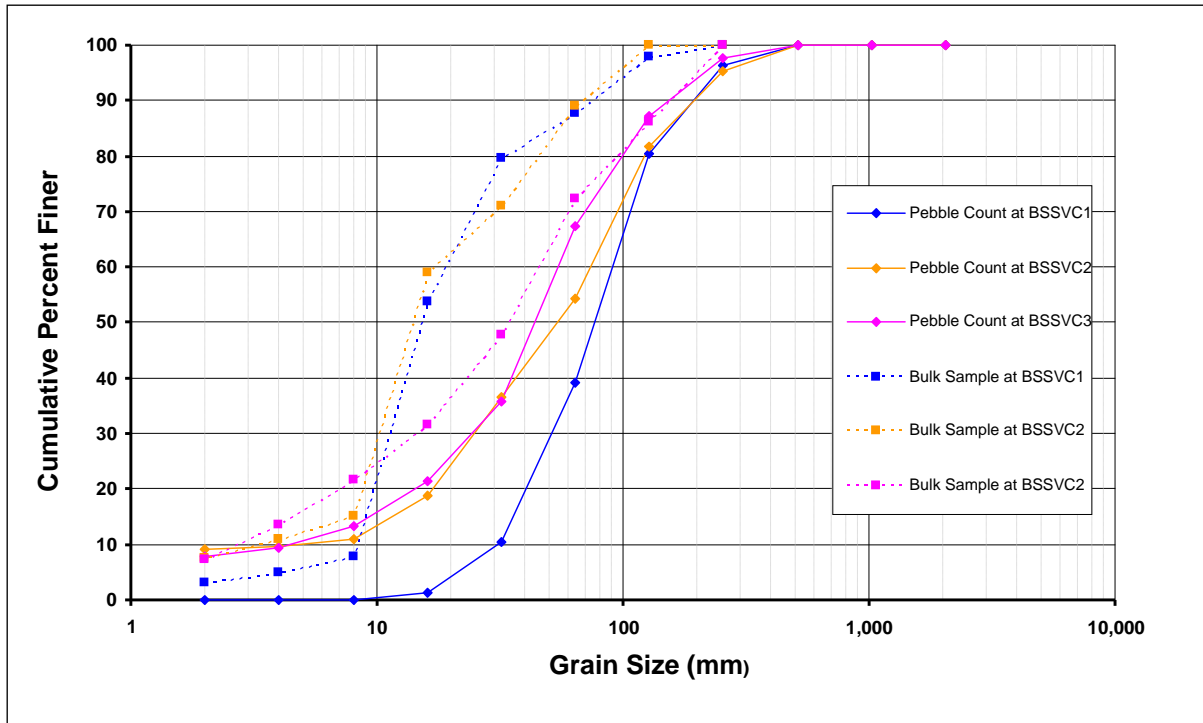


Figure A1-19. Cumulative particle-size distributions for samples collected at Lower McCloud River tributary site Squaw Valley Creek

Table A1-8. Grain-size parameters for pebble counts and bulk samples at Lower McCloud River tributary site Squaw Valley Creek

Summary Statistics	Pebble Count (mm)			Bulk Samples (mm)		
	BSSVC1	BSSVC2	BSSVC3	BSSVC1	BSSVC2	BSSVC3
D90	162	190	150	76	66	141
D84	140	140	110	49	54	116
D50	78	50	40	16	15	34
D16	40	14	11	12	9	5
D10	30	6	6	< 2	< 2	< 2
Dg	72	39	33	NA	NA	NA
σg	1.9	3.8	3.5	NA	NA	NA

ATTACHMENT 2

Sediment Transport Model Documentation

This page intentionally left blank.



EASI Model Formulation

The surface based bedload equation of Parker (1990a,b) is expressed for a wide rectangular channel for which channel geometry can be expressed as a channel width. This equation is modified for the Enhanced Acronym Series (1&2) with Interface (EASI) program so that it can also calculate transport at a given cross section. Details of the surface based bedload equation of Parker can be found in the original references (Parker 1990a,b). Here only the most essential part of the Parker equation is presented to facilitate discussion of how the equation is modified and implemented in the EASI program.

The surface based bedload equation of Parker (1990a and 1990b) for a wide rectangular channel is as follows:

$$\frac{RgQ_G p_i}{Bu_*^3} = \alpha F_i G \left[\omega \phi_{sgo} \left(\frac{\overline{D}_i}{D_{sg}} \right)^{-\beta} \right] \quad \text{(Equation A-1)}$$

Where R denotes the submerged specific gravity of sediment; g denotes the acceleration of gravity; Q_G denotes volumetric bedload transport rate; B denotes channel width; u_* denotes shear velocity; \overline{D}_i denotes the mean grain size of the i-th subrange; p_i denotes the volumetric fraction of the i-th subrange in bedload; F_i denotes the volumetric fraction of the i-th subrange in the surface layer; D_{sg} denotes geometric mean grain size of the surface layer; ϕ_{sgo} is normalized Shields stress; ω is a function of the normalized Shields stress ϕ_{sgo} and the arithmetic standard deviation of the surface layer. Coefficients α and β are given as:

$$\alpha = 0.00218; \quad \beta = 0.0951 \quad \text{(Equation A-2a-b)}$$

Grain size is described both in diameter and in ψ -scale, which is the negative of the more commonly used ϕ -scale in geophysics community (1990a and 1990b).

$$\psi_i = -\phi_i = \log_2(D_i) \quad \text{(Equation A-3)}$$

The grain size is divided into N subgroups bounded by N+1 grain sizes ψ_1 (D_1) to ψ_{N+1} (D_{N+1}). The mean grain size of the i-th subrange is then given as:

$$\overline{\psi}_i = \frac{\psi_i + \psi_{i+1}}{2}, \quad \overline{D}_i = \sqrt{D_i D_{i+1}} \quad \text{(Equation A-4a-b)}$$

The surface layer mean grain size $\overline{\psi}_s$ and standard deviation $\sigma_{s\psi}$ are as follows,

$$\overline{\psi}_s = \sum_{i=1}^N \overline{\psi}_i F_i, \quad \sigma_{s\psi}^2 = \sum (\overline{\psi}_i - \overline{\psi}_s)^2 F_i \quad \text{(Equation A-5a-b)}$$

and the geometric mean grain size is given as:

$$D_{sg} = 2^{\overline{\psi}_s} \quad \text{(Equation A-5c)}$$



Note that the surface based bedload equation of Parker applies only to particles too coarse to be transported in suspension, and Parker further suggested that the finest grain size (D_1) be set as 2 mm as a common rule in field cases (Parker 1990a and 1990b).

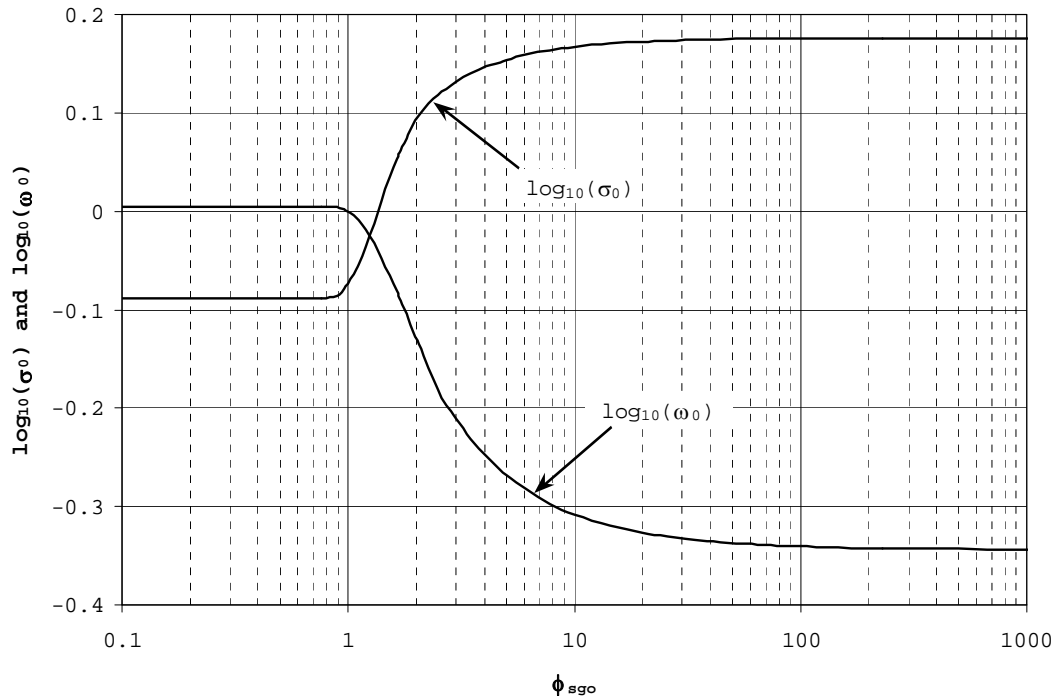


Figure A2-1. Parameters σ_0 and ω_0 as functions of ϕ_{sgo} in Parker equation

Parameter ω is a function of the normalized Shield stress ϕ_{sgo} ,

$$\omega = 1 + \frac{\sigma_0}{\sigma_{sy}} (\omega_0 - 1) \quad \text{(Equation A-6)}$$

where σ_0 and ω_0 are functions of ϕ_{sgo} given in Figure A2-1 (Parker 1990a and 1990b). The relations can also be found in tabulated form in Parker (1990a and 1990b).

The normalized Shield stress ϕ_{sgo} is acquired by dividing the surface based Shield stress τ_{sg}^* by a reference stress τ_r^* ,

$$\phi_{sgo} = \frac{\tau_{sg}^*}{\tau_r^*} \quad \text{(Equation A-7)}$$

where the reference Shield stress τ_r^* was originally proposed by Parker (1990a and 1990b) as 0.0386. However, for this study the reference Shield stress τ_r^* at each intensive study site was



determined from the relation proposed by Mueller *et al.* (2005) described in detail below (Section 2), which was calibrated with data from the tracer rock study where possible. The surface based Shield stress τ_{sg}^* is defined as:

$$\tau_{sg}^* = \frac{u_*^2}{RgD_{sg}} \tag{Equation A-8}$$

Shear velocity u^* is assumed to obey the Manning-Strickler resistance relation,

$$\frac{U}{u_*} = 8.1 \left(\frac{h}{k_s} \right)^{1/6} \tag{Equation A-9}$$

in which U denotes flow velocity; h denotes water depth and k_s denotes roughness height. Roughness height is defined slightly differently from the original work of Parker (1990a and 1990b) for simplicity,

$$k_s = 2D_{sg} \sigma_{sg}^{1.28} \tag{Equation A-10}$$

where σ_{sg} denotes surface layer geometric standard deviation,

$$\sigma_{sg} = 2^{\sigma_{s\psi}} \tag{Equation A-11}$$

Note that the roughness height given in Equation (A-10) is an approximation of the original value given by Parker (1990a and 1990b), in which the roughness height was defined as twice of surface layer D_{90} .

In case of a normal flow, shear velocity u_* can be expressed as:

$$u_* = \sqrt{ghS} \tag{Equation A-12}$$

in which S is channel bed slope.

A roughness correction was used in the sediment transport modeling for this study due to the abundance of large roughness elements on the channel bed in the McCloud River. Large, relatively immobile grains in mountain stream channels consume a significant portion of the total shear stress thereby reducing the stress available for transporting finer, mobile sediment (Yager *et al.* 2007). Roughness, represented by traditional Manning's n , is partitioned into a mobile grain roughness (n_D) and a main channel roughness (n_c) using the following logic according to Peter Wilcock (personal communication, P. Wilcock, Professor, Department of Engineering at Johns Hopkins University, Baltimore, MD, and Y. Cui, Sediment Transport Modeler, Stillwater Sciences, Berkeley, CA, January 15, 2008).

Manning's flow resistance equation (SI Units) can be written as follows:

$$U = \frac{\sqrt{SR_h}^{2/3}}{n} \tag{Equation A-13}$$



where n is the Manning's resistance coefficient, and R_h is hydraulic radius. By multiplying Equation A-13 by $(\rho g)^{2/3} S^{1/6}$, rearranging, and then raising to the $(3/2)$ power, Equation A-13 can be manipulated into the following formulation for total boundary shear stress τ_0 :

$$\rho g S^{1/4} (nU)^{3/2} = \tau_0 \tag{Equation A-14}$$

Similar to the reasoning behind the Einstein drag partition, we assume that Equation A-14 holds not only for the total roughness n , giving the total boundary stress τ_0 , but, if we replace n with a roughness pertaining only to the grains (n_D), we get the grain stress τ' :

$$\rho g S^{1/4} (n_D U)^{3/2} = \tau' \tag{Equation A-15}$$

Again, using the reasoning of Einstein's drag partition, we assume that the same velocity U holds true for Equations A-14 and A-15. By dividing Equation A-15 with Equation A-14, the following equation results:

$$\tau' = \left(\frac{n_D}{n} \right)^{3/2} \tau_0 \tag{Equation A-16}$$

Because ρ , g , and S are constant for τ' and τ_0 , Equation A-16 can also be written as:

$$h' = \left(\frac{n_D}{n} \right)^{3/2} h \tag{Equation A-17}$$

where h' is the grain stress depth. The grain roughness n_D can be calculated from the Manning Strickler relation by substituting Equations A-12 and A-13 into Equation A-9 for the following relation where k_s is expressed in meters:

$$n_D = 0.04(k_s)^{1/6} \tag{Equation A-18}$$

Shear stress τ' calculated with Equation A-16 is used for bedload transport calculations in place of the total shear stress τ_0 , resulting in a reduced bedload transport rate due to the presence of roughness elements.

Function G in Parker's surface based bedload equation (Equation A-1) is given by Parker (1990a and 1990b) as:

$$G(\phi) = \begin{cases} 5474 \left(1 - \frac{0.853}{\phi} \right)^{4.5} & \phi > 1.59 \\ \exp[4.2(\phi - 1) - 9.28(\phi - 1)^2] & 1 \leq \phi \leq 1.59 \\ \phi^{14.2} & \phi < 1 \end{cases} \tag{Equation A-19}$$



In case of an arbitrary cross section, the cross section is divided into the main channel and a floodplain. In this case sediment transport over floodplain is assumed to be insignificant. The surface based bedload equation of Parker (Equation A-1) and the Manning-Strickler resistance relation (Equation A-9) are modified as follows,

$$\frac{RQ_G P_i}{A_c S u_*} = \alpha F_i G \left(\omega \phi_{sgo} \left(\overline{D}_i / D_{sg} \right)^{-\beta} \right) \quad \text{(Equation A-20)}$$

$$Q_{wc} = \frac{1}{n_c} A_c R_{hc}^{2/3} S^{1/2} \quad \text{(Equation A-21)}$$

$$\frac{U_c}{u_*} = 8.1 \left(\frac{R_{hc}}{k_s} \right)^{1/6} \quad \text{(Equation A-22)}$$

where A_c denotes flow area in the main channel; U_c denotes velocity in the main channel, R_{hc} denotes hydraulic radius of the flow in the main channel,

$$R_{hc} = \frac{A_c}{P_c} \quad \text{(Equation A-23)}$$

and P_c denotes the wet perimeter of the main channel. When a main channel Mannings n_c is provided, Equation A-21 is used to calculate main channel discharge, but when one is not provided Equation A-22 with Equation A-27 is used. Shear velocity, roughness height and grain size parameters in Equations A-20 and A-22 all refer to those in the main channel.

Floodplain hydraulics and flow continuity are brought in to close the equations,

$$Q_{wf} = \frac{1}{n_f} A_f R_{hf}^{2/3} S^{1/2} \quad \text{(Equation A-24)}$$

$$Q_{wf} + Q_{wc} = Q_w \quad \text{(Equation A-25)}$$

$$R_{hf} = \frac{A_f}{P_f} \quad \text{(Equation A-26)}$$

$$U_c = \frac{Q_{wc}}{A_c} \quad \text{(Equation A-27)}$$

where n_f denotes Manning's n for on the floodplain; A_f denotes flow area in floodplain; P_f denotes the wet perimeter of the floodplain; R_{hf} denotes hydraulic radius of the floodplain; Q_{wf} and Q_{wc} denotes the discharge on floodplain and main channel respectively.

Equations A-21 through A-26 are solved iteratively using input cross-section data. Once these equations are solved, total boundary shear stress τ_0 is calculated as:

$$\tau_0 = \rho g R_{hc} S \quad \text{(Equation A-28)}$$



Total grain shear stress τ' available to transport the mobile sediment fraction can then be calculated using Equations A-16 and A-18.

Model Assumptions

The following assumptions and limitations pertain to applying Parker's surface-based bedload equation (Parker 1990a and 1990b in the EASI model):

- Flow is assumed to be normal (steady and uniform) flow.
- Friction slope (energy slope) is approximated by the reach-averaged water surface slope surveyed at relatively low discharges.
- Sediment densities are assumed to be $2,650 \text{ kg m}^{-3}$.
- The channel is assumed prismatic (continuous channel shape throughout the reach being modeled) based on the shape of the cross-section input; as a result, cross-sections used in the model should be located in uniform and representative sites of the entire reach.
- If floodplains exist at the cross-section, sediment transport occurs only in the main channel while the floodplains convey part of the flow at discharges that overtop the bank and connect with the floodplain.
- Simulated sediment transport capacities should be viewed as long-term averages.
- As with any sediment transport equation, sediment transport capacities calculated with EASI model usually have an error factor of 2 to 3 but can be larger.

Manning's n Calculation

Modeling results presented in this study are sensitive to the selected Manning's n values as they are critical to computed flow depths and subsequent shear stress and bedload transport estimates. Manning's n , as are other coefficients that estimate roughness, is a highly variable parameter that depends on several factors including: surface roughness, vegetation, channel size and shape, channel irregularities, channel obstruction, and stage and discharge. Roughness coefficients at a given station will vary based on stage and discharge and generally decrease as stage and hydraulic radius increase, which further complicates the selection of a single Manning's n value to model an entire flow record. Furthermore, Manning's n values are much greater for high gradient cobble- and boulder-bed streams than for low gradient streams with similar relative roughness (Jarrett 1987). All of these factors introduce significant uncertainty in Manning's n values and sediment transport estimates presented in this study. As a result, a variety of methods were used to estimate Manning's n , and sediment transport results are presented using a range of Manning's n values.

An estimate for the main channel Manning's n used in Equations A-16, A-17, and A-21 was determined from published empirical relations and from roughness values calculated from stage-discharge observations at the sediment transport modeling cross-sections that were monitored as part of Study Description BR-S4 (see TM-65, *Assess Ongoing Project Effects on Riparian*



Vegetation Community Types in the Project Area [PG&E 2009]). The following published empirical relations were used to estimate Manning’s *n*:

Bathurst’s (1985) relation for higher gradient, gravel-bed streams;

$$n = \frac{(0.3193R_h^{0.167})}{[5.62\log(R_h / D_{84}) + 4]} \quad \text{(Equation A-29)}$$

Jarrett’s (1984) relation for high gradient (> 0.002) coarse-grained (D_{84} from 0.1 to 0.8 m) streams;

$$n = 0.32S^{0.38}R_h^{-0.16} \quad \text{(Equation A-30)}$$

and Smart and Jaeggi’s (1983) relation for high gradients (up to 0.2) streams with high sediment transport rates:

$$n = \frac{(0.3193R_h^{0.167})}{5.75[1 - \exp(-0.05(R_h / D_{90})(1 / S^{0.5}))]^{0.5} \log(8.2(R_h / D_{90}))} \quad \text{(Equation A-31)}$$

Study Description BR-S4 (see TM-65, *Assess Ongoing Project Effects on Riparian Vegetation Community Types in the Project Area* [PG&E 2009]) utilized observed data combined with historic gage to develop roughness coefficient to discharge regression relationships. Stage-discharge observations were made at all of the sediment transport modeling cross-sections at three discharges: approximately 175, 600, and 800 cfs. Roughness coefficients were back calculated based on these observations and surveyed slope and channel geometry data. These observed roughness coefficients were used to develop a regression relationship between discharge and roughness coefficients (note that the relationships developed as part of Study Description BR-S4 used the friction factor from the Darcy-Weisbach equation, which was converted to Manning’s *n* for this study). Regression relationships at individual cross-sections were extended to higher discharges based on stage-discharge points at the USGS gaging station (McCloud River at Ah-Di-Na, USGS Gage No. 11367800) located at cross section 2B for the GS-S2 Study. Using these regression relationships, the estimated Manning’s *n* for a 2-year return peak flow under unimpaired hydrologic conditions (Table 9) was used to help develop the range of Manning’s *n* used in the sediment transport modeling.

Estimated average annual coarse sediment transport capacity and bed mobility thresholds were given at a high, middle, and low amount (Table 10). The primary variable between these model scenarios was the Manning’s *n* estimate (Table A2-1). Note that a “high” Manning’s *n* estimate in Table A2-1 leads to decreased sediment transport capacity and produces the “low” sediment transport capacities in Table 10. Manning’s *n* values for the 2-year unimpaired peak flow from the field based regression relationships in TM-65, *Assess Ongoing Project Effects on Riparian Vegetation Community Types in the Project Area* (PG&E 2009) were consistently higher than the published empirical relations (Equations A-29, A-30, and A-31) and provided the “high” value in Table A2-1. The median value from Equations A-29, A-30, and A-31 was used to provide the



“low” estimate. An average of the two methods generally provided the “middle” Manning’s *n* estimate in Table A2-1; although some calibration of the middle value was done based on tracer rock observations. The generally accepted range of Manning’s *n* estimates for steep mountain streams with no vegetation in channel, usually steep banks, with trees and brush on banks submerged at high flows, and a cobble and large boulder bottom is 0.040 to 0.070 (Chow 1959). Values in Table A2-1 are generally within this range and show a decreasing trend with distance downstream of McCloud Dam as slope decreases.

Table A2-1. Range of main channel Manning’s *n* estimates used in the sediment transport modeling at the five intensive study sites on the Lower McCloud River

Site	Distance Downstream of McCloud Dam (km)	Slope (%)	Main Channel Manning’s <i>n</i> Estimates		
			High	Middle	Low
Site 1	1.71	1.35	0.080	0.071	0.061
Site 2	5.49	1.19	0.072	0.063	0.054
Site 3	11.33	0.74	0.060	0.054	0.047
Site 4	16.77	0.94	0.063	0.056	0.049
Site 5	20.78	0.43	0.047	0.043	0.040

List of Notations used in Attachment 2

- A area of the flow;
- B channel width;
- D_i the lower bound grain size of the *i*-th subrange;
- \overline{D}_i mean grain size of the *i*-th subrange ($= \sqrt{D_i D_{i+1}}$);
- D_{84} grain size for which 84% of the distribution is finer than;
- D_{90} grain size for which 90% of the distribution is finer than;
- D_{sg} geometric mean grain size of the surface layer;
- F_i volumetric fraction of the *i*-th subrange in the surface layer;
- g* acceleration of gravity;
- h* water depth;
- h' grain stress depth;
- k_s roughness height;
- n* Manning’s roughness coefficient;
- n_D mobile grain roughness coefficient;
- P* wet perimeter of the channel;
- p_i volumetric fraction of the *i*-th subrange in bedload;
- Q_G gravel transport rate;



Q_w	water discharge;
Q_{wc}	water discharge main channel;
Q_{wf}	water discharge floodplain;
R	submerged specific gravity of gravel;
R_h	hydraulic radius of the flow;
R_{hc}	hydraulic radius of the flow in the main channel;
R_{hf}	hydraulic radius of the flow on the floodplain;
S	reach-averaged channel bed slope;
U	flow velocity;
U_C	flow velocity in the main channel;
u^*	shear velocity;
α	coefficient in Parker equation (= 0.00218);
β	hiding coefficient in Parker equation (= 0.0951);
ρ	density of water
ϕ_{sgo}	normalized Shield stress;
σ_0	parameter in Parker equation (is a function of ϕ_{sgo});
σ_{sg}	geometric standard deviation of the surface layer;
$\sigma_{s\psi}$	arithmetic standard deviation of the surface layer;
τ_r^*	reference Shield stress;
τ_{sg}^*	surface based Shield stress;
τ_0	total boundary shear stress;
τ'	mobile grain shear stress;
ω	parameter in Parker equation (is a function of $\sigma_{s\psi}$ and ϕ_{sgo});
ω_0	parameter in Parker equation (is a function of ϕ_{sgo});
ψ_i	the lower bound of the i-th subrange grain size in ψ -scale, $\psi_i = \log_2(D_i)$, where D_i is grain size in mm;
$\bar{\psi}_i$	mean grain size of the i-th subrange in ψ -scale ($= \frac{\psi_i + \psi_{i+1}}{2}$);
$\bar{\psi}_s$	mean grain size of the surface layer in ψ -scale.

Literature Cited

- Bathurst, J.C. 1985. Flow resistance estimation in mountain streams. ASCE Journal of Hydraulic Engineering 111:625–641.
- Chow, V.T. 1959. Open channel hydraulics. McGraw-Hill Book Co., New York. 512 pp.
- Jarrett, R.D. 1987. Errors in slope-area computations of peak discharges in mountain streams. Journal of Hydrology 96:53–67.
- Jarrett, R.D. 1984. Hydraulics of high gradient streams. ASCE Journal of Hydraulics Division 110:1519–1539.



- Mueller, E. R., J.Pitlick, and J. M. Nelson. 2005. Variation in the reference Shields stress for bed load transport in gravel-bed streams and rivers. *Water Resources Research* 41:W04006, doi: 10.1029/2004WR003692
- Parker, G. 1990a. Surface-based bedload transport relation for gravel rivers. *Journal of Hydraulic Research* 28:417-436.
- Parker, G. 1990b. The acronym series of PASCAL program for computing bedload transport in gravel rivers. External Memorandum M-220. St. Anthony Falls Laboratory, University of Minnesota.
- PG&E. 2009. Assess potential ongoing Project effects on riparian vegetation community types in the Project Area (BR-S4), Technical Memo 65. McCloud-Pit Project, FERC Project No. 2106, San Francisco, CA. In progress.
- Smart, G.M. and M.N.R. Jaeggi. 1983. Sediment transport on steep slopes. *Versuchsanstalt fur Wasserbau, Hydrologie und Glaziologie*, 64, Zurich Institute of Technology, Zurich, Switzerland.
- Yager, E.M., J.W. Kirchner, and W.E. Dietrich. 2007. Calculating bed load transport in steep boulder bed channels. *Water Resources. Research* 43: DOI:10.1029/2006WR005432.
- Yager, E., M. Schmeckle, W.E. Dietrich, and J.W. Kirchner. 2004. The effect of large roughness elements on local flow and bedload transport. American Geophysical Union, AGU Fall Meeting: Abstract #H41G-05.

ATTACHMENT 3

Exceedance Probability Curves

This page intentionally left blank.

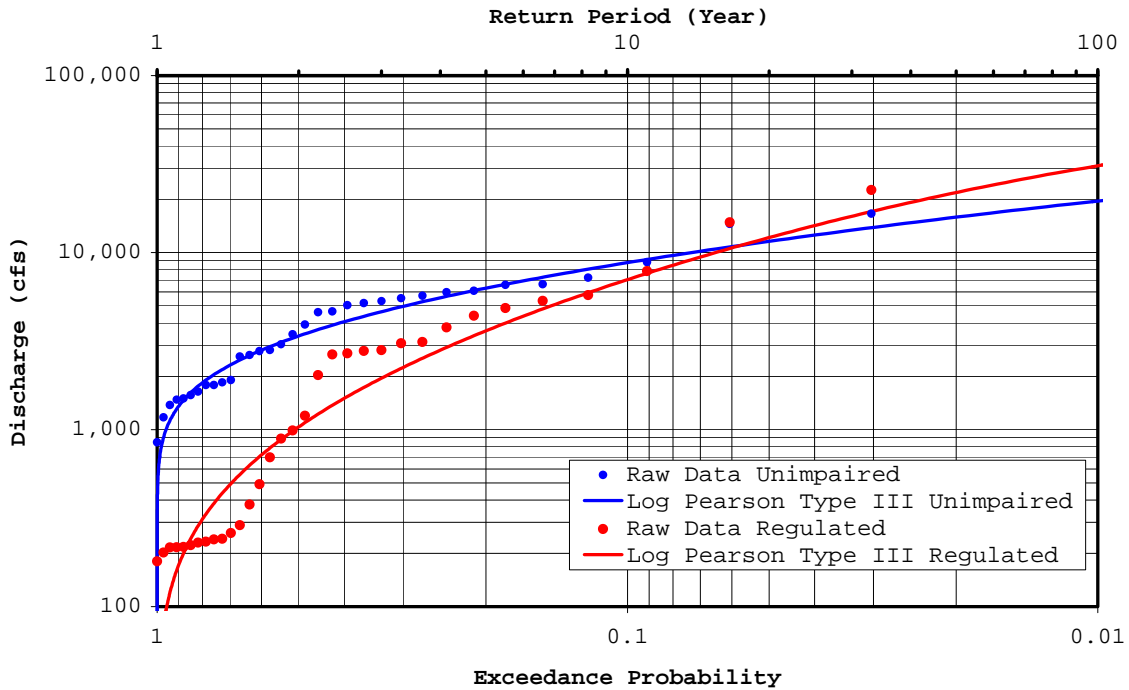


Figure A3-1. Log Pearson Type III peak flow analysis of annual maximum daily flow for regulated and unimpaired conditions at Intensive Study Site 1.

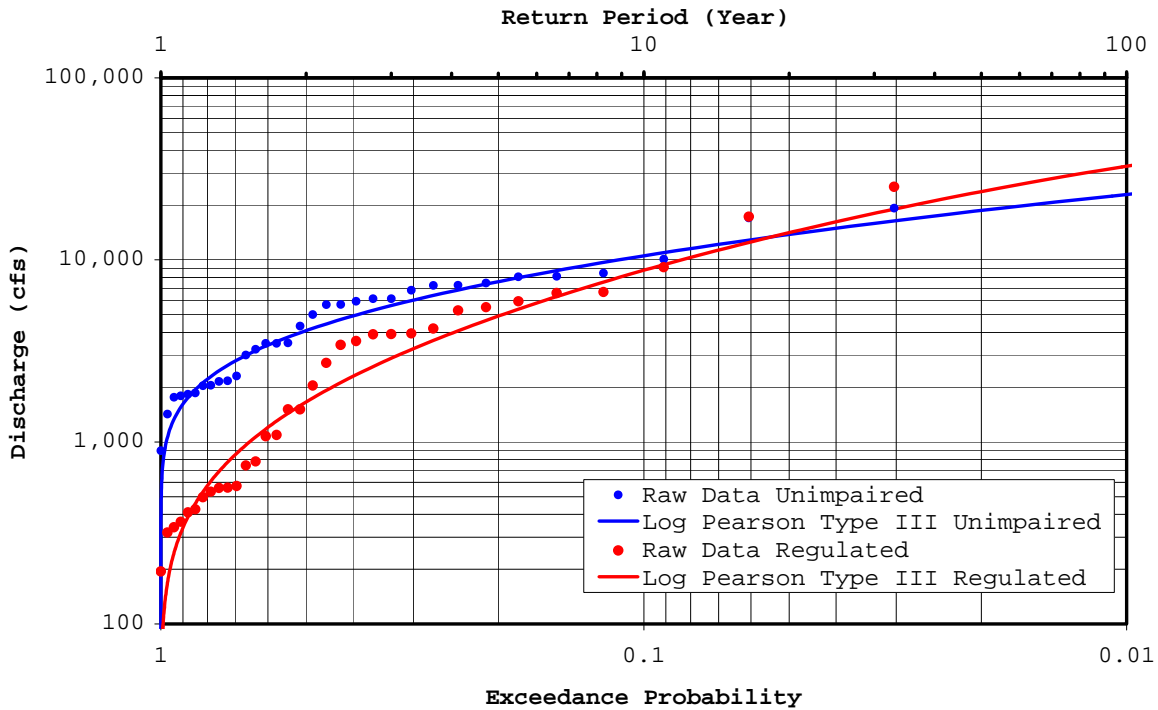


Figure A3-2. Log Pearson Type III peak flow analysis of annual maximum daily flow for regulated and unimpaired conditions at Intensive Study Site 2.

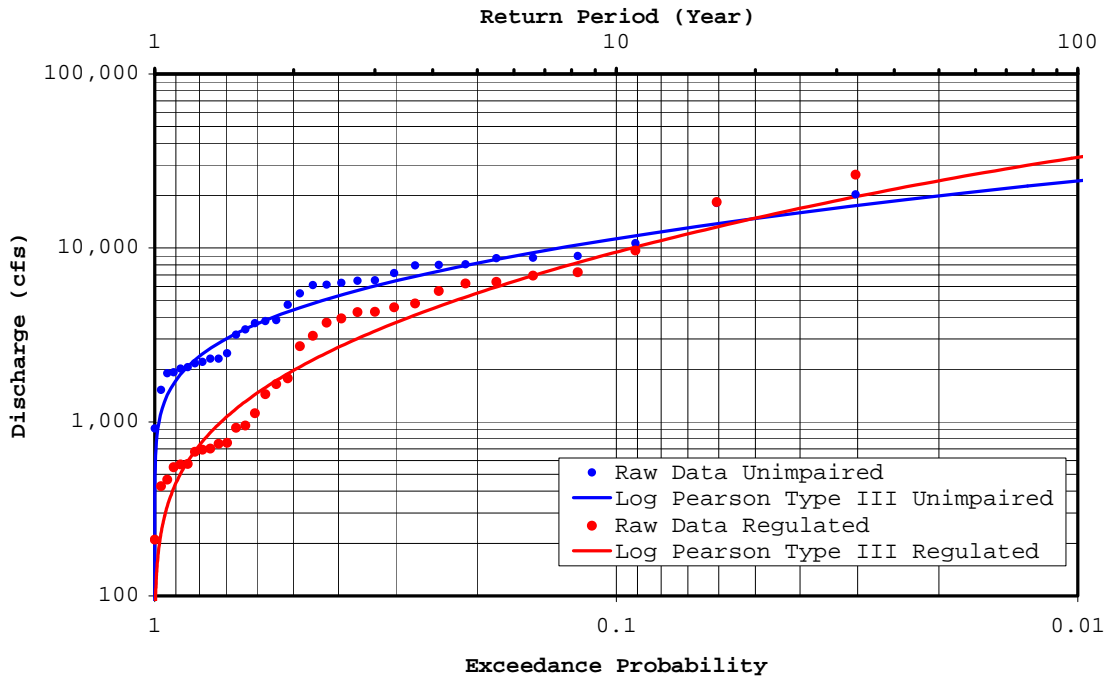


Figure A3-3. Log Pearson Type III peak flow analysis of annual maximum daily flow for regulated and unimpaired conditions at Intensive Study Site 3.

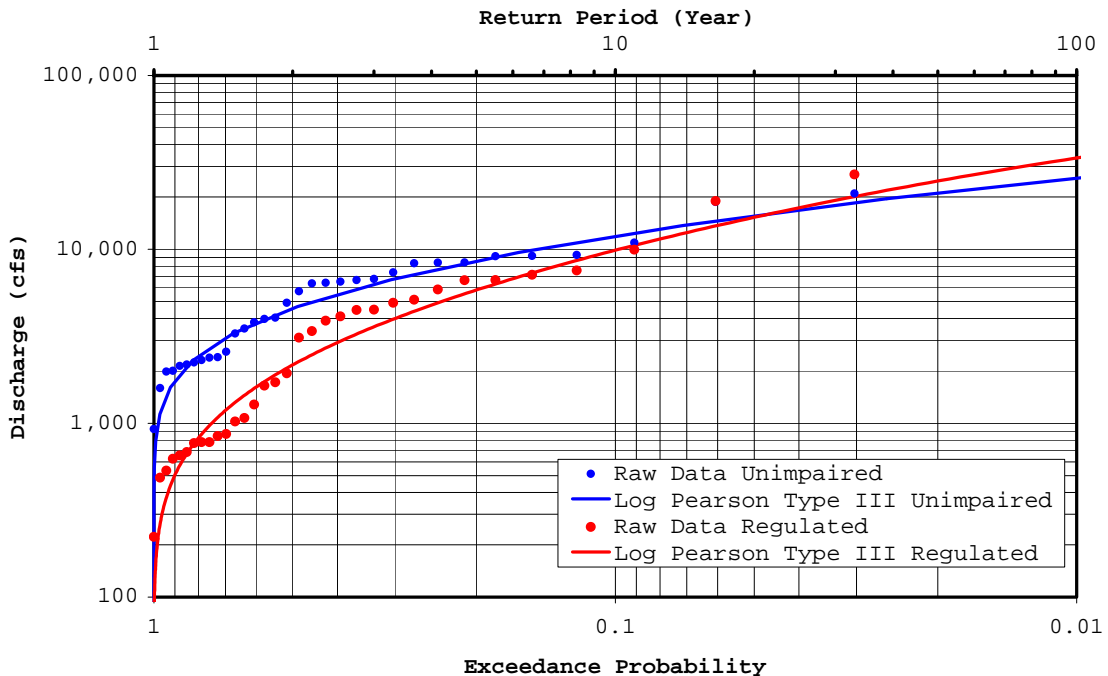


Figure A3-4. Log Pearson Type III peak flow analysis of annual maximum daily flow for regulated and unimpaired conditions at Intensive Study Site 4.

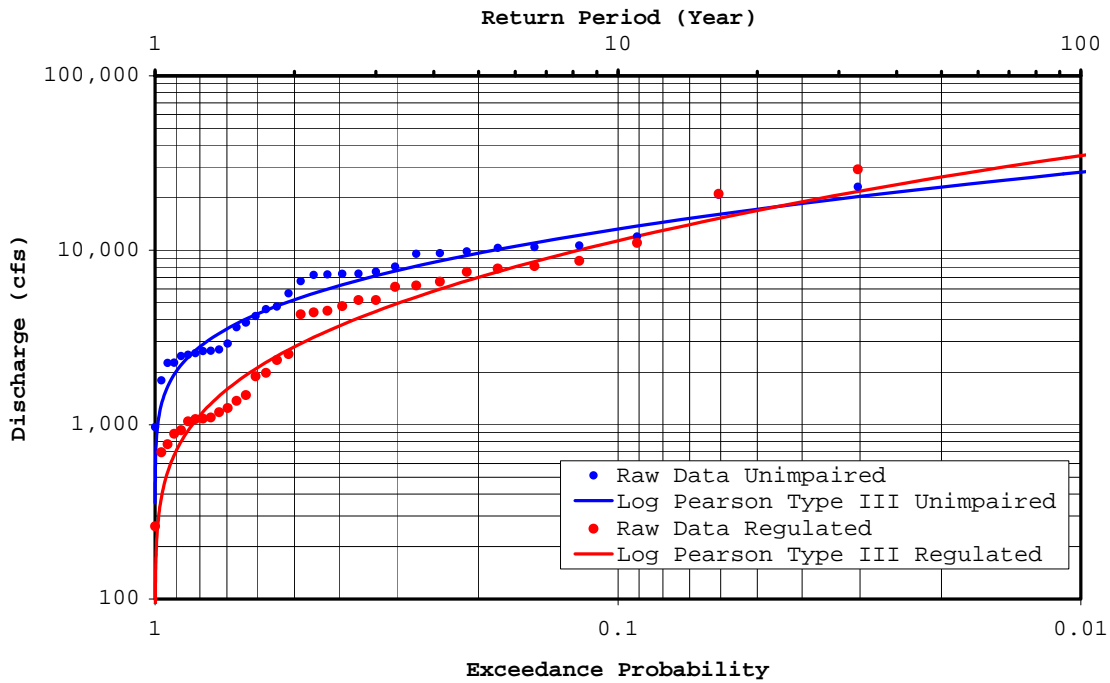


Figure A3-5. Log Pearson Type III peak flow analysis of annual maximum daily flow for regulated and unimpaired conditions at Intensive Study Site 5.

This page intentionally left blank.

ATTACHMENT 4

**Comparison of predicted bedload grain size
distributions with bulk samples of mobile material at
Intensive Study Sites**

This page intentionally left blank

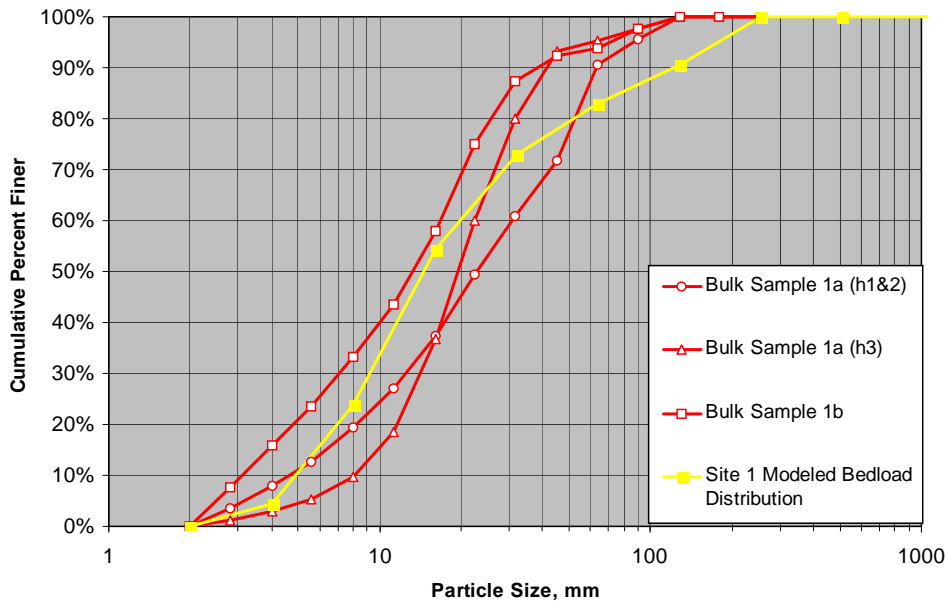


Figure A4-1. Comparison of grain size distributions from field bulk samples and modeled bedload distributions modeled with EASI model for Intensive Study Site 1 (distribution truncated at 2 mm to exclude sand and finer material from the analysis).

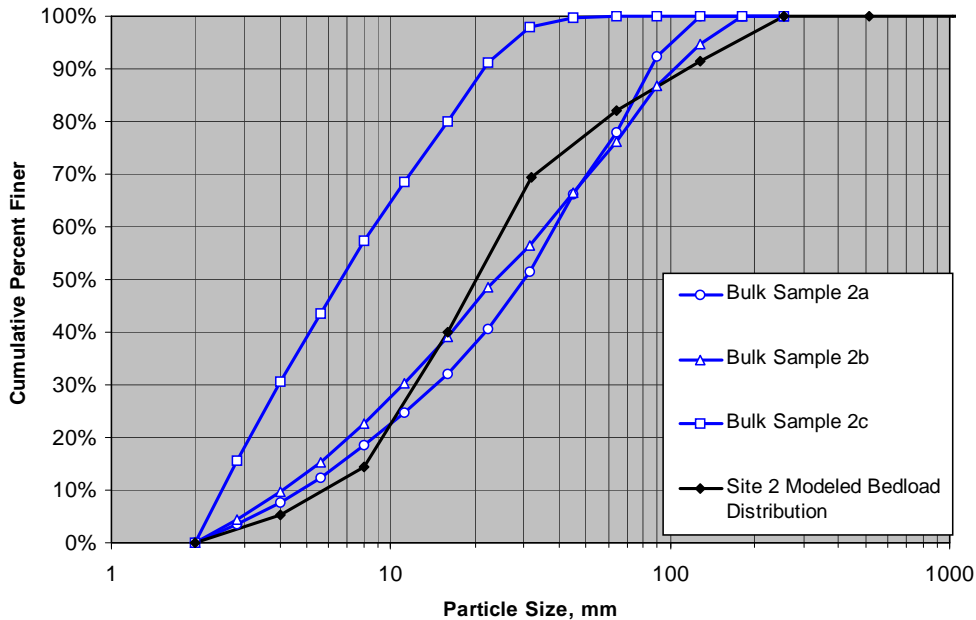


Figure A4-2. Comparison of grain size distributions from field bulk samples and modeled bedload distributions modeled with EASI model for Intensive Study Site 2 (distribution truncated at 2 mm to exclude sand and finer material from the analysis).

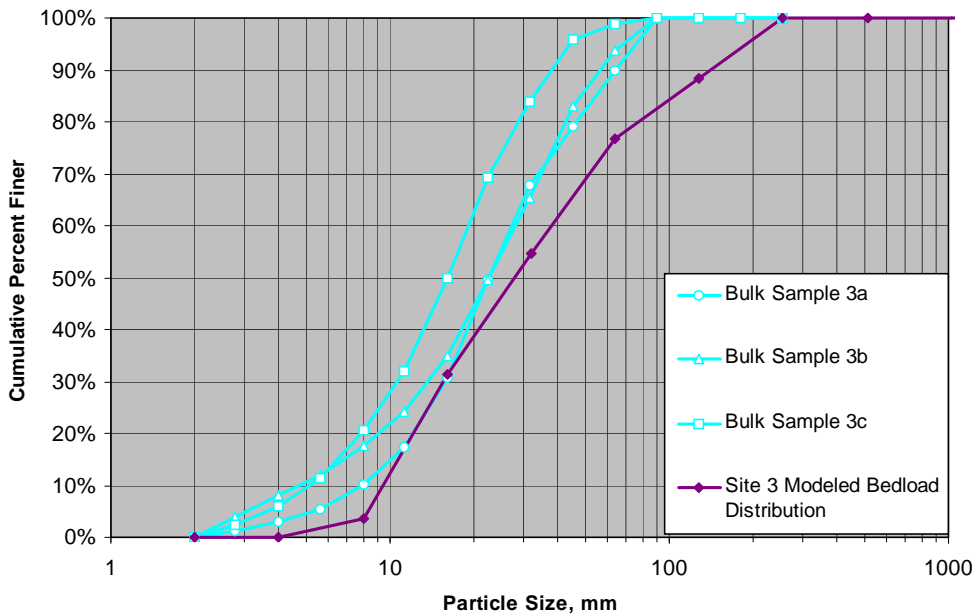


Figure A4-3. Comparison of grain size distributions from field bulk samples and modeled bedload distributions modeled with EASI model for Intensive Study Site 3 (distribution truncated at 2 mm to exclude sand and finer material from the analysis).

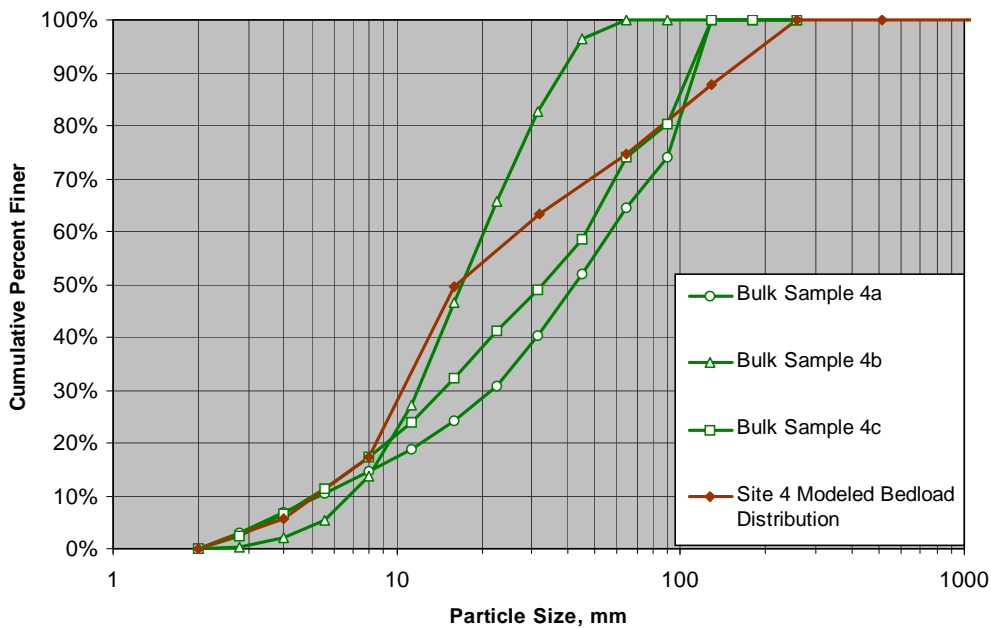


Figure A4-4. Comparison of grain size distributions from field bulk samples and modeled bedload distributions modeled with EASI model for Intensive Study Site 4 (distribution truncated at 2 mm to exclude sand and finer material from the analysis).

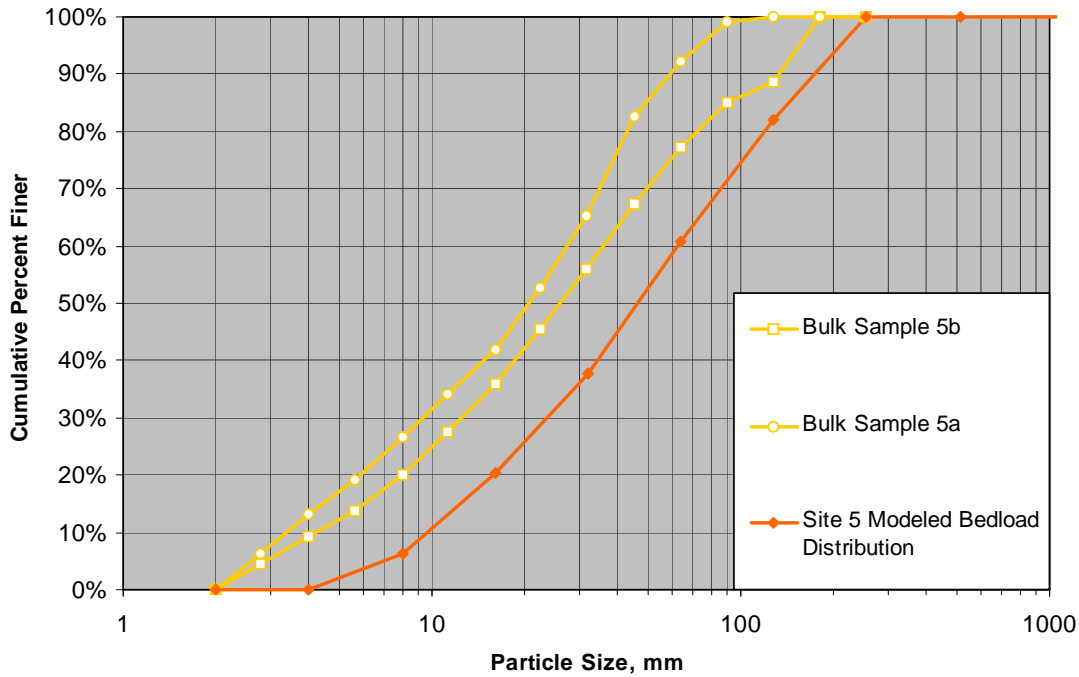


Figure A4-5. Comparison of grain size distributions from field bulk samples and modeled bedload distributions modeled with EASI model for Intensive Study Site 5 (distribution truncated at 2 mm to exclude sand and finer material from the analysis).

ATTACHMENT 5

Sample Data Sheet for Sediment Storage Mapping

This page intentionally left blank.



CHANNEL SEDIMENT STORAGE	Crew: _____	DATE: _____
		Page _____ of _____

Level I habitat type (circle one): Flatwater, Riffle, Pool

Level IV habitat type: _____

Habitat Unit #: _____

bed: _____

Channel type: _____

* Include intermediate morphologies as needed.

Slope: _____

Survey length: _____ (m)

% area of unmappable transitory active

XS	W _{wet}	W _{bf}
1		
2		
3		
4		

Storage element #	Geomorphic feature	Activity class	Facies		Est. D ₅₀ /D ₈₄	Datum	Average Dimensions (m)			Indicators of residence time			
			dom.	subdom.			thickness	width	length	veg	round	bright	sorting

Notes:

Channel types: pool riffle (PR), forced pool riffle, (fPR), pool riffle-plane bed (PRPB), plane bed (PB), plane bed-step pool (PBSP), step pool (SP), step pool-cascade (SPCA), cascade (CA), bedrock (BR).

Geomorphic feature: transitory active channel bed (CB), mid-channel bar (MB), lateral bar (LB), point bar (PB), pool tail (P), lee or stoss deposit (LD), step pool deposit (SP), debris flow deposit (DF), tributary fan deposit (TF), floodplain bench (FB), terrace (T), colluvium (C).

Activity class: active (A) – mobile at RI <5 yr, no or sparse woody veg, low relief; semiactive (SA) – mobile RI >5 yr but within W_{bf}, predom. woody riparian shrubs and small trees

Datum: plane bed (PB), alluvial thalweg (AT), bedrock thalweg (BT), probe to resistant material (P).

Vegetation: (1) bare, (2) herbaceous w/ limited woody riparian, (3) young woody riparian encroachment, (4) dense/mature woody riparian w/ few upland sp, (5) conifers and broadleaf upland sp.

Roundness: (1) angular, (2) subangular, (3) subrounded, (4) rounded. **Brightness:** (1) light, (2) dark, (3) algae, (4) moss/lichen. **Sorting:** (1) well sorted, (2) mod. sorted, (3) poorly sorted.

This page intentionally left blank.

ATTACHMENT 6

Sediment storage mapping results in the Lower McCloud River from McCloud Dam to Squaw Valley Creek

This page intentionally left blank.



Distance from Dam (km)	Survey Length (m)	Channel Type		Channel Gradient	Unit Stream Power (ω)	% TMB ^b	Unit Storage Area, m ² 100m ⁻²			Unit Storage Volume, m ³ 100 m ⁻²		
		Montgomery and Buffington ^a	DFG Level 1				Active	Semi-active	Total	Active	Semi-active	Total
0.42	52	SP	pool	0.0050	170	5	8	1	9	8	0	8
1.21	126	PB	flatwater	0.0247	796	5	1	0	1	0	0	0
1.42	60	SP	pool	0.0020	82	2	1	0	1	0	0	0
1.74	248	PB, SP	flatwater	0.0133	394	20	2	0	3	0	0	0
2.18	130	PB	flatwater	0.0126	318	10	3	0	3	1	0	1
2.63	25	PB, SP	pool	0.0085	281	5	4	0	4	0	0	0
2.76	86	PB, SP	flatwater	0.0219	1,217	5	2	0	2	1	0	1
3.11	75	SP	pool	0.0159	722	5	18	0	18	26	0	26
3.28	35	SP	pool	0.0034	172	5	7	6	12	1	5	6
3.62	105	PB, SP	flatwater	0.0131	379	5	2	1	3	1	0	1
4.56	57	SP	pool	0.0025	123	5	5	9	14	3	8	11
4.63	42	PB, SP	flatwater	0.0180	656	5	2	0	2	1	0	1
4.70	87	SP	pool	0.0045	149	2	22	0	22	31	0	31
5.03	35	SP	pool	0.0100	298	5	4	8	12	1	3	4
5.09	47	SP	pool	0.0020	91	2	7	6	12	1	1	2
5.19	146	PB	flatwater	0.0097	382	30	1	0	1	0	0	0
5.64	303	PB	flatwater	0.0130	387	30	4	0	4	1	0	1
6.28	69	PB, SP	flatwater	0.0110	383	10	2	0	2	1	0	1
6.36	71	SP	pool	0.0045	189	2	20	0	20	22	0	22
6.90	88	PB	flatwater	0.0130	345	40	3	0	3	0	0	0
7.17	88	SP	pool	0.0034	128	40	33	0	33	53	0	53



Distance from Dam (km)	Survey Length (m)	Channel Type		Channel Gradient	Unit Stream Power (ω)	% TMB ^b	Unit Storage Area, m ² 100m ⁻²			Unit Storage Volume, m ³ 100 m ⁻²			
		Montgomery and Buffington ^a	DFG Level 1				Active	Semi-active	Total	Active	Semi-active	Total	
7.26	77	PB	riffle	0.0349	925	10	0	0	0	0	0	0	0
7.45	210	PB, SP	flatwater	0.0071	255	40	5	0	5	1	0	1	1
7.74	143	PB	riffle	0.0142	366	60	1	0	1	0	0	0	0
7.90	108	SP	pool	0.0031	115	70	39	2	41	57	0	58	58
8.12	109	PB	flatwater	0.0103	255	60	12	3	15	3	1	5	5
8.47	92	PB	riffle	0.0115	286	80	23	0	23	4	0	4	4
9.67	80	SP	pool	0.0032	106	50	22.9	0.0	22.9	12.4	0.0	12.4	12.4
10.07	153	PB	flatwater	0.0140	419	20	7.0	1.4	8.4	1.9	0.6	2.5	2.5
10.50	95	PBSP	flatwater	0.0193	878	20	7.2	0.0	7.2	12.3	0.0	12.3	12.3
11.00	116	SP	pool	0.0020	78	60	29.0	0.0	29.0	33.8	0.0	33.8	33.8
11.55	203	PB	flatwater	0.0073	234	50	9.8	0.0	9.8	4.9	0.0	4.9	4.9
11.75	100	SP	pool	0.0021	76	60	43.9	0.0	43.9	22.5	0.0	22.5	22.5
12.89	184	PB	flatwater	0.0132	395	60	2.9	0.0	2.9	0.8	0.0	0.8	0.8
13.29	49	SP	pool	0.0027	97	20	46.9	0.0	46.9	70.4	0.0	70.4	70.4
13.97	154	PB	flatwater	0.0131	514	30	9.9	0.0	9.9	9.7	0.0	9.7	9.7
14.52	49	SP	pool	0.0070	233	60	24.8	0.0	24.8	16.0	0.0	16.0	16.0
15.74	125	PB	flatwater	0.0059	196	60	6.4	2.0	8.4	3.4	0.4	3.8	3.8
16.05	144	SP	pool	0.0027	107	60	19.1	0.0	19.1	8.6	0.0	8.6	8.6
16.62	172	PB	flatwater	0.0066	204	40	6.1	0.0	6.1	1.7	0.0	1.7	1.7
17.05	95	SP	pool	0.0020	59	60	21.7	2.2	23.9	10.6	1.0	11.6	11.6
17.21	242	PB	flatwater	0.0094	215	40	2.0	0.0	2.0	1.0	0.0	1.0	1.0



Distance from Dam (km)	Survey Length (m)	Channel Type		Channel Gradient	Unit Stream Power (ω)	% TMB ^b	Unit Storage Area, m ² 100m ⁻²			Unit Storage Volume, m ³ 100 m ⁻²		
		Montgomery and Buffington ^a	DFG Level 1				Active	Semi-active	Total	Active	Semi-active	Total
18.45	291	PBSP	flatwater	0.0090	307	40	4.7	0.0	4.7	1.4	0.0	1.4
18.92	106	SP	pool	0.0013	35	50	18.2	0.0	18.2	41.4	2.7	44.1
20.61	86	SP	pool	0.0042	177	30	11.0	10.5	21.4	16.5	0.0	16.5
20.72	98	PB	flatwater	0.0060	268	30	4.0	0.0	4.0	1.1	0.0	1.1
21.38	286	PB	flatwater	0.0043	145	30	5.7	0.0	5.7	1.4	0.0	1.4
21.67	128	SP	pool	0.0023	93	50	41.6	0.0	41.6	66.3	0.0	66.3
22.35	78	PBSP	flatwater	0.0210	474	50	2.3	0.0	2.3	0.5	0.0	0.5
22.59	56	SP	pool	0.0016	54	50	6.1	0.0	6.1	3.1	0.0	3.1

^a Plane bed (PB), step pool (SP)

^b Transitory mobile bed (TMB)